CAPITAL UNIVERSITY OF SCIENCE AND TECHNOLOGY, ISLAMABAD

Anti-diabetic Attributes of Methanolic Extract of Okra Leaves and Molecular Docking of Bioactive Compound with IRS-Proteins

by

Nimra Suleman

A thesis submitted in partial fulfillment for the degree of Master of Science

in the

Faculty of Health and Life Sciences
Department of Bioinformatics and Biosciences

2025

I want to dedicate this achievement to my beloved parents and siblings, honorable teachers, friends, and classmates who always encouraged and supported me in every crucial time during my studies to achieve my tasks and secure this degree.

CERTIFICATE OF APPROVAL

Anti-diabetic Attributes of Methanolic Extract of Okra Leaves and Molecular Docking of Bioactive Compound with IRS-Proteins

by

Nimra Suleman

(MBS233020)

THESIS EXAMINING COMMITTEE

S. No.	Examiner	Name	Organization
(a)	External Examiner	Dr. Zaheer Ahmed	AIOU, Islamabad
(b)	Internal Examiner	Dr, Arshia Amin Butt	CUST, Islamabad
(c)	Supervisor	Dr. Rizwan Ur Rehman	CUST, Islamabad

Dr. Rizwan Ur Rehman
Thesis Supervisor
October, 2025

Dr. Syeda Marriam Bakhtiar
Head
Dept. of Bioinfo. & Biosciences
October, 2025

Dr. Sahar Fazal
Dean
Faculty of Health & Life Sciences
October, 2025

Author's Declaration

I, **Nimra Suleman** hereby state that my MS thesis titled "**Anti-diabetic Attributes of Methanolic Extract of Okra Leaves and Molecular Docking of Bioactive Compound with IRS-Proteins**" is my own work and has not been submitted previously by me for taking any degree from Capital University of Science and Technology, Islamabad or anywhere else in the country/abroad.

At any time if my statement is found to be incorrect even after my graduation, the University has the right to withdraw my MS Degree.

(Nimra Suleman)

Registration No: MBS233020

Plagiarism Undertaking

I solemnly declare that research work presented in this thesis titled "**Anti-diabetic Attributes of Methanolic Extract of Okra Leaves and Molecular Docking of Bioactive Compound with IRS-Proteins**" is solely my research work with no significant contribution from any other person. Small contribution/help wherever taken has been duly acknowledged and that complete thesis has been written by me.

I understand the zero tolerance policy of the HEC and Capital University of Science and Technology towards plagiarism. Therefore, I as an author of the above titled thesis declare that no portion of my thesis has been plagiarized and any material used as reference is properly referred/cited.

I undertake that if I am found guilty of any formal plagiarism in the above titled thesis even after award of MS Degree, the University reserves the right to withdraw/revoke my MS degree and that HEC and the University have the right to publish my name on the HEC/University website on which names of students are placed who submitted plagiarized work.

(Nimra Suleman)

Registration No: MBS233020

Acknowledgement

First, thanks to the most powerful and most beneficial Allah Almighty, who inculcated skills, knowledge, and endless effort in me to reach here and accomplish my research work. A special thanks to my thesis supervisor for his help, support, interest, and valuable time. Thanks for supervising and motivating me throughout the way to accomplish this thesis. I am grateful to my institute, Capital University of Science and Technology (CUST) Islamabad. This research work is funded by NRPU HEC project no. 16186 and I am highly thankful to HEC for supporting and funding for this project. I would like to thank my family for providing me with unfailing support and continuous encouragement. I would like to express my cordial gratitude towards my sweet parents and my siblings. I would like to thank my friends for helping and motivating me. Finally, I appreciate all the encouragement I have received from several others who have been involved in some way or another with this research work for the accomplishment of my tasks in hand.

(Nimra Suleman)

Abstract

Diabetes mellitus is a serious worldwide public health issue that is accompanied by abnormalities in the metabolism. The present study investigates the phytochemical profiling, through different chromatographical techniques, and therapeutic potential of methanolic leaf extract of *Abelmoschus esculentus* (okra), with a focus on its antioxidant and antidiabetic properties against type 2 *diabetes mellitus*. Okra has demonstrated to exhibit therapeutic characteristics treating range of diseases. Initially, Thin Layer Chromatography (TLC) of leaf extract was performed to determine an optimized solvent system for the separation of phytoconstituents. Based on this, Column Chromatography was employed to fractionate the extract. The fractions were made based on the same band distance appeared on TLC. The obtained fractions were screened for biological activity using in vitro antioxidant assays, including DPPH and Total Polyphenolic Content, and antidiabetic assays such as α-amylase and α-glucosidase inhibition. F2 fraction exhibited the maximum antioxidant, antidiabetic and TPC features followed by F1 and F3. The most bioactive fractions were subjected to High-Performance Liquid Chromatography (HPLC) analysis to identify potential phytochemicals based on retention time data compared with literature. Based on HPLC, Rutin was tentatively identified as a major bioactive compound. To explore its therapeutic relevance, molecular docking studies were performed using rutin as the ligand against key proteins involved in the insulin receptor signaling (IRS) pathway including IRS1, PPARG, and Akt. The docking results revealed that Rutin demonstrated the strongest binding affinity toward Akt, indicating its potential in modulating insulin signaling and its promise as a natural antidiabetic agent. These findings suggest that okra leaves are a valuable source of bioactive compounds with possible applications in diabetes management. The *invitro* and *insilico* findings warrant further investigation into bioavailability, the *invivo* efficacy and clinical potential of okra derived compounds for the containment of T2DM.

Keywords: *Abelmoschus esculentus*, chromatography, rutin, antioxidant activity, antidiabetic assay, molecular docking

Contents

List of Figures

List of Tables

Abbreviations

AMPK	AMP-activated protein kinase
DM	Diabetes mellitus
DPPH	2, 2-diphenyl-1-1picrylhydrazyl reagent
GDM	Gestational Diabetes mellitus
MODY	Maturity onset diabetes of the young
NADH	Nicotinamide adenine dinucleotide
T2DM	Type II Diabetes mellitus
TZD	Thiazolidinediones

Chapter 1

Introduction

Diabetes mellitus is a serious worldwide public well-being issue i.e. typified via abnormalities in carbohydrates metabolism, which results in blood glucose levels that are persistently raised because of decreased insulin function or production. It happens when blood glucose, sometimes referred to as blood sugar, concentrations rise too high [1]. Diabetes can be classified as follows: An autoimmune attack on β-cells causes type 1 diabetes, which usually results in total lack of insulin production, including latent autoimmune diabetes in adulthood [2]. A non-autoimmune, progressive decrease in β-cell insulin production causes type II diabetes, that is frequently linked to resistance of insulin as well as metabolic syndrome [2].

According to a study, approximately 537 million adults amongst the ages of 20 and 79 are presently impacted through diabetes, constituting 10.5% of this demographic globally. Projections suggest that by 2030, this figure will climb to 643 million and further to 783 million that is 11.3% and 12.2% respectively by 2045. Additionally, around 240 million individuals worldwide have diabetes but have not been diagnosed, indicating that nearly half of adults with the condition are unaware of their status [3].

The clinical sign of diabetes envelops a range of indications reflecting the basic metabolic derangements. Classical side effects incorporate polyuria (intemperate urination), polydipsia (expanded thirst), and polyphagia (expanded starvation),

coming about from osmotic diuresis and cellular vitality hardship The clinical appearance of diabetes envelops a range of side effects reflecting the basic metabolic derangements.

Classical indications incorporate polyuria (over the top urination), polydipsia (expanded thirst), and polyphagia (expanded starvation), coming about from osmotic diuresis and cellular vitality hardship. Unexplained weight misfortune happens overwhelmingly in Type 1 *diabetes mellitus* due to catabolic state and protein squandering. Patients regularly report weariness, obscured vision from glucose-induced changes in focal point ebb and flow, and expanded helplessness to contaminations, especially influencing the skin and urinary tract. Nocturia disturbs rest designs, whereas slow-healing wounds result from impeded microcirculation and safe work.

In serious cases, diabetic ketoacidosis may display with Kussmaul breathing, fruity breath odor, and modified awareness [4]. Overweight or weight was the single most critical indicator of diabetes. Need of work out, a destitute count calories, current smoking, and forbearance from liquor utilize were all related with an altogether expanded chance of diabetes, indeed after alteration for the body-mass file [5].

These complications encompass illnesses such as coronary artery disease, heart attacks, stroke, and atherosclerosis [6]. Moreover, increase in blood pressure puts additional stress on the heart, contributes in vascular damage, and amplifies the risk of experiencing a heart attack [7].

Amidst diabetics, hypertension is highly prevalent and ranks as one of the most dominant disorders worldwide. The co-occurrence of these two illnesses considerably enhances the probability of complications entail retinopathy and nephropathy [8].

Dealing diabetes can also affect mental well-being. Compared to people without diabetes, people with diabetes can develop depression two to three times higher as compared to non-diabetic ones [6]. These complications largely stem from persistently elevated blood glucose levels. Insulin and glucagon play crucial roles in maintaining glucose and lipid homeostasis through signaling pathways [9].

Attaining lasting metabolic stability in diabetes requires a blend of lifestyle adjustments and pharmaceutical interventions. Achieving glycated hemoglobin levels close to normal substantially diminishes the risks associated with both macrovascular and microvascular complications. Presently, there exists a range of treatments, including oral and injectable options, for managing *diabetes mellitus* specifically in type II.

Treatment practices directed at delaying the onset or advancement of diabetes-related complications underscore the importance of maintaining optimal glycemic control. The primary approach should prioritize lifestyle modifications. While lifestyle changes have demonstrated significant benefits, sustaining them long-term can pose challenges for many patients. Metformin continues to be the preferred preliminary treatment for the majority of patients. The selection of alternative or second-line treatments must be centered on the particular requirements of each patient [10].

In earlier times, the primary focus of diabetes medications was to manage and normalize blood glucose levels within the bloodstream. However, many modern drugs were associated with numerous side effects that could lead to significant medical issues during treatment. Consequently, plants had been employed as alternative medicines for an extended period and played a pivotal role in diabetes management. Moreover, in recent years, newly discovered bioactive compounds isolated from plants exhibited superior antidiabetic properties compared to conventional oral hypoglycemic agents utilized in clinical treatment [11].

A part of the *Malvaceae* family, *Abelmoschus esculentus* moreover known as okra, woman finger and bhindi has interesting physical characteristics [12]. Okra flourishes in zones with scope and unmistakably tall stickiness levels. It is exceedingly helpless to cold temperatures and shows hindered development when uncovered to conditions underneath 15 ^{o}C [13]. The plant incorporates a durable, upright stem that can develop up to one or two meters in stature. It has distinctive levels of pubescence and every so often has ruddy or purplish tones. With serrated edges and recognizable veins, its palmately lobed clears out are heart-shaped on the base and run in length from 10 to 25 cm. The pentamerous, single, the yellow

petals of axillary blossoms feature a scarlet or purple core. Plant produces long, furrowed, pentagonal seed units (natural products) that are 10-25 cm long after fertilization. Various circular, kidney-shaped seeds are found interior the locules of these natural products, gathered in vertical columns [14].

Okra leaves have various restorative properties that have been recognized in conventional pharmacological frameworks over different societies. Pharmacological considers have uncovered that okra holds antidiabetic, anti-fatigue, antioxidant, neuroprotective, and antihyperlipidemic exercises [15–19]. The clears out show hepatoprotective impacts against chemical-induced liver harm and have immunomodulatory properties that upgrade resistant framework work [20]. Furthermore, they contain mucilage that gives demulcent impacts, alleviating kindled mucous films and advancing stomach related wellbeing [21].

Okra seed and mash have considerable phenolic substance, counting flavonoids such as quercetin and rutin, procyanidins (B1 and B2), catechin and epicatechin. These compounds contribute altogether to the leaves' strong antioxidant properties, which work through numerous instruments such as free radical rummaging and enactment of endogenous antioxidant defense frameworks. The antioxidant capability of okra leaf extricates connects unequivocally with their add up to phenolic substance, as calculated through 2,2-Diphenyl-1-picrylhydrazyl (DPPH), 2,2'-Azino-bis 3-ethylbenzothiazoline-6-sulfonic corrosive (ABTS) measures. The positions are profiled by this antioxidant.

Docking refers to the process of positioning molecules in optimal orientations to facilitate their interaction with a receptor. This phenomenon occurs rapidly within a cell, where molecules bind together to form a stable complex [22].

1.1 Problem Statement

With diabetes cases projected to reach 592 million by 2035, already available drugs including insulin, metformin, as well as sulfonylureas are involved in causing adverse effects, prompting a need for alternative treatments.

1.2 Aim & Objectives

The present study is aimed to address this knowledge gap by isolating and identifying the specific bioactive compounds from okra leaf extract through different chromatographic techniques, followed by determining their antidiabetic efficacy through computational tools.

The **objectives** of the study are as follows:

1. To separate and identify bioactive compounds of *Abelmoschus esculentus* (okra) via thin-layer chromatography, Column chromatography and HPLC analysis.
2. To assess binding affinities of okra compounds with IRS-proteins through molecular docking.

1.3 Scope

The research seeks to delve into its properties for regulating blood sugar, uncover bioactive components, gain insights into its mode of operation, and play a role in the creation of cost effective and secure pharmaceutical choices for diabetes treatment. Furthermore, the investigation extends to examining *Abelmoschus esculentus (L.) Moench*'s wider health advantages, encompassing its antioxidative attributes, all with the overarching objective of progressing scientific understanding in the realms of herbal medicine and diabetes care.

1.4 Impact on Society

Diabetes exerts a notable influence on society, encompassing challenges within healthcare, financial ramifications, and an expanding public health concern. Genetic and environmental elements contribute to this impact, while investigations into alternative remedies like *Abelmoschus esculentus (L.) Moench* offer potential solutions for diabetes management.

Chapter 2

Literature Review

2.1 *Diabetes Mellitus*

Diabetes mellitus is a complex metabolic disorder categorized by persistent hyperglycemia, triggered by a combination of faults in secretion of insulin, insulin activity, or both, and results in a disturbance in carbohydrates, lipids, and proteins metabolism. The state has the capability to cause long term damage, dysfunction and ultimate organ damage. The clinical signs can comprise intense thirst, frequent urination, vision problems, and weight loss that is unintentional. In severe circumstances, life-threatening metabolic derangements, either ketoacidosis or hyperosmolar hyperglycemic state can occur, and may proceed to unconsciousness, coma, and death without treatment.

Often, there are no or minor symptoms, and thus severe hyperglycemia, enough to cause structural and physiological changes, can remain unrecognized for ages formerly the disease is discovered. Long-term complications of diabetes include advanced retinopathy (that can result in blindness), nephropathy (which may lead to kidney failure), additionally neuropathy, which places the person in danger of foot ulcers, amputations of limb, Charcot foot plus ankle deformities, and autonomic malfunction, including sexual dysfunction. In addition to that, diabetics are exposed to high risks of cardiovascular, peripheral vascular, and cerebral vascular diseases. The diabetes disease process (pathogenesis) is multifactorial, but

generally involves the destruction of the pancreatic 8-cells (through an autoimmune attack) (insulin deficiency) and/or a decreased cellular response to insulin. The dysregulation of metabolism is a consequence of a decreased insulin effect on target tissues that could be caused by insulin resistance or absolute insulin deficiency.

Type I *diabetes mellitus* mainly involves destruction of -cells, which needs exterior insulin to prevent life-threatening ketoacidosis and metabolic crisis. This subtype is usually characterized by the presence of autoimmune markers, i.e., islet cell, anti-GAD or antibodies of insulin. Nevertheless, in some groups of people there is no observation of autoimmune etiology, especially non-Europeans, and it is then classified as idiopathic Type 1 diabetes.

The most prevalent type is type 2 *diabetes mellitus*, where there are instantaneous failings in secretion of insulin and its activity, and also dysfunction may prevail during clinical presentation.

Glucose intolerance is involved in gestational diabetics whose beginning or first recognition occurs in the course of pregnancy, regardless of the mode of treatment or continuation after pregnancy. The classification leaves room open to undiagnosed pre-existing hyperglycemia [23].

2.1.1 Types of *Diabetes Mellitus*

2.1.1.1 Type I *Diabetes Mellitus*

This kind of diabetes, that was formerly known by the name of juvenile-onset diabetes, Type I diabetes or insulin-dependent diabetes and is initiated by an autoimmune-mediated failure of the pancreatic 8-cells. The natural history of α-cell depletion has great interindividual variation, with some patients having a sudden course to others showing a more progressive deterioration [24].

The fulminant subtype is chiefly showed in children population but adults can also affected by this [25]. The steady system of development generally arises in adult

groups, as well as occasionally it is mentioned as latent autoimmune diabetes in adults (LADA). There are few examples especially in pediatric and adolescent patients whereby the first clinical manifestation of the disease could be diabetic ketoacidosis [26].

Baseline fasting hyperglycemia of mild degree with pronounced metabolic instability, and prompt development of severe hyperglycemia or ketoacidosis in response to physiological stresses, e.g. infection, systemic disease. Intact endogenous insulin production, especially in adult patients, in whom some beta-cells functionality can lead to prevention of ketoacidotic crises even over long periods, perhaps decades [27].

The patients afflicted by this variant of Type 1 *Diabetes mellitus* inevitably reach the point where they are completely dependent on insulin to support the vital metabolic processes, at the same time being under a high threat of emerging diabetic ketoacidosis [28]. At this advanced stage of illness, the functionality of the pancreatic -cell is seriously impaired, as shown by a severe reduction or absence of insulin secretion manifested by negligible or undetectable plasma C-peptide levels [29].

Immunological evidence of pancreatic -cell destruction, namely: autoantibodies of glutamic acid decarboxylase (GAD65), insulin autoantibodies (IAAs) and islet cell autoantibodies (ICAs) can be shown in nearby 85-90 percent in Type I *Diabetes mellitus* patients when they first display fasting hyperglycemia [30].

Although it has been shown that Type I *Diabetes mellitus* of this kind exhibits peak incidence including pediatric as well as adolescent ages, it can occur at any age in the age spectrum with reports of incidence cases occurring as early as childhood and as late as older adulthood (up to 90 years) [31].

Its pathogenesis includes a genetic predisposition to beta -cell autoimmunity as well as environmental factors. Well, concomitant obesity does not exclude the analysis in sufferers. Moreover, such patients often have comorbid autoimmune endocrinopathies for example Graves' disease, Addisons disease and Hashimoto thyroiditis [32].

In type I-idiopathic form, there are few kinds whose etiopathogenesis is not defined. These patients are characterized by the constant insulin deficiency and ketoacidotic tendency, however, they do not show any immunological signs of -cell autoimmunity [33].

Epidemiological research indicates that populations of African and Asian descent have a prevalence of this type of diabetes. There is a divergent clinical form seen especially in African patients which shows intermittent dependence on insulin, with variable need of exogenous insulin replacement and episodic ketoacidotic crises [34].

2.1.1.2 Type II *Diabetes mellitus*

Diabetes mellitus of this kind, which was formerly recognized as non-insulin-dependent diabetes or adult-onset diabetes, is an illness in metabolism, that is triggered through relative insulin deficit but not absolute insulinopenia. The affected individuals normally have a massive insulin resistance which is clinically characterized by reduced cellular sensitivity to endogenous insulin [35, 36].

At the onset of the disease and often during its clinical course, the patients still have enough endogenous insulin secretion that does not allow the direct use of insulin as a life-saving therapy. The reason is that this type of diabetes can go unnoticed over a long period of time, because its moderate hyperglycemia is often not noticed, causing no classical symptoms. Notably, in spite of its lazy manifestation, this condition poses high risk to both macrovascular and microvascular diabetic complications [35, 37].

The large percentage of the people by means of this kind of diabetes are obese and this is a metabolic condition that directly leads to the pathogenesis and worsening of insulin resistance [38, 39]. There is a large group of patients that fall below the traditional anthropometric definitions of obesity but still have increased adiposity, especially the visceral fat distribution including abdominal area [40]. Diabetic ketoacidosis (DKA) does not occur normally in this particular form of diabetes

and the majority of the episodes of DKA are triggered by acute physiologic stressors, especially infectious diseases [41, 42]. Even though people with this type of diabetes could have circulating insulin levels in the normal or even high range, their sustained hyperglycemia proves relative insulin deficiency, as they have an insufficient 82cell secretory response to elevated blood glucose concentrations [43].

The most common metabolic disturbance is the defect in insulin secretion which is not sufficient to overcome the existing insulin resistance, representing a dual deficiency in -cell functionality and peripheral glucose uptake. Conversely, there is a clearly defined group of individuals who have maintained insulin sensitivity but severe α-cell dysfunction, representing an isolated secretory defect. Although therapeutic intervention, consisting of adipose tissue decreased, increased physical activity, and glucose-lowering pharmacotherapy, can partially correct the insulin resistance syndrome, full recovery of normoglycemic metabolic homeostasis is infrequent in the established disease [44, 45]. *Diabetes mellitus* of Type II has been demonstrated to positively correlate with increasing age, high body mass index, as well as a sedentary lifestyle pattern [46, 47].

The epidemiology of this condition is characterized by increased prevalence in women who had gestational *Diabetes mellitus* (GDM) and in people with metabolic comorbidities such as hypertension, and dyslipidemia. There is great epidemiologic diversity among racial and ethnic groups, which is indicative of intricate relations between genes and the environment [46–49].

This disease illustrates a major heritable element, and compelling data have been provided that a polygenic susceptibility is common and often presents itself as a family aggregation of cases [48–50].

2.1.1.3 Gestational Hyperglycemia and Diabetes

Gestational *Diabetes mellitus* (GDM) is abnormal glucose metabolism of widely varying degree of intensity with onset or first identification during pregnancy. This diagnostic category does not change, based on:(1) the need for insulin treatment,

or (2) the possible occurrence of glucose metabolism derangements after pregnancy. Significantly, the definition does not exclude the presence of previously unknow subclinical diabetes and prediabetes subtypes or subtypes of overt T2DM preceding pregnancy.

Females with known diabetes are classified as having 'pregestational diabetes in pregnancy' rather than GDM. These women need to have diabetes addressed throughout the entire perinatal period - preconception, antenatal andpostnatal care.

During pregnancy (1st and beginning of 2nd trimester), there is a physiological decrease in fasting and postprandial glucose levels relative to non pregnant reference rangevalues. Increased plasma glucose concentrations at this early gestational age may imply pre existing diabetes, where evidence based thresholds for the diagnosis of abnormal glycemia in earlygestation have not been clearly defined [23].

2.1.2 Other Specific Types with Their Causes

2.1.2.1 Genetic Defects of Beta-cell Function

Unigenic defects in beta-cell physiology may be depicted in various types of the diabetic state, usually presenting with mild hyperglycaemia at a young age (typically less than 25 years). They are generally transmissible autosomal dominant fashion. These patients, previously denominated as having maturity onset diabetes of the young (MODY), exhibit defective insulin release and limited or no insulin resistance [51, 52].

Monogenic diabetes, as current studies show, stems from pathogenic variants occurring at three different genomic locations. The dominantly prevalent of these, illustrating for approximately 70% of cases, involves mutations to the HNF1α gene (that's hepatocyte nuclear factor 1-alpha). You'll find that gene on chromosome 12q24.31, and it's vital for how pancreatic α-cells develop and secrete insulin. This transcription factor is very important for development [53].

Now, when we discuss genetic factors, it's worth noting a specific subtype tied to variations, pathogenic ones at that, in the GCK gene. The gene, encoding glucokinase, is found on chromosome 7p13. This particular genetic arrangement has important implications to consider [54, 55].

Glucokinase helps turn glucose into glucose-6-phosphate, which then gets metabolized. This process enhances insulin release from pancreatic beta cells. So, glucokinase serves as the primary glucose sensor in these cells. However, mutations in the glucokinase gene can disrupt this function. When this occurs, higher glucose levels are required to achieve a normal insulin response. Additionally, a variation in the HNF4α gene, located on chromosome 20q, can also impact insulin release [56].

HNF4α operates as a transcription factor, and it is key factor in controlling how HNF1α gets expressed. Recent findings regarding genetic variants indicate that mutations in the IPF-1 gene, which is a transcription factor, may play a significant role. In cases where this mutation is homozygous, it can lead to a complete absence of the pancreas [57].

Scientists are currently investigating specific genetic differences among individuals who exhibit similar medical symptoms. Notably, alterations like missense mutations in mitochondrial DNA have been identified as potential causes of both diabetes and hearing loss concurrently [58]. The primary mutation is located at nucleotide 3243 in the mitochondrial tRNA gene for Leucine, where an adenine-to-guanine transition occurs. This molecular change is commonly associated with MELAS syndrome, abbreviated for Mitochondrial Encephalomyopathy, Lactic Acidosis, and Stroke-like episodes.

Interestingly, *Diabetes mellitus* is not present in this condition. This absence suggests different pathways or specific vulnerabilities in tissues, contributing to the distinct symptoms of this genetic variation [59]. Sometimes, families possess genetic traits that hinder the proper conversion of proinsulin into insulin. These traits often follow an autosomal dominant inheritance pattern, and the carbohydrate intolerance that results is generally manageable, representing a minor

challenge [60, 61]. Additionally, some families may have mutant insulin molecules that do not bind to the receptor as effectively as intended. This intriguing phenomenon is linked to autosomal transmission and can involve either stable or slightly abnormal carbohydrate metabolism [62, 63].

2.1.2.2 Genetic Defects in Insulin Action

Heritable variations can interfere with insulin function and impact metabolism. The consequences of these mutations can range widely, from increased insulin levels with only slight rises in blood sugar to the onset of symptomatic diabetes. In all instances, they typically leave a noticeable impact [64, 65]. Acanthosis nigricans is a dermatological issue observed in some individuals with these genetic variations. In females, symptoms may also include virilization and over-sized, cystic ovaries. This syndrome was previously referred to as Type A insulin resistance [64].

Both leprechaunism and Rabson-Mendenhall syndrome are two types of juvenile syndromes that have altered the insulin receptor gene, with resultant changes in insulin receptor functionality. Furthermore, they are associated with profound levels of insulin tolerance [65] The first demonstrates unique facial characteristics while the latter is characterized by anormalities in teeth, nails, and pineal gland hyperplasia.

2.1.2.3 Diseases of the Exocrine Pancreas

Diabetes can result from damage to the pancreas. Conditions that predispose to this outcome are pancreatitis, trauma, and infections. It is also imbalanced blood sugar levels in the shadow of pancreatic carcinoma or post-pancreatectomy. When the pancreas is compromised, overt diabetes may develop [66, 67]. Diabetes will not manifest unless there has been significant damage to the pancreas. And yet, tiny adenocarcinomas, just minor disturbances in the pancreatic environment, can cause diabetes. This suggests a complex mechanism that involves more than just the simple loss of α-cell mass [68].

Cystic fibrosis and haemochromatosis destroy the beta cells of insulin secretion and reduce the amount of insulin that is actually secreted [69, 70].

Radiation of abdominal cramps to the back, pancreatic calcifications seen on X-ray and ductal dilatation are what FCP will typically present with [71] ketoacidosis-tolerance in fibro-calculous-pancreatic-diabetes.

Autopsy shows pancreatic fibrosis and calcified stones blocking exocrine ducts. Endocrinopathies take the main stage of this hormonal play. Growth hormone, cortisol, glucagon, and epinephrine are insulin antagonists. Over secretion of these hormones results in a diabetes battle. Conditions of acromegaly, Cushing's syndrome, glucagonoma, and phaeochromocytoma drive into the limelight creating turmoil in glucose homeostasis [72].

When the overproduction of hormones is brought under control, high blood sugar levels typically resolve. Tumors such as somatostaminomas and aldosteronomas may cause diabetes.

They do this by damaging insulin secretion to a degree and thus also contribute to patients having persistently elevated blood sugar levels [73, 74]. Hyperglycaemia generally resolves following successful elemination of the tumor.

2.1.2.4 Drug or Chemical-induced Diabetes

Certain medications can interfere with insulin's function in the body. While these drugs may not lead to a diabetes diagnosis, they can certainly contribute to insulin resistance [75, 76]. The classification of these conditions often lacks clarity, leaving us questioning whether it's beta-cell dysfunction or insulin resistance. Additionally, substances like Vacor, a common rodenticide, and pentamidine can severely damage pancreatic beta cells, resulting in lasting effects [77–79].

Fortunately, such adverse reactions are quite rare. However, various medications and hormones can disrupt insulin's effectiveness, including nicotinic acid and glucocorticoids, which can alter how insulin functions [75, 76].

2.1.3 Prevalence

In the field of diabetes, the latest statistics are striking: over 500 million people globally are living with this condition, with the elderly population significantly impacted. Projections indicate a dramatic increase, with Africa expected to see a 134% rise, South-East Asia a 68% increase, and Europe a steady climb of 13%. In the United States, diabetes affects 37 million individuals, representing 11.3% of the population. In Australia, approximately one in twenty people, or about 1.3 million individuals, are managing diabetes.

China has the highest number of cases, with an astonishing 141 million people living with diabetes. Additionally, around 283,000 Americans under the age of 20 are facing this challenge, and the U.S. sees approximately 1.4 million new diagnoses each year [80].

Globally, about 463 million adults are living with diabetes, with a significant 90% diagnosed with T2DM. According to "The News," Pakistan ranks third in diabetes prevalence worldwide, following China and India. The rates in Pakistan show a concerning trend, rising from 11.77% in 2016 to 16.98% in 2018, and peaking at 17.1% in 2019

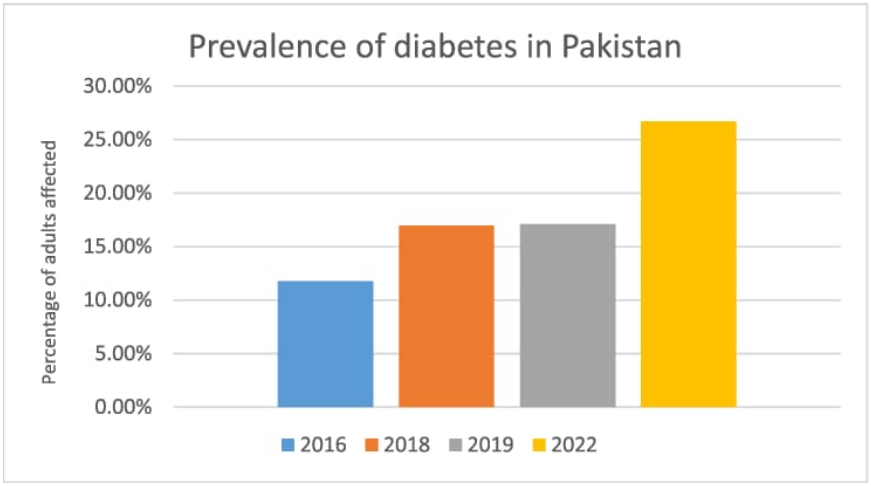

FIGURE 2.1: Prevalence of diabetes in Pakistan.

The International Diabetes Federation's 2022 report indicates a diabetes incidence of 26.7% among adults in Pakistan, equating to around 33 million cases.

This figure 2.1 is not only alarmingly high but also continues to rise each year. Unfortunately, many individuals remain undiagnosed, which exacerbates the true prevalence and the risks associated with untreated diabetes complications [81].

The graph had depicted the prevalence of diabetes. In 2016, approximately 11.7% of adults were affected by diabetes. The prevalence rose to around 16.9% in 2018 and similar in 2019 art about 17.1%. By 2022, the percentage of affected adults significantly increased to approximately 28%. [80]

Consider this situation, approximately 537 million people aged 20 to 79 are living with diabetes. This represents a significant 10.5% of the global population in this age group. Looking forward, projections indicate that by 2045, the prevalence of diabetes could rise to over 12% worldwide [80].

2.1.3.1 Prevalence of Diabetes in Pakistan

According to the International Diabetes Federation, the prevalence of diabetes in Pakistan has reached an estimated 34.5 million individuals in 2024, predominantly among those aged 20 to 70 years. Alarmingly, this figure is projected to rise to 70.2 million by 2050 [82]. The actual burden is likely even higher, as a considerable proportion of cases remain undiagnosed, thereby increasing both the true prevalence and the risk of severe complications in the absence of timely treatment.

The World Health Organization (WHO) reported that diabetes was the leading cause of mortality in 2019, accounting for approximately 1.5 million deaths worldwide [83]. With the disease disproportionately affecting low- and middle-income countries, Pakistan remains particularly vulnerable to diabetes-related morbidity and mortality.

Several risk factors predispose individuals, especially adults, to the development of diabetes, most notably genetic susceptibility and lifestyle modifications. These include obesity, physical inactivity, and the excessive consumption of processed foods with high sugar content. Based on WHO Asia-Pacific cut-off parameters, the overall weighted prevalence of generalized obesity in Pakistan was found to be

57.9% (42% in males and 58% in females), while central obesity was recorded at 73.1% (37.3% in males and 62.7% in females) [84]. The widespread availability of processed foods, combined with insufficient physical activity, also places children at increasing risk of developing diabetes in the future.

Furthermore, the incidence of diabetes is markedly higher in urban areas (15.1%) compared to rural regions (1.6%) [85]. This urban–rural disparity, compounded by the ongoing migration from rural to urban areas and subsequent adoption of sedentary urban lifestyles, underscores the urgency of addressing this escalating public health crisis.

2.1.4 Role of Modern Medicines in Managing Diabetes

A recent study revealed that the treatment landscape for *Diabetes mellitus* revolved around one key aim: normalizing plasma glucose levels. During this era, a repertoire of six essential medication categories and two injectable classes was widely adopted to keep blood sugar in check. This lineup featured tablet-form biguanides, sulfonylureas, thiazolidinediones, and alpha-glucosidase inhibitors [86].

2.1.4.1 Oral Drugs

When addressing the complex issues of metabolic challenges such as insulin resistance or inadequate insulin production, oral medications are utilized to manage these conditions. These treatments are most efficient when taken simultaneously along with a balanced diet and regular exercise [87].

2.1.4.2 Sulfonylureas

Sulfonylureas (refer to Figure 2.2) have become essential in enhancing the body's insulin production. However, some users have experienced weight gain early in their treatment. Additionally, a few individuals have reported allergic reactions related to sulfonylurea use. On the other hand, metformin, a long-established

medication, effectively lowers blood sugar levels by reducing endogenous glucose production. Nevertheless, individuals with diabetes often face challenges when prescribed metformin, as it can lead to a condition known as acidosis, characterized by an excess of acid in the bloodstream.

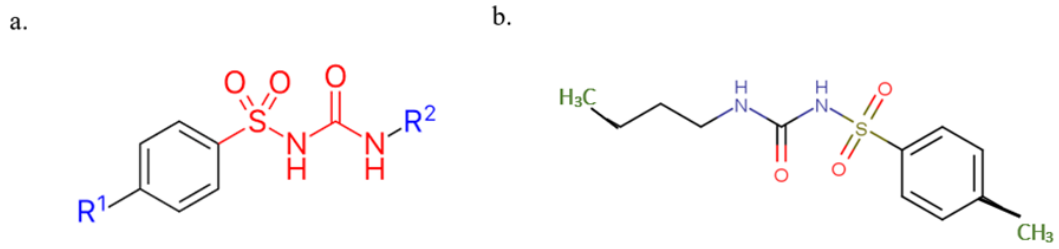

FIGURE 2.2: (a) The side chains that differentiate sulfonylurea compounds are indicated in blue, and the sulfonylurea backbone is highlighted in red in figure of the fundamental structure of sulfonylureas. (b) The methyl group (R1) and butane chain (R2) of tolbutamide, a sulfonylurea medication, are both shown in green

Symptoms can include nausea, circulatory shock, or difficulty breathing. Due to these risks, metformin is generally less preferred for patients with impaired kidney function, reduced cardiac performance, or a history of alcohol abuse [87].

2.1.4.3 Gliflozins

Gliflozins, effective agents in glucose management, include dapagliflozin, empagliflozin, and canagliflozin. These medications enhance urinary sugar excretion, which aids in lowering blood sugar levels. On the other hand, the gliflozins may be associated with side effects such as vaginal thrush and an increased risk of acidosis, which can lead to complications from excessive blood acidity.

In the past, alpha-glucosidase inhibitors were prominent in the cure of T2DM. While they are no longer the primary choice, these medications work by slowing glucose absorption in the gastrointestinal tract, with acarbose being the most frequently prescribed option. However, acarbose has limitations, as it does not significantly reduce blood sugar levels compared to other available treatments [87].

2.1.5 Metformin

Metformin (Figure 2.3) stands out as the primary treatment for Type 2 *Diabetes mellitus* (T2DM). This effective medication surpasses other oral options due to its impressive performance. Its benefits include modifying gut microbiota and activating mucosal AMP-activated protein kinase (AMPK), which plays a pivotal part in maintaining the integrity of our intestinal barrier [88].

Extensive research reveals several mechanisms through which metformin inhibits gluconeogenesis. By blocking mitochondrial glycerol phosphate dehydrogenase and nicotinamide adenine dinucleotide (NADH) coenzyme Q oxidoreductase in the mitochondrial electron transport chain (MET), metformin shifts the balance, leading to an increased AMP/ATP ratio that activates AMPK. It also engages liver kinase B1 to stimulate hepatic AMPK.

Generally, metformin is a reliable option for diabetes management. However, some individuals may have mild gastrointestinal side effects [88].

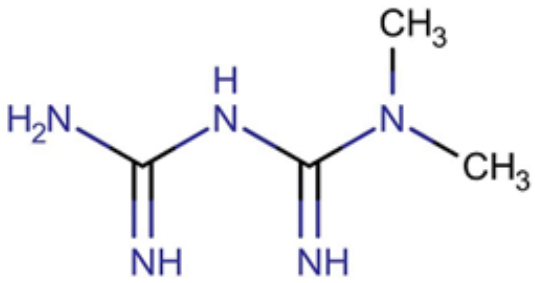

FIGURE 2.3: The chemical structure of metformin

2.1.5.1 Thiazolidinediones: Insulin Sensitivity Enhancers

Thiazolidinediones (TZD) (Figure 2.4) emerge as key players in enhancing insulin sensitivity. By acting as effective inhibitors for nuclear peroxisome proliferator-activated receptor-gamma (PPAR-α), they help orchestrate metabolic balance. These PPARs are crucial in regulating genes associated with fat development and insulin signaling, influencing muscle, adipose tissue, and liver function.

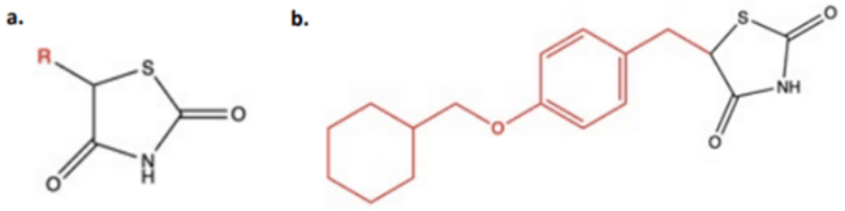

FIGURE 2.4: (a) This diagram shows the general structure of thiazolidinediones, with the backbone shown in black and side chain highlighted in red. (b) Ciglitazone is example of thiazolidinedione medication [89]

TZDs influence fat and carbohydrate metabolism by binding to PPARs. This process improves glucose uptake while carefully decreasing glucose production [88]. However, it is important to acknowledge that two prevalent adverse influences may include liquid retention and obesity [89].

2.1.5.2 Biguanides

Phenformin, buformin, and metformin are the three biguanides that are used to treat diabetes. Because of their link to lactic acidosis, the first two named were no longer used in the United States of America [90]. Metformin, derived from *Galega officinalis L.*, also known as French lilac, originates from galegine, a guanidine derivative found in this perennial herb.

Galega officinalis has been recognized for centuries for its ability to alleviate diabetes symptoms. Metformin successfully completed clinical trials in 1995 and was subsequently approved for use in the United States. While the exact mode of action of biguanides, such as metformin, remains unclear, they do not require the existence of functional pancreatic beta cells in order to lower blood glucose levels.

Reduced plasma glucagon levels, hepatic gluconeogenesis, gastrointestinal tract slowdown, enterocyte improvement of glucose to lactate conversion, direct stimulation of glycolysis in tissues, and enhanced elimination of glucose from the bloodstream are some of the hypothesised mechanisms of action [90]. Patients with insulin-resistant hyperglycemia and persistent obesity are frequently given biguanides. Known for its ability to preserve insulin, metformin has an advantage

over sulfonylureas and insulin in that it does not cause hypoglycemia or encourage weight gain. Metformin's GI tract adverse impacts are the most prevalent, and lactic acidosis is a possible side effect [90].

2.1.5.3 Meglitinides

A new class of insulin secretagogues is represented by meglitinides (figure 2.5). First approved by the FDA for clinical use in 1998, repaglinide is the first drug in this category. By affecting potassium efflux through potassium channels, these drugs regulate the release of insulin from beta cells. Meglitinides share molecular binding sites with sulfonylureas, with two sites in common and one distinct site. However, unlike sulfonylureas, meglitinides do not directly affect insulin exocytosis [90].

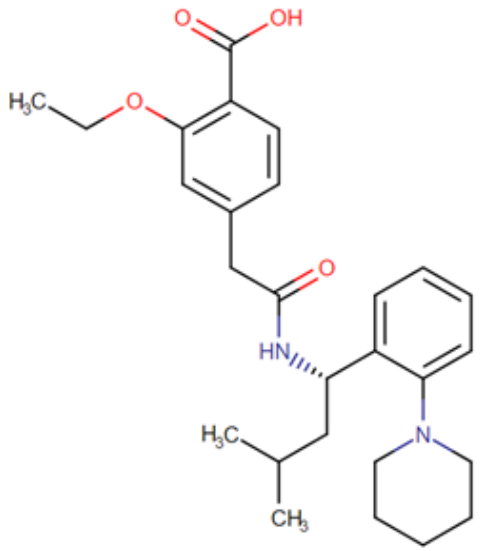

FIGURE 2.5: Chemical structure of the Meglitinide repaglinide [90]

2.1.5.4 Injectable Drugs

Additionally, there were two types of injectable drugs used for diabetes management in the past: incretin mimetics and insulin [86]. Incretin mimetics, which resembled hormones, were administered by injection in conjunction with metformin and/or sulfonylurea tablets, rather than as a replacement for oral antidiabetic

tablets. These injectable drugs were delivered beneath the skin using pre-filled pens and stimulated the pancreas to increase insulin production. Nausea and vomiting are possible side effects of incretin mimetics, including liraglutide, dulaglutide, lixisenatide, exenatide, and albiglutide. Additionally, blood pressure lowering drugs (antihypertensives), less dosage of acetylsalicylic acid (the active ingredient in medications like Aspirin) to prevent blood clot formation, and statins to lower cholesterol levels were among the drugs intended to lower the risk of cardiovascular diseases [91].

2.1.5.5 Lifestyle Change

While medications provide valuable support, lifestyle changes play a crucial role in managing diabetes. Adopting a healthier diet and introducing regular physical activity into your routine are essential steps toward achieving optimal health outcomes alongside medical treatments.

Factors such as blood pressure, weight management, and blood glucose levels are significantly influenced by our dietary choices. The merits of exercise and workout are countless; it enhances insulin sensitivity, improves glycemic control, regulates blood pressure and lipid levels, promotes weight loss, and strengthens cardiovascular health [88].

2.1.5.6 Biological Activity of α- & α-Glucosidase Inhibitors

Recent research has revealed a wealth of alpha-glucosidase inhibitors derived from natural sources, particularly plants. A range of promising compounds has surfaced, including secondary metabolites such as phenols, terpenoids, alkaloids, and flavonoids. The role of triglycosides in metabolic processes is increasingly recognized, especially in the production of glycoproteins and glycolipids, as well as in carbohydrate digestion. Glucosidases are emerging as a significant pharmaceutical target; these enzymes break down the glycosidic bonds, secreting glucose from the non-reducing end of oligo or polysaccharide chains, which is essential for glycoprotein synthesis.

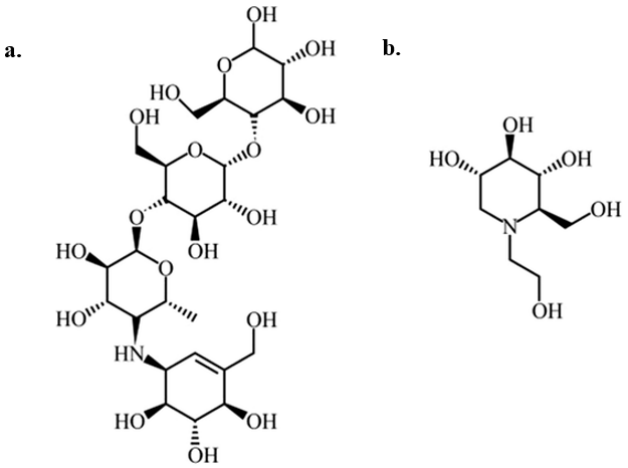

FIGURE 2.6: Chemical structures of anti-diabetic medications: (a) acarbose, (b) miglitol

Research is emerging around glucosidase inhibitors as potential treatments for lysosomal storage disorders, diabetes, HIV, and even metastatic cancer, highlighting their significant therapeutic potential. Furthermore, these inhibitors can clarify biochemical pathways and shed light on the complex structure-activity relationships necessary to understand an enzyme's transition state. Various types of glucosidase inhibitors, including disaccharides, amino sugars, carbasugars, thiosugars, and non-sugar derivatives, have garnered considerable interest. The primary objective of the study was to present the main classes of glucosidase inhibitors and their biological effects on α- and α-glucosidases [92].

2.1.6 T2DM Prevention- Glucose Metabolism

2.1.6.1 Metabolism of Glucose

Emerging research is showcasing glucosidase inhibitors as potential treatments for lysosomal storage disorders, diabetes, HIV, and even metastatic cancer, highlighting their important therapeutic possibilities. These inhibitors also help clarify biochemical pathways and provide insights into the complex structure-activity relationships needed to understand an enzyme's transition state. Different types of glucosidase inhibitors, such as disaccharides, amino sugars, carbasugars, thiosugars, and non-sugar derivatives, have gained significant attention [93].

In the intricate performance of metabolism, glycolysis stands out as a key player. This catabolic pathway skillfully transforms glucose into ATP, the essential energy currency for our cells [94].

TABLE 2.1: The metabolic cascade influencing blood glucose level [95]

Phenomenon	**Explanation**	**Glucose Level**	**Organ**
Glycolysis	When glucose molecules disrupt, two three carbon atoms are produced (pyruvate).	↓ glucose	Liver
Gluconeogenesis	From non-carbohydrate and carbohydrate precursors, new glucose molecules are formed.	↑ glucose	Liver
Glycogenolysis	When glucose is broken down from glycogen,	↑ glucose	Kidney & Liver
Glycogenesis	Glycogen synthesis involves the insertion of glucose molecules to chains of glycogen.	↓ glucose	Muscle & Liver

2.1.7 Insulin and the Regulation of Blood Sugar Levels

Located within the pancreatic islets of Langerhans, the α-cells are key players in our body's glucose regulation. These dedicated cells produce insulin, a crucial hormone for maintaining glucose balance (see Figure 2.7). Insulin promotes the entry of glucose into cells and regulates the metabolism of complex biomolecules. The production of insulin is influenced by fluctuating glucose levels.

A variety of hormones, including growth hormone and estrogens, can also impact insulin release [96]. When glucose levels increase, the pancreatic beta-cells respond by insulin secretion, which encourages glucose uptake while reducing its production [97]. Insulin binds to specific receptors in muscle, liver, and fat tissues, triggering a series of phosphorylation events that promote the movement of glucose transporters (GLUT) to cell membranes. This phenomenon effectively lowers blood glucose levels and enhances cellular glucose uptake.

However, type 2 *Diabetes mellitus* introduces a challenge of insulin resistance. This condition prevents the liver and skeletal muscles from responding adequately to insulin, impeding glucose absorption and increasing gluconeogenesis in the liver [98].

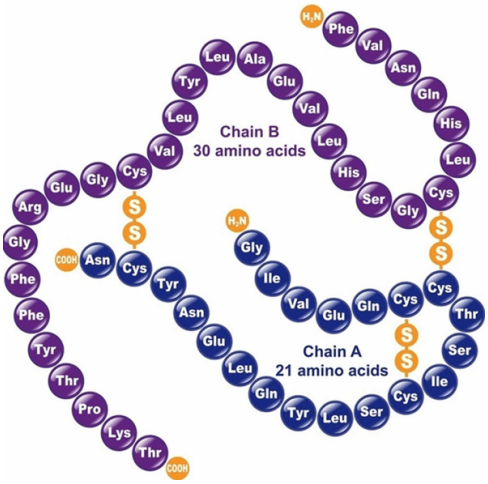

FIGURE 2.7: The chemical structure of Insulin

Insulin, secreted by the diligent beta cells, plays a pivotal part in mediating glucose levels in muscles and the liver. It facilitates the uptake of glucose into cells and converts it into glycogen through glycogenesis, effectively reducing glucose concentrations. At the same time, insulin inhibits gluconeogenesis, the production of glucose from internal stores, ensuring balanced glucose management.

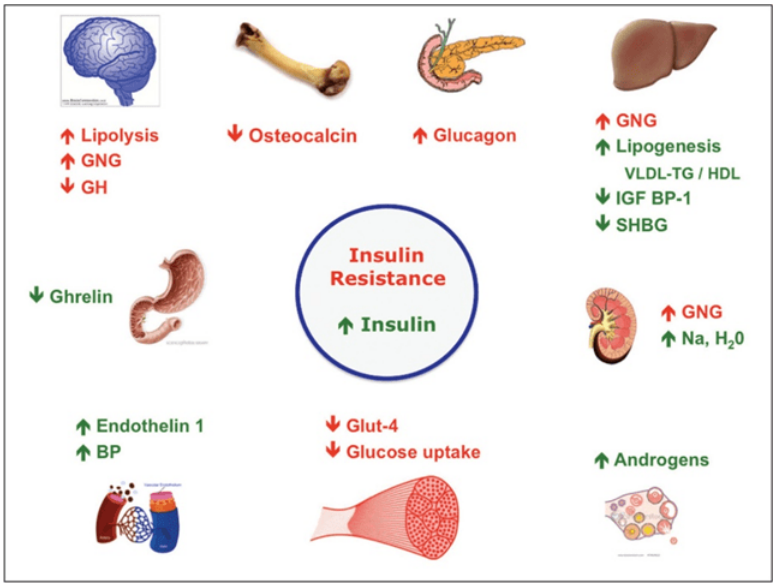

FIGURE 2.8: Showing the workflow of insulin resistance within the human body [99]

Pancreatic hormones prompt GLUT4 transporters to migrate from the interior of cells to their surface. This swift translocation facilitates efficient glucose storage in muscle and fat cells, executing their insulin-dependent function (refer to Fig. 2.8). Unfortunately, insulin resistance often emerges in the progression of T2DM, featured by impairments in glucose uptake mechanisms [9].

2.1.8 Insulin Signaling Pathways

The intricate mechanisms of insulin function are revealed through a complex network of signaling pathways. Various phytochemicals, including alkaloids, flavonoids, and terpenoids, play active roles in triggering different insulin signaling routes (refer to Fig. 2.10) [40].

Insulin receptors, consisting of two beta subunits that bind insulin and two with tyrosine kinase activity, serve as pivotal components in this sophisticated process. Upon insulin binding, a structural change occurs, amplifying kinase activity and activating ATP and substrate-binding sites. This sets off a precisely orchestrated cascade of interactions with intracellular molecules, such as insulin receptor substrate (IRS-1) [41].

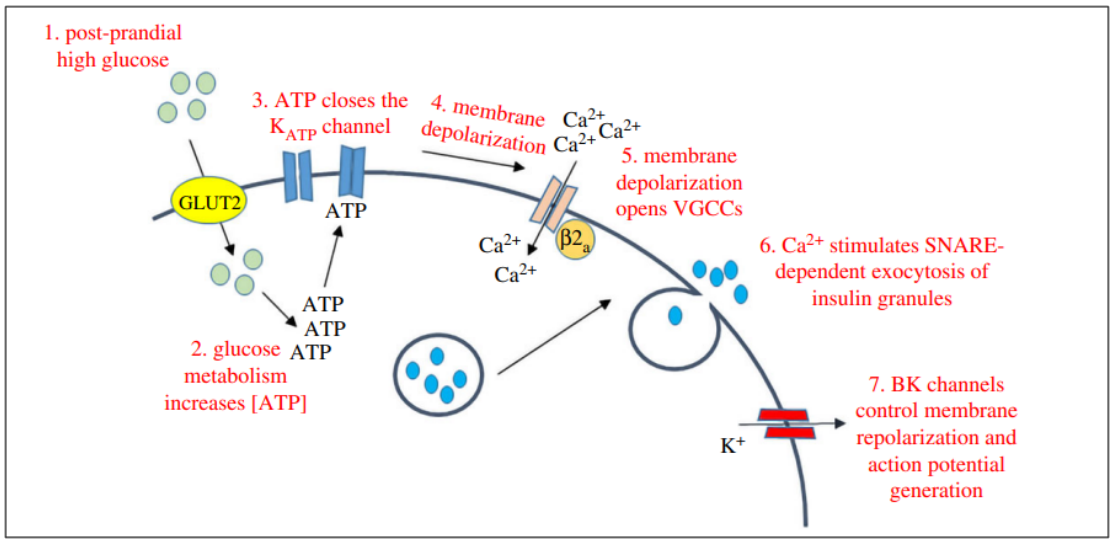

FIGURE 2.9: Shows glucose induced insulin secretion in pancreatic α-cells [100]

Upon activation, IRS-1 triggers a remarkable cascade of signaling events, recruiting kinases such as phosphoinositide 3-kinase (PI3K) and protein kinase B

(PKB/AkT). AkT, a serine/threonine kinase, plays a pivotal role in insulin signaling, moving to the cell membrane and initiating a series of phosphorylation events that enhance insulin signaling processes [101].

Furthermore, peroxisome proliferator-activated receptors (PPARs), essential transcription factors, regulate lipid and glucose metabolism in pancreatic beta cells, coordinating the critical function of insulin secretion [102].

2.1.8.1 Insulin Secretion

Insulin is produced by pancreatic beta-cells at a baseline rate and at significantly higher rates in response to glucose and other stimuli. Elevated blood glucose levels cause cells' levels of adenosine triphosphate (ATP) to rise, which inhibits ATP-dependent potassium channels. This closure results in a decrease in out-ward potassium current, depolarizing the beta-cell and activation of calcium channels. Hormone release is triggered by the subsequent increase in intracellular calcium levels. Insulin, also known as glutathione insulin transhydrogenase, is mainly responsible for removing insulin from the bloodstream through the liver and kidneys.

It is thought that hydrolyzation of the disulfide bond between the A and B chains is taking place here. Proteolysis is used to carry out further degradation after this decrease. Because the liver is the primary target for blood flow from the portal vein, it normally removes around 60% of the insulin generated by the pancreas, whereas the kidneys only remove 35-40% of the hormone. This distribution is changed in diabetic individuals getting subcutaneous insulin injections, since the liver removes no more than 30-40% of the exogenous insulin while the kidneys remove 60% of it. Insulin has a circulation half-life of around three to five minutes [90].

2.1.8.2 The Insulin Receptor

Insulin attaches to specific receptors on different cell membranes as it enters circulation. However, the biological consequences of these insulin-receptor complexes

have only been observed in specific target organs, such as muscle, adipose tissue, and liver.

With remarkable selectivity and affinity, the insulin receptors bind insulin at picomolar concentrations. Each complete insulin receptor consists of two heterodimeric units: the alpha subunit, which is completely extracellular and serves as the target region, and the α subunit, which crosses the membrane and comprises a tyrosine kinase domain. When insulin binds to the alpha subunit outside of the cell, it initiates tyrosine kinase activity in the beta subunit.

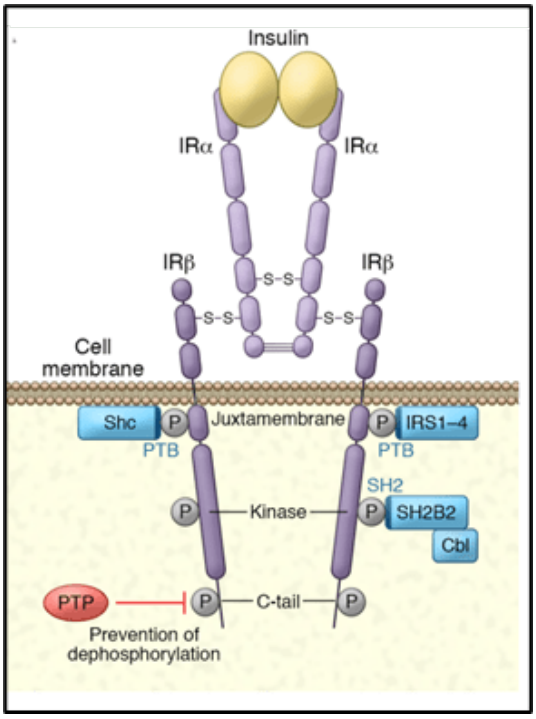

FIGURE 2.10: Structure of insulin receptor

Although the beta subunit's dimeric form can bind insulin, its affinity for doing so is much lower than that of the tetrameric form. The beta subunit's self-phosphorylation promotes the formation of beta heterodimers as well as the maintenance of the receptor tyrosine kinase's activated state. Insulin receptor concentration is lower in clinical situations including obesity and insulinoma that are marked by high circulating insulin levels. Target cells appear to use this natural process of downregulating insulin receptors to limit their responsiveness to high hormone concentrations [90].

2.1.8.3 Influence of Insulin on Its Targets

Insulin promotes the storage of fat and glucose inside certain target cells and has an impact on cell division and metabolic activities in a variety of organs.

2.1.8.4 Impact on Glucose Transporters

Insulin has a substantial influence on a number of transporters that help travel glucose across plasma membrane. Diabetes is linked to these transporters in both its onset and manifestation. Insulin releases GLUT 4, a crucial factor in lowering blood glucose levels, from storage membrane-bound sacs within the cell and inserts it into the membranes of muscle and fat cells. Deficits in the movement of glucose into pancreatic α-cells by GLUT 2 may also be a factor in the reduced insulin production seen in type II diabetes [90].

2.1.8.5 Impact on the Liver

When endogenous insulin reaches the portal circulation, it mostly affects the liver. Here, it plays a role in stimulating the storage of glucose as glycogen and reestablishing a fed state in the liver by inhibiting multiple catabolic processes, including ketogenesis and glycogenolysis.

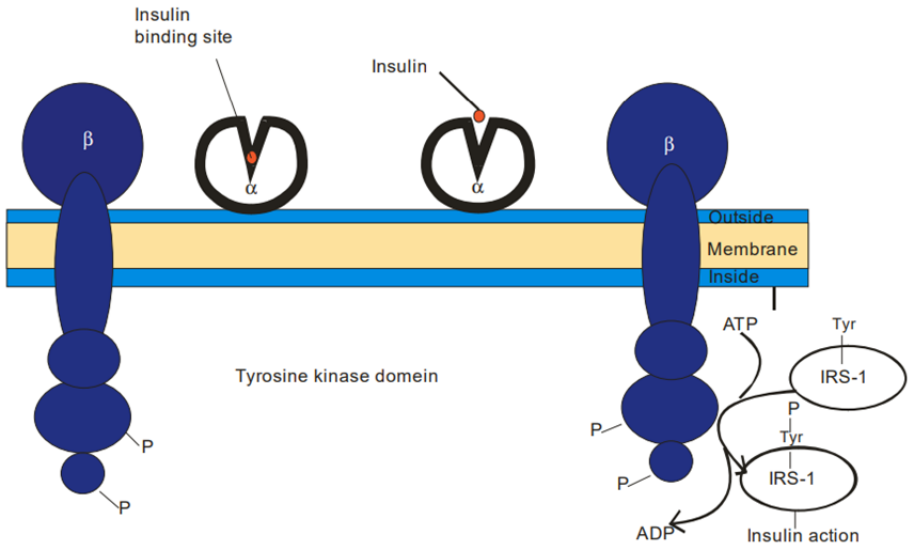

FIGURE 2.11: Schematic diagram of the probable structure of the insulin receptor tetramer in the activated state [90]

Insulin exerts its effects on the liver by directly inducing phosphorylation events. This activation enhances enzymes like pyruvate kinase, phosphofructokinase, and glucokinase, which promote glucose storage and utilization pathways. On the other hand, gluconeogenic enzymes that are normally active during the post-absorptive state such as fructose bisphosphatase, phosphoenolpyruvate carboxykinase, and pyruvate carboxylase are inhibited by insulin. Insulin directly induces phosphorylation processes, which impact the liver.

This activation increases the activity of enzymes such as phosphofructokinase, glucokinase, and pyruvate kinase that support the pathways involved in the storage and utilisation of glucose. Insulin, on the other hand, inhibits gluconeogenic enzymes that are typically active during the post-absorptive state, including pyruvate carboxylase, fructose bisphosphatase, and phosphoenolpyruvate carboxykinase. (Figure 2.11).

2.1.8.6 Impact on Muscle

Insulin increases amino acid transport and ribosome activity to promote protein synthesis. In order to restore glycogen reserves lost by muscular exercise, it also promotes the synthesis of new glycogen. Glycogen synthase is activated, glycogen phosphorylase is inhibited, and glucose transport into muscle cells is increased during this process [103].

2.1.8.7 Impact on Adipose Tissue

Through three main pathways, insulin decreases blood levels of unoccupied fatty acids and increases triglyceride storage in adipose tissues1. It triggers the strong hydrolysis of circulating lipoproteins to liberate triglycerides by activating lipoprotein lipase. 2. Insulin promotes the absorption of glucose within cells, leading to the metabolic byproduct of glycero-phosphate synthesis. This makes it easier to esterify the fatty acids produced by hydrolyzing lipoproteins. 3.Insulin decreases intracellular lipase activity, which in turn prevents stored triglycerides from being lipolyzed within cells [90].

2.1.9 Complications of Insulin Therapy

Oral hypoglycemic agents and insulin are central to diabetes treatment, effectively managing hyperglycemia. However, they are associated with significant side effects and do not substantially alter the progression of diabetic complications [103].

1. Hypoglycemia can be brought on by skipping meals, engaging in intense physical activity, or taking more insulin than is necessary at the moment. The primary autonomic warning signals of hypoglycemia and insulin excess are symptoms related to poor central nervous system function, which might include abnormal behaviour, disorientation, and possibly even coma. Regular insulin use can cause rapid-onset hypoglycemia, which can lead to autonomic hyperactivity. This hyperactivity can include sympathetic symptoms (tachycardia, palpitations, sweating, tremors) and parasympathetic symptoms (nausea, hunger). If left untreated, this hyperactivity can escalate to convulsions and coma.

2. Insulin allergy, immunological insulin resistance caused by the development of anti-insulin antibodies, and injection site lipodystrophy are among the immunopathological.

2.2 Morphological Attributes of *Abelmoschus esculentus* Okra Plant

Abelmoschus esculentus (L.) Moench (Okra) has a place to the family Malvaceae and it is a generally developed vegetables trim developed as a part of tropical and subtropical world. The study estimated the subjective attributes of 36 genotypes of okra and reported existence of significant differences among the genotypes for plant habit, stem color, leaf and flower traits, fruit traits and seed type.

The majority of genotypes had base very branched (50%) or all over (38.89%), with all showing erect growth. Color of stem was predominantly green with reddish (72.22%) with ruddy patches and of leaf green with ruddy veins (61.11%)

and green (38.89%). Leaf pubescence was mostly slight (86.11%) and leaf shapes observed were heart-shaped, broadly praise and palmately lobed. All genotypes had pink flowers on both surfaces with one exception. The young fruit color was predominantly green with ruddy check (55.56%) or green (41.67%) with most fruit erect (69.44%) and having ringed-protrude base (69.44%). Product Conformations to Nature: Product shapes were varied, and seed shapes were reniform (11.11%), circular (44.44%) and circular (44.44%). They indicate genetic variations influenced by both natural and developmental causes and raise the possibility of a trait that could be changed by selection or crossbreeding [13].

2.3 Therapeutic Properties

2.3.1 Antimicrobial Features

Pharmaceutical plants are valuable source for antimicrobial bioactive metabolites. Various infections may be treated with the wide arrange of medicinal plants extract due to their antimicrobial activity [104]. Phytochemical analysis of methanol extract of *A. esculentus* indicated the presence of phyto-constituents like alkaloids, saponins, cardenolides, anthraquinones and tennis. Antimicrobial potential of these plant metabolites has been reported. Therefore, the presence of these secondary metaboltes could be a reason for the antimicrobial potential of medicinal plants [105].

2.3.2 Anti-diabetic Effects

A study illustrated the antidiabetic exercises of *Abelmoschus esculentus* peel and seed powder (AEPP and AESP separately). The creator appeared that organization of AEPP and AESP in diabetic rats appeared significant decrease in blood glucose level and increment in body weight than diabetic control rats. A critical expanded level of Hb, TP, and diminished level of HbA1c, SGPT were watched after the treatment of both measurements of AEPP and AESP. Too, hoisted lipid

profile levels returned to approach typical in diabetic rats after the organization of AEPP and AESP, compared to diabetic control rats [106].

2.3.3 Impact on Gut

The effects of mucilage of *A. esculentus* at concentrations of 1g/kg and observed a significant inhibition of indomethacin induced ulcer. The test extricate pretreatment fundamentally expanded the complete amount of gastric fluid substance in ethanol-ulcerated rats. Cyto-protection may be due to formation of a protective film and increase in mucous output from the superficial epithelial cells [107].

2.3.4 Hepatoprotective Action

Explorers in the quest for knowledge ventured into the healing benefits of *Abelmoschus esculentus*, the okra, for liver diseases. They decided to step out on a limb with a daring proposition of whether an ethanolic extract of okra (EEO) could protect the liver from damage. The carbon tetrachloride (CCl_4) rat model of hepatotoxicity was used to investigate these effects. At 250 and 500 mg/kg body weight doses, EEO revealed remarkable dose-based protection against liver injury. It dramatically decreased the serum markers (ALT, AST, ALP, GGT), as well as cholesterol, triglycerides and MDA, which were elevated in CCl4-injected mice [108].

2.3.5 Immunomodulatory Impacts

In an in vitro consideration, the constitution of okra (*Abelmoschus esculentus*) extricates and explored the impact of *A. esculentus* polysaccharides (AE-PS) on the development and work of dendritic cells (DCs) determined from rodent bone marrow hematopoietic cells (BMHCs) was analyzed. BMHC-based juvenile DCs were isolated from rats and treated with AE-PS. AE-PS actuated the nearness of polymorphic nuclei and stretched bulge within the BMHC-based juvenile DCs, showing DC actuation. Treatment with AE-PS expanded the MHC class II and

CD80/86 expression levels by 41% and 42%, individually. Treated cells had diminished endocytosis action. The discharge of IL-12 and IFN-α expanded altogether by 120% and 75%, individually, when treated with of AE-PS. Additionally, IL-10 production was decreased by 66%. Therefore AE-PS shows stimulatory impacts on rodent dendritic cells and advances the discharge of TH1 cytokines [109].

2.4 Overall Phenolic Content

The phenolic composition of okra leaves displays a complex cluster of bioactive compounds that altogether contribute to their helpful properties, especially their antioxidant capacity. Comprehensive phytochemical investigations have distinguished differing classes of phenolic compounds in okra leaves, with outstanding concentrations of flavonoids, hydroxycinnamic corrosive subordinates, and procyanidins. Among the flavonoid constituents, quercetin and its glycosides (quercetin - 3 - O - glucoside, quercetin - 3 - O - rutinoside) prevail, nearby critical levels of kaempferol subordinates, myricetin, and luteolin. Hydroxycinnamic acids display incorporate chlorogenic acid, caffeic acid, p-coumaric acid, and ferulic acid, whereas tannin divisions comprise basically of epicatechin and procyanidin oligomers [110].

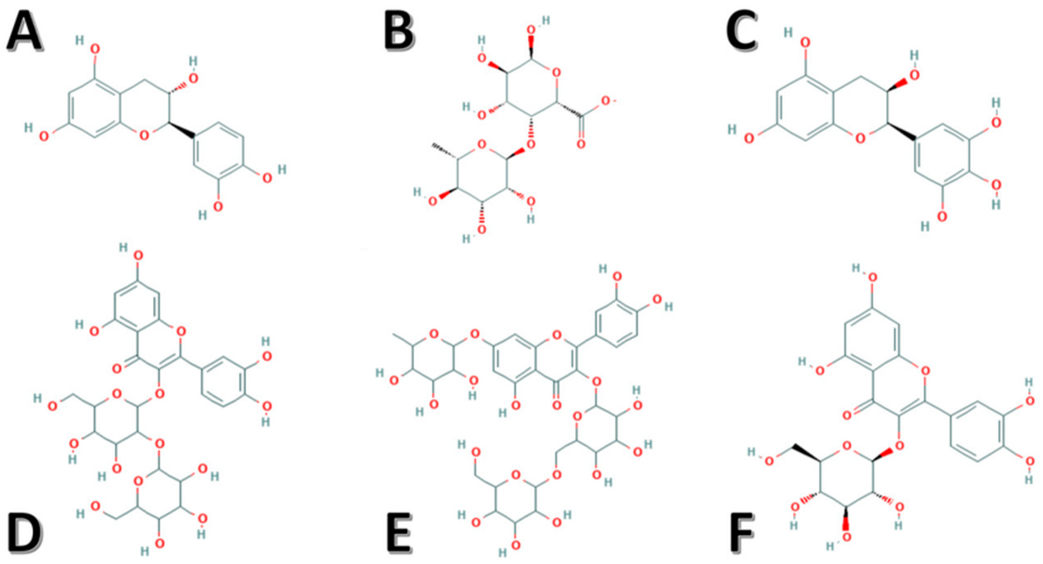

FIGURE 2.12: Chemical structures of potent bioactive compounds identified in okra *A. Catechin*, *B. Rhamnogalacturonan*, *C. Epigalalocatechin D. Quercetin* - 3 - 0 - sophosroide, *E. Quercetin* - 2 - 0 - [glucosy(1→ 6) glucoside] - 7 - 0 - rhamnoside and *F. isoquercitin*

Quantitative appraisals of add up to phenolic substance in okra clears out for the most part utilize the Folin-Ciocalteu measure, with comes about communicated as Gallic Acid Equivalents (GAE). Ponders reliably report considerable phenolic concentrations extending from 45-120 mg GAE/g dry weight, situating okra leaves among the wealthiest plant sources of phenolic compounds. This substance shows noteworthy variety impacted by numerous variables, counting cultivar hereditary qualities, development conditions, development arrange at collect, post-harvest dealing with, and extraction techniques. Agronomic hones, especially soil richness administration and water accessibility, illustrate significant effect on phenolic amassing, with direct push conditions regularly improving biosynthesis of these auxiliary metabolites as cautious reactions [111].

The leaves of *Abelmoschus esculentus* consisted of numerous naturally-occurring secondary metabolites. Lab-based anti-oxidant investigations have revealed that phenolic compounds can successfully rummage oxygen free radicals. The parts of enhancement divisions of column chromatography within the water extricates of *Abelmoschus esculentus* and its diverse parts explored more flavonoids, phenolic acids and other natural dynamic compounds. And these parts have the more grounded capacity on rummaging free radicals and decreasing control of Fe^{3+}. The anti-oxidant fundamental fixings in *Abelmoschus esculentus* ought to be flavonoids and phenolic acids. *Abelmoschus esculentus* has a noteworthy straight relationship between the antioxidant movement and of the adequacy and asset abuse of *Abelmoschus esculentus* L. substance of total flavonoids and total phenolic acids [112].

2.5 Chromatography and Separation Techniques

The fundamental idea behind chromatography is that when a mixture of molecules is placed onto a surface or solid medium, they separate as they are transported by a mobile phase as they interact with a stationary phase (fluid or stable phase). The process of separation is influenced by various molecule properties, including

adsorption (liquid-solid), partition, affinity, or differences in molecular weights [113, 114].

2.5.1 Thin Layer Chromatography

A form of "solid-liquid adsorption" chromatography is thin-layer chromatography (TLC). The solid adsorbent material that covers the glass plates makes up the fixed phase in this procedure. In TLC, you may also use common adsorbents like alumina, silica gel, and cellulose. The mobile phase travels in upward direction through the stationary phase, with capillary action causing the solvent to ascend the thin plate. This movement also transports the mixture, which was first administered to the plate's lower edge using a capillary tube, upwards at various flow rates, resulting in the separation of the analytes. The speed at which a material moves upward is determined by its polarity, the stationary phase, and the solvent [115].

To locate the position of colorless sample molecules on the chromatogram, fluorescence, radioactivity, or a particular chemical compound can be used to create a visible colored reactive product. Under ordinary or UV light, the visible color may be seen. By computing the ratio of the distance covered by the molecule to the distance covered by the solvent, the location of each molecule in the mixture is determined. The qualitative description of molecules uses this measure, termed relative mobility, which is represented by the Rf value. [116].

2.5.2 Column Chromatography

The total charge, size, form, stationary phase interaction, and binding potential of proteins are all unique features. Column chromatography is the most widely used chromatographic approach, and each of these characteristics can be employed for purification. This procedure is used to purify biomolecules. The eluent (mobile phase) is applied after the sample to be separated is initially placed to the column (stationary phase). The column material, which is placed on a fiberglass support,

guarantees the flow of these compounds, and the samples are collected at the bottom of the instrument in a manner that depends on both time and volume [117].

2.5.3 High-pressure Liquid Chromatography

Within a short amount of time, HPLC, a chromatographic method, allows for the purification and structural and functional analysis of a wide range of molecules. This approach is outstanding at separating and identifying amino acids, carbohydrates, lipids, nucleic acids, proteins, steroids, and other biologically active compounds. With a high flow rate of 0.1-5 cm/sec, the mobile phase in HPLC flows through columns at pressures between 10 and 400 atmospheres. HPLC's separation capacity is improved by using tiny particles and applying high pressure to the solvent flow rate, allowing analyses to be finished more quickly. A solvent reservoir, a high-pressure pump, a commercially available column, a detector, and a recorder are all necessary parts of an HPLC system. A computerized system regulates the length of the separation, and the substance is gathered in accordance with this [118].

2.6 Molecular Docking

The "molecular docking" anticipates the optimal ligand orientation with respect to the receptor (a protein) to form a stable compound. The degree of ligand-protein connection or binding affinity may be predicted by using scoring functions to prioritize orientation. To forecast the affinity and activity associated with a treatment, docking is frequently employed to ascertain the direction in which drug candidates may bind to protein targets. Because of this, docking is essential to the drug design and discovery process. Molecular docking aims to computationally simulate the molecular identification process and achieve an ideal conformation in order to lower the free energy of the system. It's quite hard to discover a new drug. In contemporary pharmaceutical development, the in-silico technique is the main

method employed. The use, acceptance, and value of computer-aided methods in the drug research and development process are expanding rapidly [119].

The most widely used technique for predicting ligand binding affinity and mechanism of action is protein-ligand docking. Protein-ligand docking is one successful approach for CADD. The blind docking web server CB-Dock is simple to use. It only needs the ligand file in the precise SDF format and the protein file in the PDB format in order to automatically forecast binding modes without knowing the binding locations. The sizes and centers of all of the N cavities are then determined by CB-Dock, which also predicts the protein's cavities. For docking, AutoDock Vina retrieves the pdbqt f iles of any size, via any center [120].

2.7 *In silico* Tools Used to Check the Sensitivity of IRS1

Chronic hyperglycemia is a hallmark of *diabetes mellitus*, a common metabolic disorder brought on by malfunctions in insulin production, insulin activity, or both. Plant extricates have for quite some time been examined for their capacity to change insulin pathways and proposition elective medicines. The study of these plant-derived substances has been transformed by the combination of bioinformatics and computational methods, allowing for extensive research and validation of their medicinal properties [121].

2.7.1 Retrieval of Sequence

The fundamental grouping of target proteins, like the Insulin Receptor Substrate (IRS), is basic for understanding how they work and communicate with remedial medications. These sequences are saved in the Protein Data Bank (PDB). Past examination have downloaded the IRS grouping in FASTA design from the PDB to help future examinations and demonstrating. Smith utilized the IRS arrangement got from PDBin 2020 to look at its primary and useful highlights, which supported

the recognizable proof of conceivable association locales for plant-based drugs [121].

2.7.2 ProtParam

Protein dependability and capability are exceptionally reliant upon their physicochemical characteristics. ProtParam is an internet-based device that predicts boundaries including hypothetical pI, sub-atomic weight, and how much charged buildups.

The IRS protein was studied using ProtParam by Johnson *et al.* (2019), which revealed its activity and potential interactions with chemicals derived from plants [122].

2.7.3 PDB

Knowledge of proteins' three-dimensional structure is necessary to comprehend how they interact with potential medical treatments. Template-based modeling and validation can benefit from the extensive structural data provided by the PDB.

The accuracy of molecular docking studies was improved as a result of the use of this data to estimate the IRS protein's three-dimensional structure [123].

2.7.4 PyMOL

PyMOL, a sub-atomic designs device, is ordinarily used to picture and dissect protein structures. It makes it possible for scientists to control molecules, make detailed photographs, and make animations.

Utilizing PyMOL, Thompson demon strated the interactions between IRS proteins and ligands derived from plants, assisting in the development of more potent therapeutics [124].

2.7.5 InterPro

InterPro is used to find the functional domains of the IRS protein. This web-based data set centers around monitored spaces associated with grouping and primary cooperations, uncovering utilitarian components of the protein that are basic to its job in insulin flagging and glucose digestion. researcher used this tool to refine the chemical structures of ligands, such as polyphenols and other active chemicals found in Momordica charantia plant extracts. These ligands were chosen for their ability to alter IRS protein activity and their pharmacological properties [125].

2.7.6 PkCSM

To guarantee an accurate structural representation, canonical smiles are retrieved from PubChem when necessary, loaded into ChemDraw, and then modified using ChemPro software. PkCSM is used to evaluate these plant-derived substances' ADME/T characteristics [126].

2.7.7 CB-Dock2

This apparatus approves that the chose compounds comply with Lipinski's Standard of Five, anticipating their pharmacokinetic highlights and conceivable restorative adequacy. For the purpose of determining the safety and effectiveness of plant extracts in the treatment of diabetes, it is essential to comprehend these characteristics. CB-Dock2 is utilized to perform sub-atomic docking, a computational methodology that predicts the limiting system and fondness of little particle ligands to protein targets. By automating the prediction and docking of binding sites using this online docking program, researchers can examine how plant-derived chemicals interact with the IRS protein. The creation of files for both the ligands and the target protein is the first step in molecular docking [127].

Chapter 3

Methodology

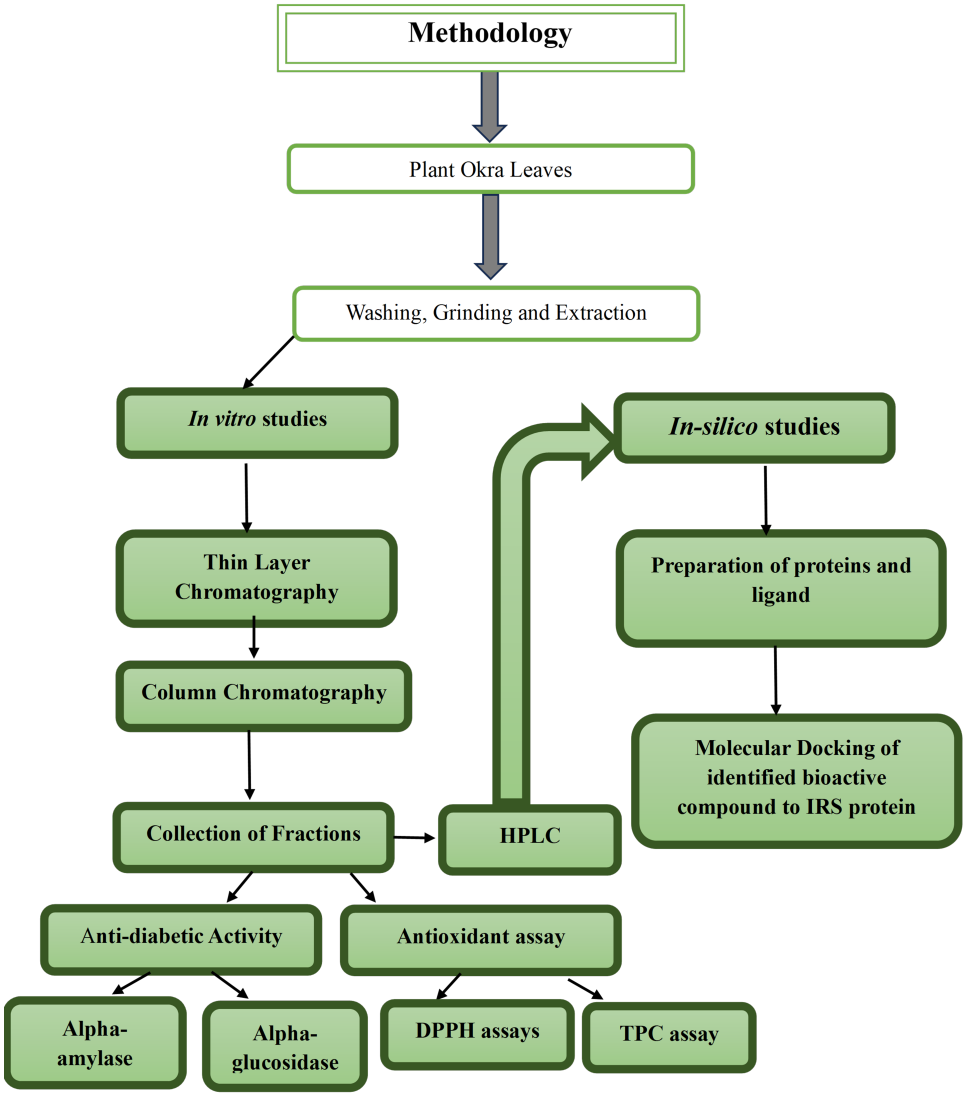

FIGURE 3.1: Overview of research methodology

3.1 Materials & Methods

3.1.1 Materials

3.1.1.1 Procurement of Raw Materials

The leaves of *Abelmoschus esculentus* obtained from the local markets of Rawalpindi and Islamabad. Methanol, Alpha-amylase, starch, 3, 5. Salicylic acid dinitro (DNSA), gallic acid, 2, 2 - diphenyl - 1 -1picrylhydrazyl reagent (DPPH), ethanol, sodium carbonate (Na2CO3), Folin-Ciocalteu reagent (FCR), chloroform, n-hexane, ethyl acetate, dichloromethane vanillin and sulfuric acid of analytical grade were procured from Sigma-Aldrich.

Spectrophotometer, weighing balance, water bath, microwave, pH meter, petri plate, beaker, conical flask, micropipette, columns, TLC plates, test tubes and test tube stand, aluminum foil, cotton, falcon tubes, funnel and filter paper, measuring cylinder, spatula

3.2 Methods

3.2.1 Washing & Drying of Medicinal Plant

The leaf extract method was adopted by following the procedure of S. Revathy *et al.*, [128] with slight modifications. Briefly, fresh leaves of the Abelmoschus esculentus were taken from the field and thoroughly washed with tap water. The leaves were cleaned and then permitted to desiccate for 15–17 days at ambient temperature. To get a uniformly colored powder, dried leaves were pulverized using a grinder. (Figure 3.2).

The methodology utilized for extract preparation as followed by S. Revathy *et al.*, [129] with a few changes. The grounded sample was taken in a beaker with the addition of solvent, and the beakers were placed at 25^{o}C for the 12-24 hours. Then

supernatants (extracts) were separated from the pellet after the centrifugation at 4000 rpm for 10 minutes. Up to the time of additional testing, extracts were kept at -4^{o}C, and each test was run in triplicate.

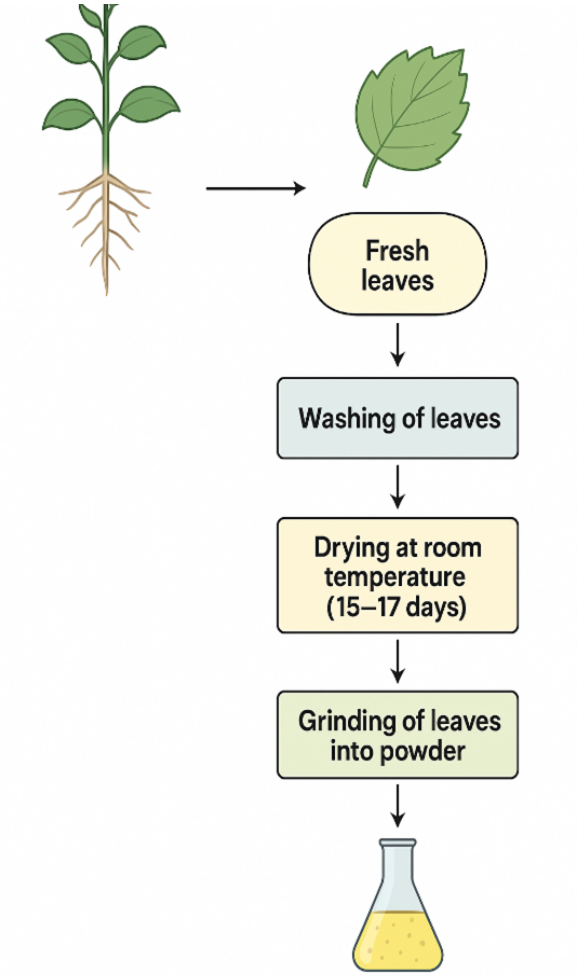

FIGURE 3.2: Sample collection and purification

3.3 Thin Layer Chromatography

TLC of okra leaf extract was performed to find the best solvent ratios after choosing the best solvent system as determined by *C. Hall, 2020* with little modifications. The TLC was performed according to the procedure mentioned in [122] with slight modifications. First of all, TLC plates were prepared after cutting them up to 5-7 cm, followed by marking of baseline by pencil about 1cm from the lower side of the plate. Then by capillary tube, stock solution of okra leaf sample was spotted on the baseline. Afterwards the TLC plates were placed in the

developing chamber containing the respective solvents [130]. In order to choose the best solvent combination system to proceed with the column chromatography, TLC were performed with different solvent systems and in different proportions as described in Table 3.1.

TABLE 3.1: The solvent system used to conduct Thin Layer Chromatography

Sr.	**Solvent System**	**Ratios/Proportions**
a.	n-hexane/ chloroform	9:01
b.	Chloroform/ Methanol	9:1, 30:1,15:1, 10:1, 20:1
c.	Dichloromethane/ Methanol	5:05
d.	n-hexane/ Ethyl-acetate	5:5, 10:1, 1:10

Compounds bands visualized on chromatoplate were further visually distinguished by the spray of vanillin-sulfuric acid reagent. The visualized banding pattern of the components in the chromatoplate were marked and the retardation factor value of each spot was assessed by the following equation:

$$Rf = \frac{distance\ travelled\ by\ the\ sample(cm)}{distance\ travelled\ by\ the\ solvent(cm)}$$

The solvent system which showed best value was used further for column chromatography. By following all the steps, column chromatography was initiated by having the solvent system with best TLC results.

3.4 Column Chromatography

Column chromatography was performed as described by C. Hall, 2020 [122] with few changes. A cylindrically-shaped glass column containing stationary phase silica gel was added gradually from the upper side with n-hexane/ethyl acetate (eluent) that passes through the column with the help of gravity. The purpose of this method is to separate substances from a mixture. The sample was introduced into the column from its top once it was prepared. The eluent was then permitted to pass through the column. Due to the distinct interaction between the stationary and mobile phases, the mixture's components will move from one phase to another

in the mobile phase over a period of time. This resulted in the separation of the mixture's constituents.

Later on, the different fractions that emerge from the column's lower side are gathered in individual tubes. During the careful separation of the mixture, each chemical was collected in separate test tubes as eluent. The excess solvent was permitted to evaporate after the pure production was collected.

The retention factor (i.e., polarity) of a substance in a given solvent system determines its elution rate [130].

3.4.1 Thin Layer Chromatography of the Column Chromatography Fractions

Each fraction is applied on activated TLC plates which were used for checking the purity of fractions by using different solvent systems.

Moving forward, the TLC plates consisting of fractions, with same distances traveled by the compounds, were mixed to proceed them as the major fractions. High performance liquid chromatography (HPLC) was used to further purify the TLC plate, which displayed the number of bands for each fraction [130].

3.5 Anti-oxidant Activity

3.5.1 Total Phenolic Compound Determination

TPC was calculated using the previously published spectrophotometric F-C reagent method with slight modification [131]. 270 μl of the methanolic extract and 1.36 ml of the 10% F-C reagent were added in the aluminum-foil-covered falcon tubes. After 5 minutes, 1.36 ml of 7.5% sodium carbonate was added, and the mixture was then mixed and permitted to sit at 45^{o}C in an incubator with distilled water for 30 minutes.

Experiment was performed in triplicates. The absorbance was determined with a spectro-photometer set at 765 nm. TPC was determined using gallic acid concentrations (0 – 120 ppm) as the standard and a calibrated curve (R2 = 0.895).

3.5.2 Radical Scavenging Assay 2, 2-Diphenyl - 1 - Picryl-hydrazyl

With just minor adjustments, the DPPH test, which was previously reported by [132], was utilised to assess the extracts' anti-oxidant activity. The experiment was conducted by using 0.004% (w/v) DPPH solution prepared in ethanol.

Experiment was performed in triplicates. A sample of extracts (200 μl) was mixed with 0.1 molar tris base HCL buffer (250 μl) and then the DPPH reagent (1 ml) was added. At 517 nm, the absorbance was determined with a spectrophotometer. This formula was utilised to determine the activity of scavenging free radicals:

$$Scavengeprecentages = \frac{A_{blank} - A_{sample}}{A_{blanks}} \times 100$$

A_{sample} of the treatment with plant extract absorbance is at 517 nm. A_{blank} is the sample's absorbance at 517 nm without plant extract.

3.6 Anti-diabetic Activity

3.6.1 Inhibition of Alpha-amylase Activity

The medicinal plant extract's inhibitory activity for alpha-amylase was determined by using previously reported methods with a few modifications [133]. Experiment was performed in triplicates.

The inhibitory effect of extracts-amylase activity was quantified using di-nitrosalicylic acid. For this purpose, 0.5% alpha-amylase solution was prepared in distilled water. To maintain the pH of the mixture, 20 mM sodium phosphate buffer (pH

6.9) was added after 100 μl of plant extract was added to the 100 μl alpha-amylase solution. Ten minutes at 37^{o}C were dedicated to pre-incubating the solution.

A 1% starch solution was made with distilled water, and 200 μl of this solution was added to the pre-incubated solution. Before adding 1 ml of 1% DNSA, the solution was once more incubated for 10 minutes at 25^{o}C. To stop the process, one millilitre of di-nitro salicylic acid was introduced, and the mixture was then brought to a boil for five minutes.

The reaction mixtures were diluted 1:5 with water and permitted to cool to ambient temperature before their absorbance was assessed at 540 nm using a spectrophotometer. The below- mentioned equation was ustilized to evaluate the enzyme's inhibition percentage:

$$Alphaamylaseinhibitionpercentage = \frac{A_{control} - A_{treatement}}{A_{control}} \times 100\%$$

$A_{treatement}$ is defined as the absorbance of the plant extract treatment at 540 nm. An absorbance of the sample without plant extract at 540 nm is called a control. Additionally, a control sample was run in triplicate.

3.6.2 Alpha-glucosidase Inhibitory Assay

The impact of the plant extract on α-glucosidase activity was investigated following the methodology explained by Kim *et al.* [134] with slight changes using α-glucosidase from S. cerevisiae. Mix 250 μl of phosphate buffer (pH 6.8), 100 μl. test sample, and 250 μl. of 0.5% starch solution, then pre-incubate at 37^{o}C for 5 minutes. Add 100 μl. alpha-glucosidase enzyme (0.5 U/mL) and incubate at 37^{o}C for exactly 30 minutes.

Stop the reaction by adding 500 μl. DNSA reagent, boil for 5 minutes, cool to ambient temperature, and read absorbance at 540 nm. Include controls without enzyme (blank) and without inhibitor (100% activity control). The DNS reagent contains 2.18 g DNS and30 g sodium potassium tartrate dissolved in 80 mL of 0.5

M NaOH.

$$\%Inhibition = [\frac{Abs_{control} - Abs_{extract}}{sAbs_{control}}] \times 100$$

This method measures reducing sugars released from starch hydrolysis and is ideal for plant extract screening since it's less affected by natural pigments compared to PNPG method.

3.7 Compounds Identification by High Pressure Liquid Chromatography

Standards of Rutin was procurred from Sigma Aldrich, USA. The HPLC grades of Acetonitrile, ammonium acetate and methanol were purchased from (MERCK®), Germany. Remaining chemicals utilized were of analytical grade. The standard and the methanolic okra leaf extract stock solutions were prepared at 1 mg/ml.

3.7.1 Chromatographic Conditions

The procedure mentioned by Laghari *et al.*, [135] was adopted with few changs. The sample were prepared by adding 600μL of methanol to 200μL of the sample. The purified samples were then loaded in mass-type vials for analysis. The chemicals employed include HPLC-grade acetonitrile (gradient type), HPLC-grade methanol and Type I water. Detection was performed using a DAD detector at wavelengths of 254 nm, with a C18 column for separation. The eluent consists of 100% Milli-Q water in pump A and 100% acetonitrile in pump B, maintained at room temperature. The HPLC isolation was carried out at a flow rate of 2 mL/min, with pressure constraints set at 0 bars (low) and 900 bars (high).

Each sample was injected in 10μL volumes, and the total run time is 42 minutes. The method followed isocratic and gradient conditions: initial conditions of 5% B (acetonitrile) and 95% A (water) for the first 2 minutes, followed by a shift to 20% B over the next minute. A gradient then increases B from 20% to 95% over

30 minutes, held for 3 minutes, before returning to initial conditions in 5 minutes and equilibrating for an additional 2 minutes.

3.8 Protein Selection and Preparation

3.8.1 Target Protein Selection

First of all, targeted protein was selected i.e., IRS-1, AkT, and PPAR from literature review.

3.8.2 3D Structure of Protein

A 3D structure of IRS protein was acquired from Protein data bank (PDB) in pdb format. The PDB provided the crystal structure of the IRS-1, AkT, and PPAR protein.

3.8.3 Physicochemical Properties of Protein

The physicochemical attributes, such as molecular weight, theoretical pI, amino acid constitution, atomic build-up, aiphatic index, instability index, esxpected shelf-life, extinction coefficient, and grand average of hydropathy of the target protein i.e., Akt, PPARG and IRS1, was computed using Expasy ProtParam tool [136].

3.8.4 Cleaning of Protein

Cleaning of targeted protein involves removal of water molecules and ligands. And this purification was done using PyMol.

3.8.5 Functional Domain

Protein functional domains and conserved sites are identified via the InterPro database. It has classified proteins into families based on their sequences [137]. The IRS-1 protein's functional domains were identified using InterPro database.

3.9 Selection of Ligands

Ligand of Rutin was selected from the HPLC results

3.9.1 Structures of Ligands

A public database of chemical structures and the findings of their biological analyses is available at PubChem [138]. In PubChem, a vast range of chemical information is accessible, including syntheses, journal articles, patents, drug labeling, spectrum information, clinical studies, and molecular structures and characteristics [139]. From PubChem, structures of ligands were acquired in sdf format.

3.9.2 Energy Minimization of Ligands

With the downloaded ligands, energy reduction was carried out prior to molecular docking via Chem3d Pro 12.0. The configurational structure with the least total potential energy is the result of the energy minimization method [140].

3.10 Molecular Docking

Docking is a computational-based approach that selects the best posture every structure produces to a categorized-order. This is done by determining the correct interacting pose of a target protein and ligand complex and evaluation of the strength of the interaction utilizing a range of scoring functions.

Docking techniques aim to fit a ligand into a protein's binding site by optimizing hydrophobic, electrostatic, and steric interactions, ultimately predicting the interacting free energy of the target protein [141].

A well-known docking application named Auto dock. The user-friendly blind docking web service CBDock, which predicts a protein's binding sites and determines its centers and sizes using a special curvature-based cavity identification method, is used to perform docking with Vina. This makes it possible to forecast binding modes automatically without requiring knowledge of binding sites. For our chosen ligands against the targeted protein, we employed CB-Dock in this instance [129].

3.11 Ligand Protein Interaction

For determining the kind of amino acids residues, interaction with the ligand using BIOVIA Discovery Studio software was utilized [142]. The biological ability of the protein was compared with the ligand i.e., the antagonistic capability of compounds using Discovery Studio software (DS) [143].

3.12 Virtual Screening

3.12.1 Lipinski Rule of Five

Lipinski's Rule of Five (RO5) physicochemical parameter standards would be met by an ideal therapeutic molecule. It forecasts the drug-like characteristics of a chemical molecule intended for oral administration that has a certain biological function. A compound will have greater bioavailability and improved pharmacokinetic characteristics in the organism's metabolic process if it fulfills these criteria [144]. Following is the Lipinski's rule of five:

1. Hydrogen bond acceptors ≤ 10
2. Hydrogen bond donors ≤ 5

3. Molecular weight < 500 g/mol.

4. LogP < 5

5. Rotatable bonds < 10

6. Calculation of Lipinski's Ro5 of compounds were done using the pkCSM tool.

3.12.2 ADMET Properties

In addition to biological activity, a successful drug's therapeutic effect depends on a suitable ADMET profile [141]. Pre-clinical optimization, which addresses the physicochemical properties and in silico toxicity assessment, is the next phase in the computer-aided drug design pipeline that must be completed before a hit molecule can be generated and deployed to use. A compound's ADME characteristics are determined by its pharmacokinetic profile. The method used for anticipating and optimizing pharmacokinetic and toxicity qualities is called pkCSM [145].

Utilizing the pkCSM server, the ADMET characteristic of particular phytochemicals were predicted. To anticipate the ADMET properties, SMILES of the chosen ligans was uploaded to the pkCSM computational tool. The pkCSM server provided a range of parameters for the profiles of selected compounds, including those related to absorption, distribution, metabolism, excretion and toxicity [146].

3.13 Statistical Analysis

The experiments for anti-oxidant (DPPH assay), TPC, anti-diabetic (α-amylase and α-glucosidase inhibition) activities were carried out three times to guarantee precision and reliability. Each experimental data set was recorded and analyzed through Microsoft Excel software. The data representation included mean values

along with standard deviation (SD) to show central trends and replicate variability. The evaluation of extract effectiveness for antioxidant and anti-diabetic activities used percentage inhibition measurements. The IC50 values were determined through regression analysis of both DPPH, TPC, α-amylase and α-glucosidase inhibition data to quantify extract potency. Statistical methods enabled the researchers to assess different solvent extracts and determine which extraction method produced the most potent results [147].

Chapter 4

Results

4.1 Thin Layer Chromatography

Phenolics are better analyzed using TLC, particularly in raw plant extracts. Several TLC methods are available for separating phenolics from raw plant extracts. These methods are inexpensive and enable simultaneous detection on the same TLC plate in a short analysis period [148].

Following the extract preparation, we dove into thin layer chromatography. This technique helped us pinpoint the most effective solvent system. Only then could we seamlessly transition to column chromatography. Multiple solvent systems find their place in the world of thin layer chromatography.

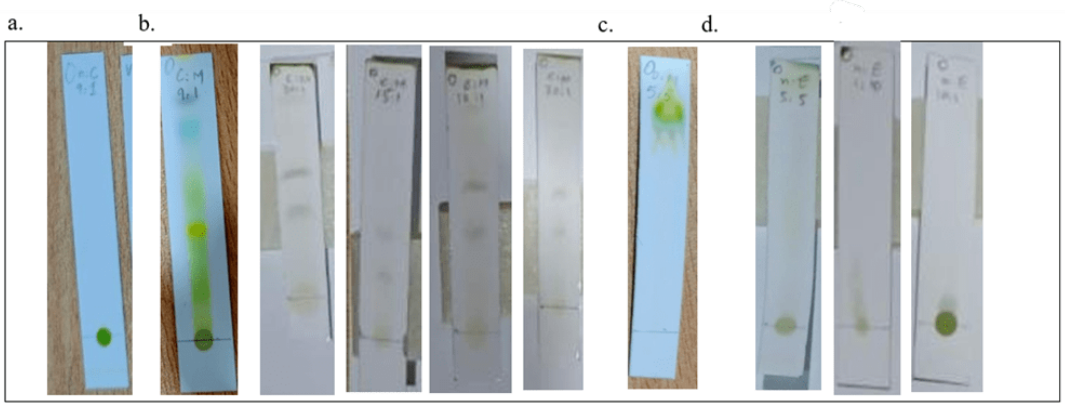

FIGURE 4.1: The chromatoplates of Okra leaf extract stock solution in different proportions of different solvent combinations a. n-hexane/ chloroform (9:1) b. Chloroform/ Methanol (9:1, 30:1,15:1, 10:1, 20:1) c. Dichloromethane/ Methanol (5:5) d. n-hexane/ Ethyl-acetate (5:5, 1:10, 10:1)

To identify the ideal column chromatography system, we tested an array of solvent solutions in our TLC endeavors. After thorough evaluation, n-hexane and ethyl acetate emerged as our leading candidates, displaying promising results. We then conducted TLCs using various ratios of n-hexane and ethyl acetate, illuminating the outcomes under the captivating light of a UV lamp.

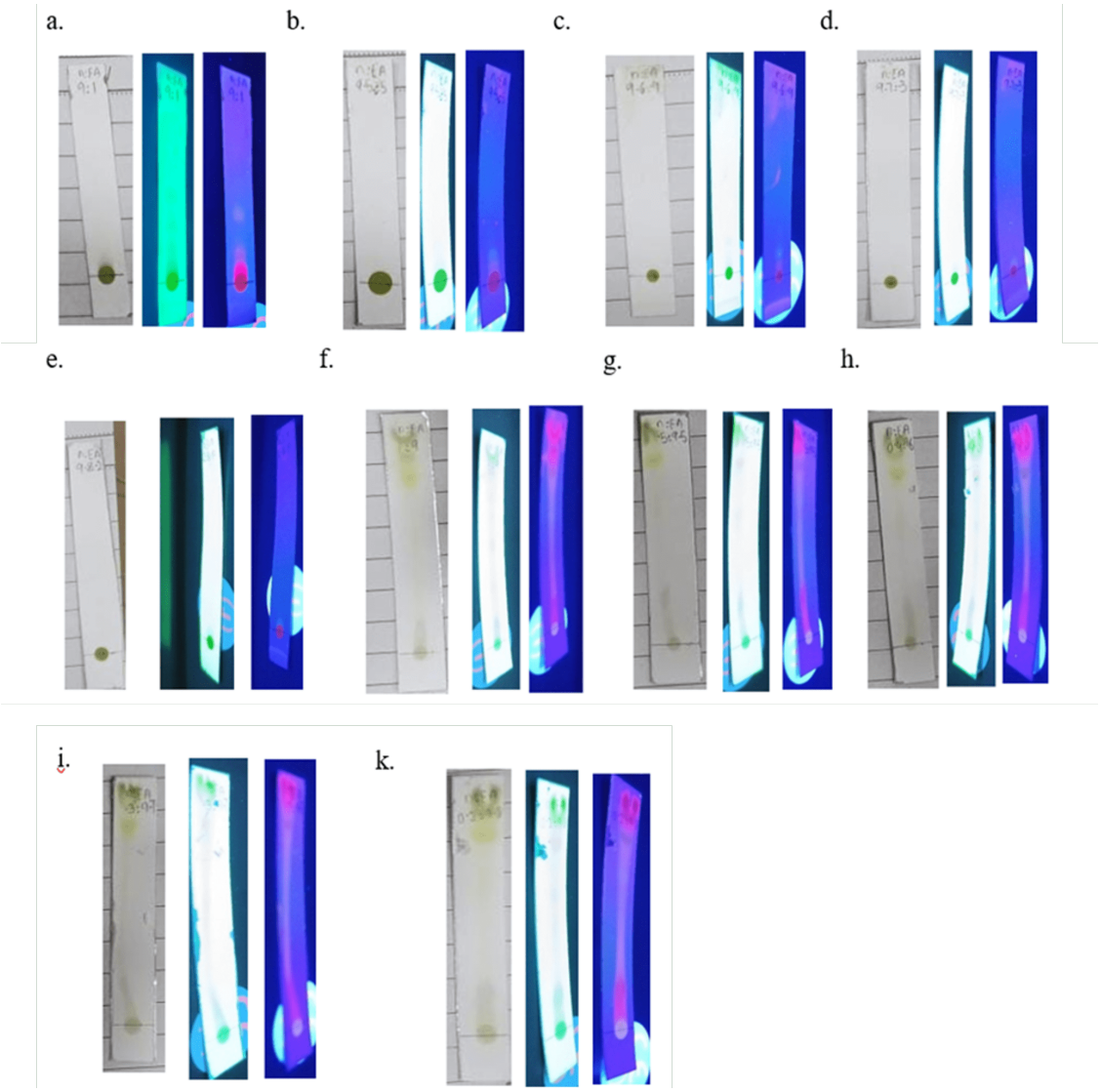

FIGURE 4.2: The chromatoplates in different solvent systems in n-hexane/ ethyl acetate in different proportions a. 10:1 b. 20:1 c. 30:1 d. 40:1 e. 50:1 f. 1:10 g. 1:20 h. 1:30 i. 1:40 j. 1:50

To proceed with column chromatography, we conducted additional TLCs. We modified the polarity of the n-hexane/ethyl acetate solvent mixture. Subsequently, we visualized the results using vanillin-sulfuric acid on a hot plate.

TABLE 4.1: The conduction of further TLCs with the selected solvent system

Sr.	**Solvent system**	**Proportion**
a.	n-hexane/ethyl acetate	10:1
b.	n-hexane/ethyl acetate	5:1
c.	n-hexane/ethyl acetate	3:1
d.	n-hexane/ethyl acetate	2:1
e.	n-hexane/ethyl acetate	1:1

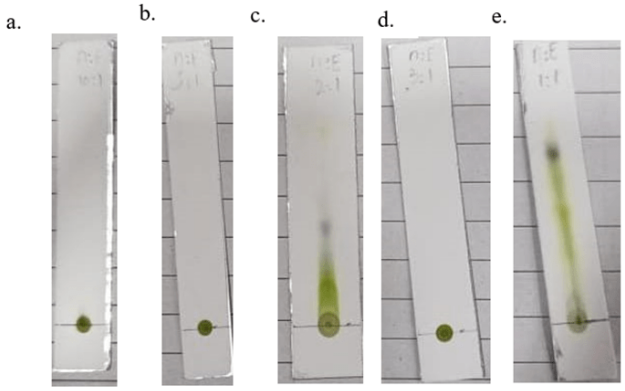

FIGURE 4.3: TLC performed with the n-hexane/Ethyl acetate solvent system in several ratios a.10:1, b.5:1, c. 2:1, d. 3:1, e. 1:1

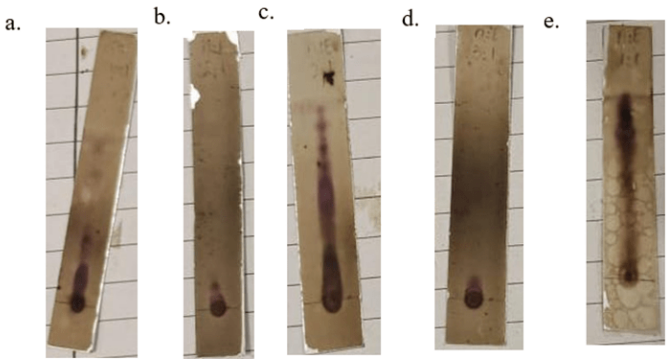

FIGURE 4.4: TLC performed with the n-hexane/Ethyl acetate solvent system in several ratios visualized using vanillin-sulfuric acid reagent on hot plate a.10:1, b.5:1, c. 2:1, d. 3:1, e. 1:1

4.2 Column Chromatography

Column chromatography is an effective technique for separating substances based on their differential adsorption to the adsorbent. As compounds traverse the column, they move at discreet rates influenced by their affinities for both the adsorbent and the solvent or mixture, allowing for the separation into distinct fractions.

These fractions are typically collected in solution as they exit the column at different times. The core principle of column chromatography lies in the adsorption of solutes onto a stationary phase, which facilitates the separation of the mixture into its individual components.

The stationary phase is densely packed within a glass or metal column. The mobile phase, known as the eluent, is introduced through a pumping system or by applying gas pressure after the analyte mixture has been added. The stationary phase can either be a thin film applied to the column's interior or small particles (the matrix) that are packed into the column. As the eluent flows down, the analytes separate according to their distribution coefficients and are collected in the eluate as they pass through the apparatus [149].

Following our TLC experiments with various solvent systems, we proceeded with column chromatography. We utilized silica gel as the stationary phase and introduced a mixture of n-hexane and ethyl acetate into the glass-column. The fractions were collected in test tubes positioned beneath the column.

FIGURE 4.5: Column filled with the stationary phase and eluent used for Column Chromatography

As a result, multiple fractions were collected for each solvent. The solvent combinations and the corresponding number of fractions collected are listed in the table 4.2 below.

TABLE 4.2: No. of fraction accumulation by passing the eluent through the Column

Sr.	Mobile Phase/ Eluent	Collected Fractions number
a.	100% n-hexane	8
b.	n-hexane/ethyl acetate (10:1)	5
c.	n-hexane/ethyl acetate (5:1)	5
d.	n-hexane/ethyl acetate (3:1)	4
e.	n-hexane/ethyl acetate (2:1)	4
f.	n-hexane/ethyl acetate (1:1)	3
g.	n-hexane/ethyl acetate (1:2)	4
h.	n-hexane/ethyl acetate (1:3)	4
i.	n-hexane/ethyl acetate (1:5)	4
j.	n-hexane/ethyl acetate (1:10)	4
k.	100% ethyl acetate	4

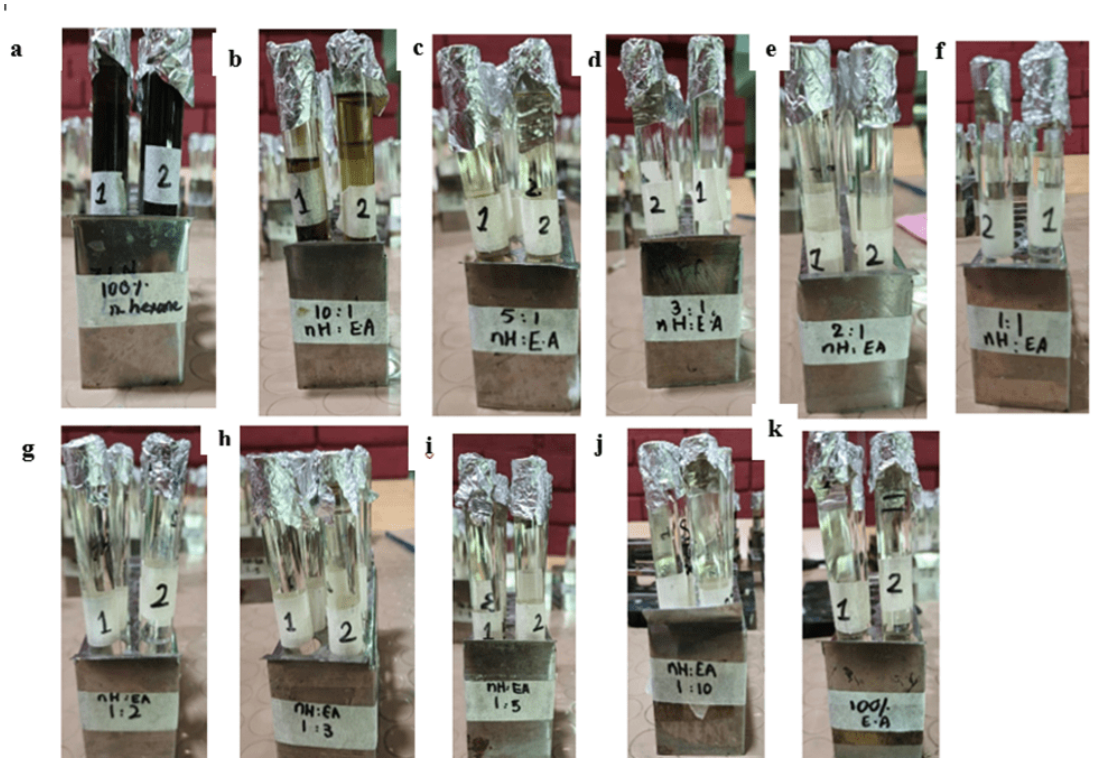

FIGURE 4.6: Fractions of different eluents collected in separate test tubes a. 100% n-hexane, b. n-hexane/ethyl acetate (10:1), c. n-hexane/ethyl acetate (5:1), d. n-hexane/ethyl acetate (3:1), e. n-hexane/ethyl acetate (2:1), f. n-hexane/ethyl acetate (1:1), g. n-hexane/ethyl acetate (1:2), h. n-hexane/ethyl acetate (1:3), i. n-hexane/ethyl acetate (1:5), j. n-hexane/ethyl acetate (1:10), k. 100% ethyl acetate

4.2.1 TLCs of Fractions Collected from Eluent

Each fraction of the specific eluent was collected in separate test tubes. Once the fractions were collected, TLCs were conducted on each eluent fraction using discrete solvent systems, specifically n-hexane/ethyl acetate in various proportions (1:1, 1:2, 1:3, 1:5, 1:10) to evaluate the banding and movement of the compounds, as illustrated in the figure below.

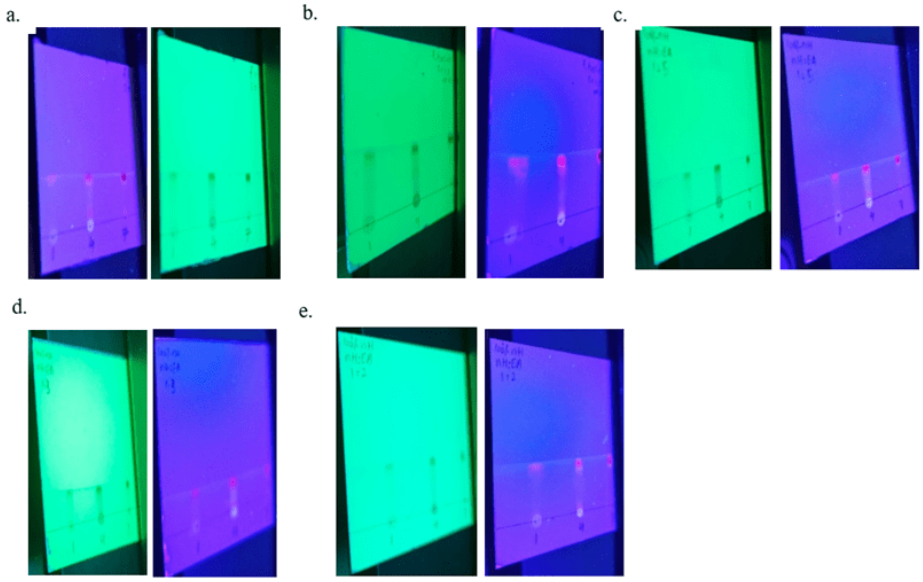

FIGURE 4.7: chromoplates of no. of fractions collected after passing the eluent of n-hexane 100% in different n-hexane/ethyl acetate proportions a. 1:1, b. 1:10, c. 1:5, d. 1:3, e. 1:2

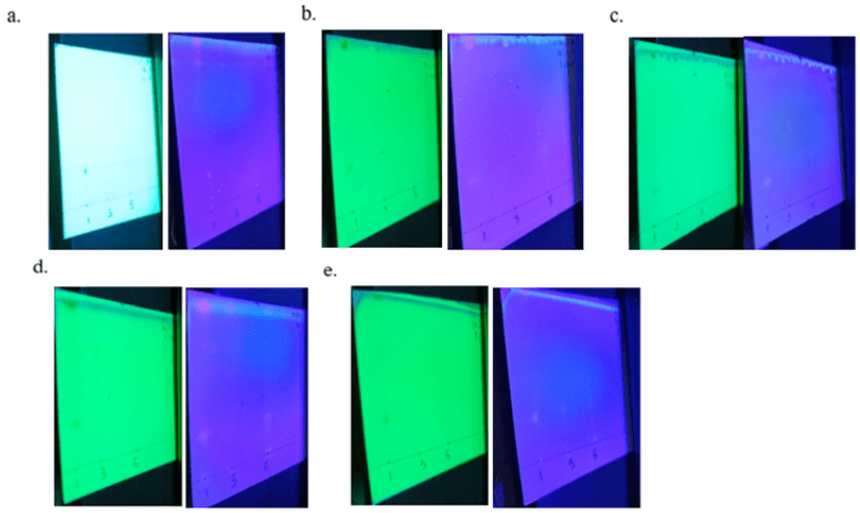

FIGURE 4.8: Chromoplates of no. of fractions collected after passing the eluent of n-hexane/ethyl acetate (10:1) in different n-hexane/ethyl acetate proportions a. 1:1, b. 1:10, c. 1:5, d. 1:3, e. 1:2

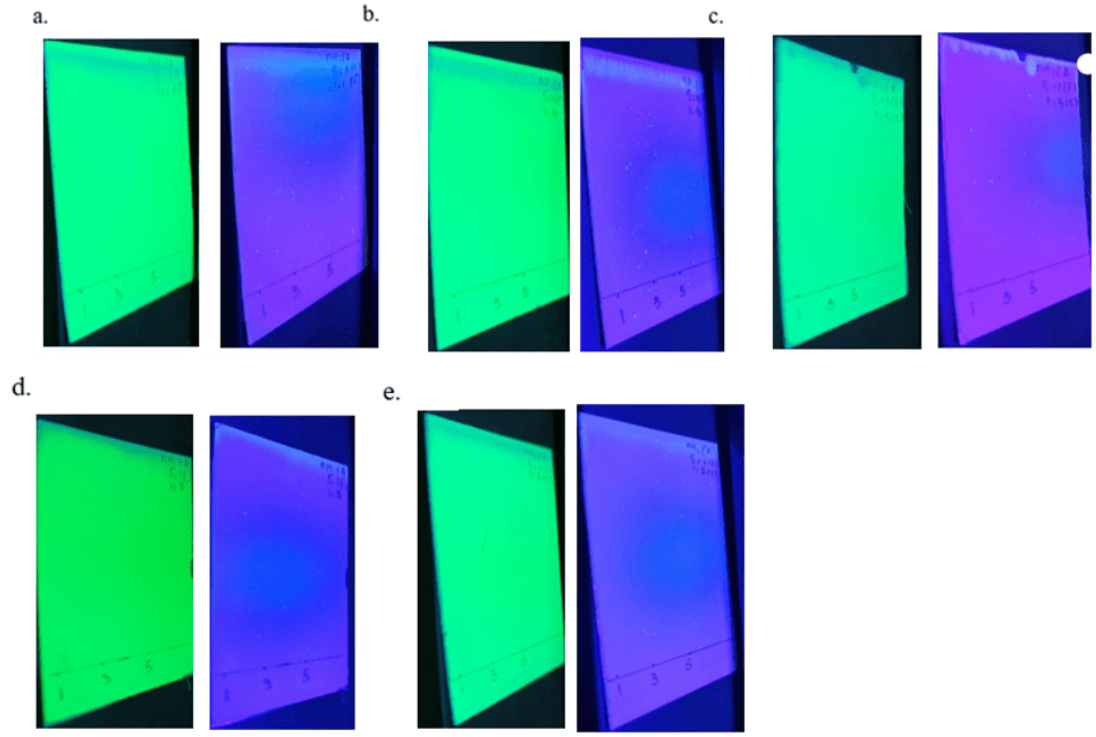

FIGURE 4.9: Chromoplates of no. of fractions collected after passing the eluent of n-hexane/ethyl acetate (5:1) in different n-hexane/ethyl acetate proportions a. 1:1, b. 1:10, c. 1:5, d. 1:3, e. 1:2

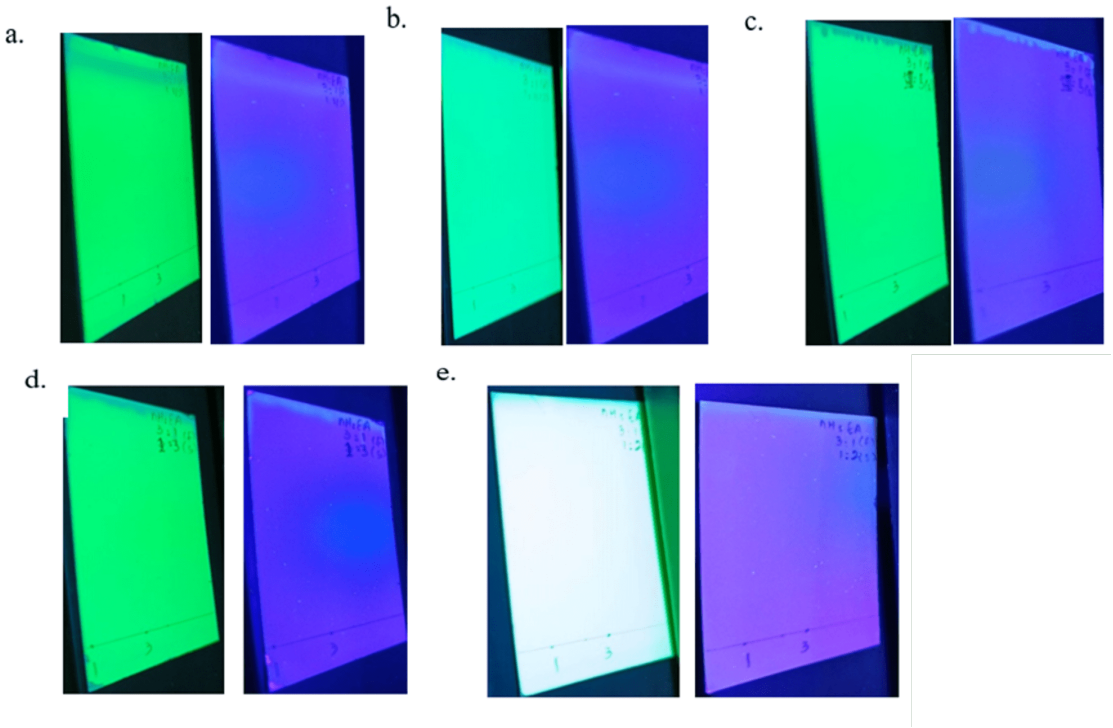

FIGURE 4.10: Chromoplates of no. of fractions collected after passing the eluent of n-hexane/ethyl acetate (3:1) in different n-hexane/ethyl acetate proportions a. 1:1, b. 1:10, c. 1:5, d. 1:3, e. 1:2

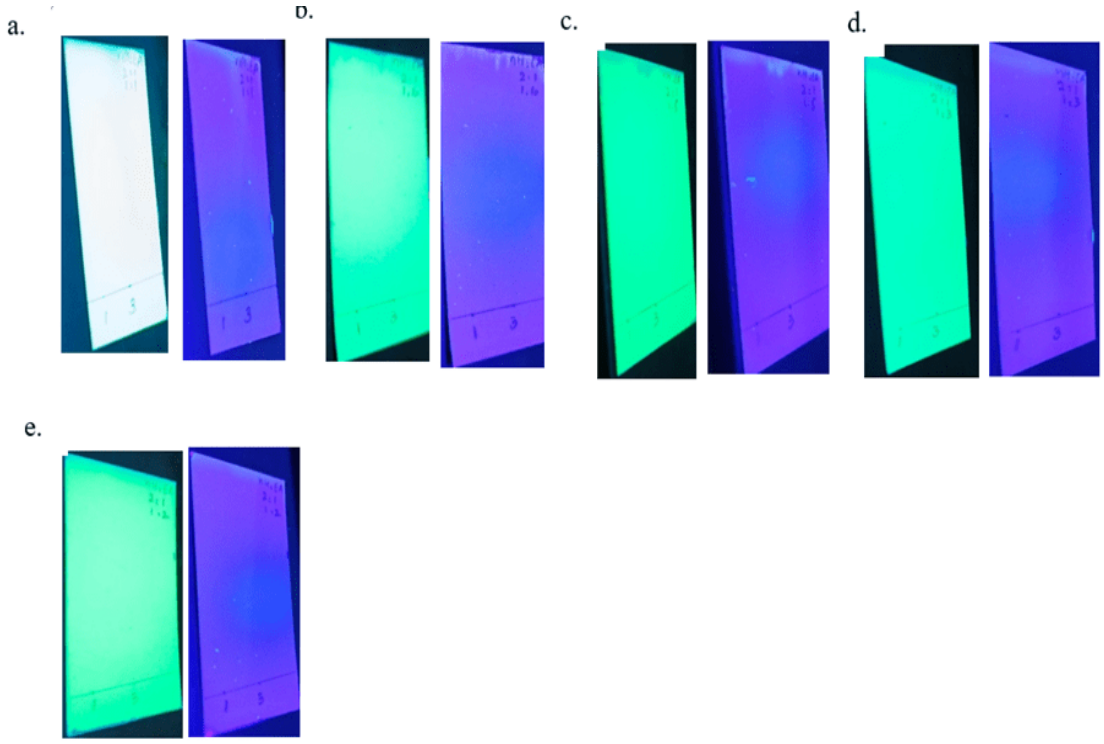

FIGURE 4.11: Chromoplates of no. of fractions collected after passing the eluent of n-hexane/ethyl acetate (2:1) in different n-hexane/ethyl acetate proportions a. 1:1, b. 1:10, c. 1:5, d. 1:3, e. 1:2

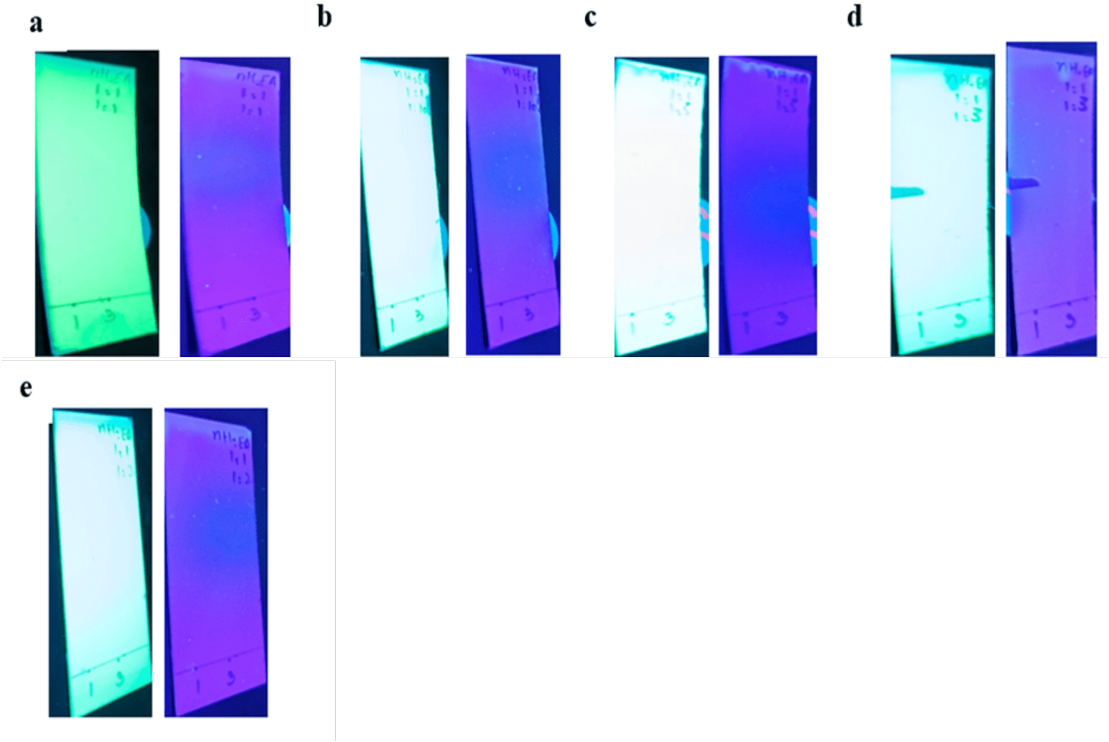

FIGURE 4.12: Chromoplates of no. of fractions collected after passing the eluent of n-hexane/ethyl acetate (1:1) in different n-hexane/ethyl acetate proportions a. 1:1, b. 1:10, c. 1:5, d. 1:3, e. 1:2

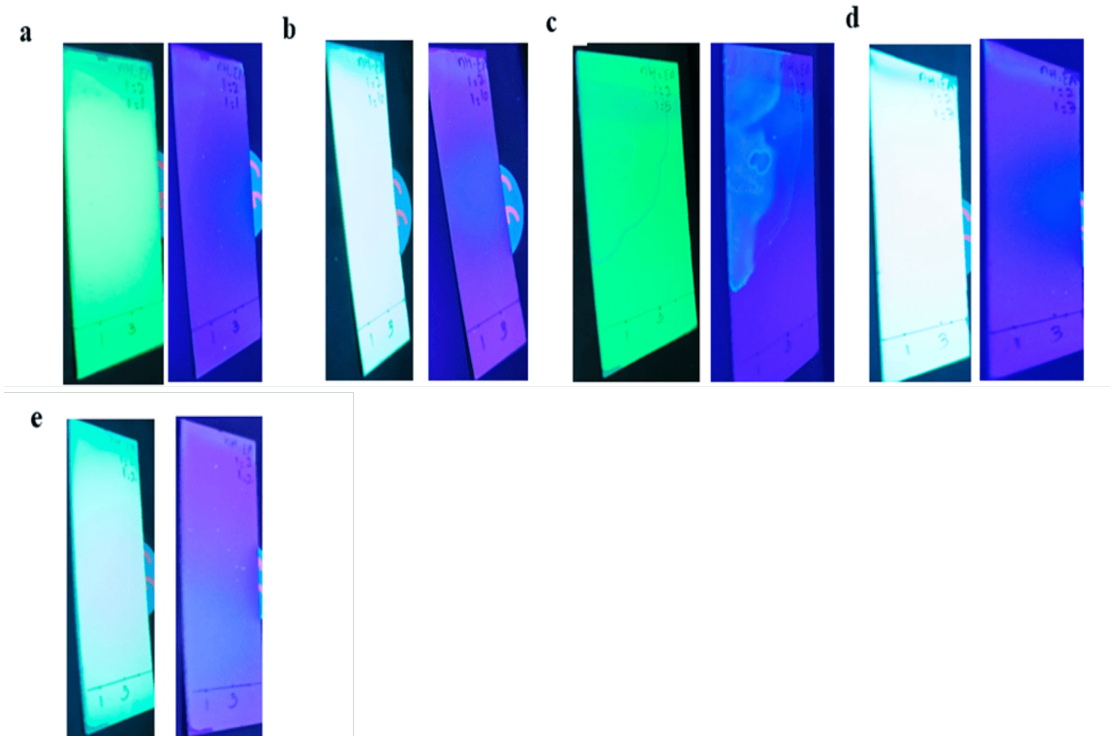

FIGURE 4.13: Chromoplates of no. of fractions collected after passing the eluent of n-hexane/ethyl acetate (1:2) in different n-hexane/ethyl acetate proportions a. 1:1, b. 1:10, c. 1:5, d. 1:3, e. 1:2

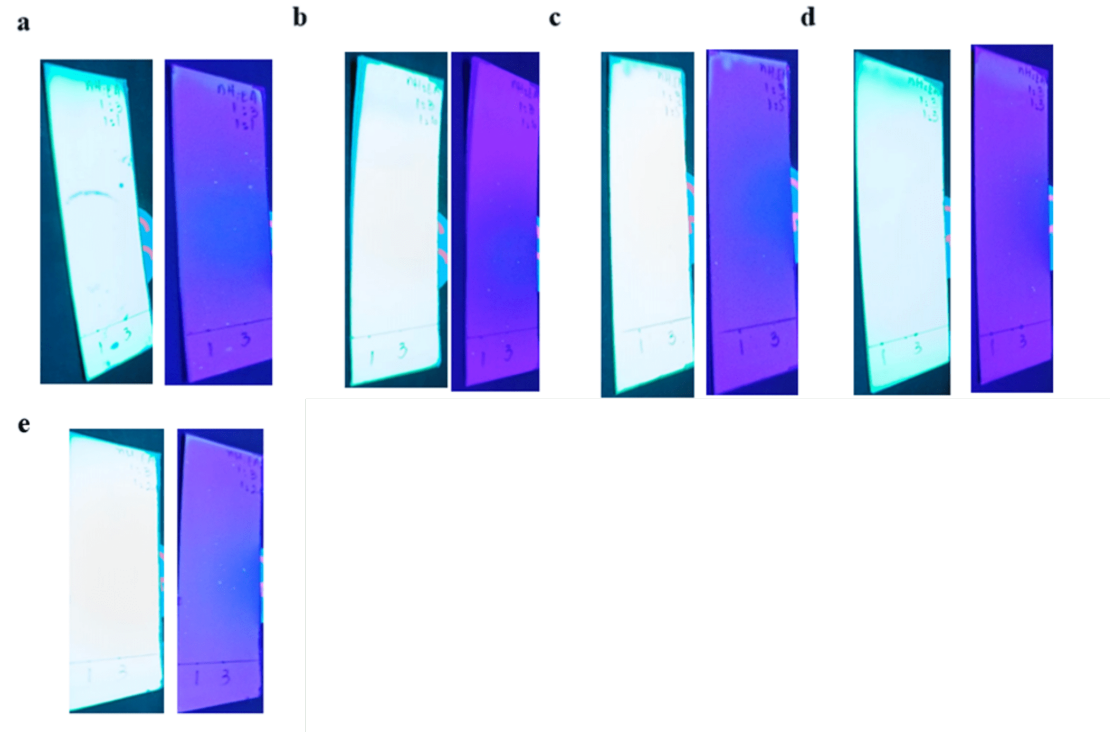

FIGURE 4.14: Chromoplates of no. of fractions collected after passing the eluent of n-hexane/ethyl acetate (1:3) in different n-hexane/ethyl acetate proportions a. 1:1, b. 1:10, c. 1:5, d. 1:3, e. 1:2

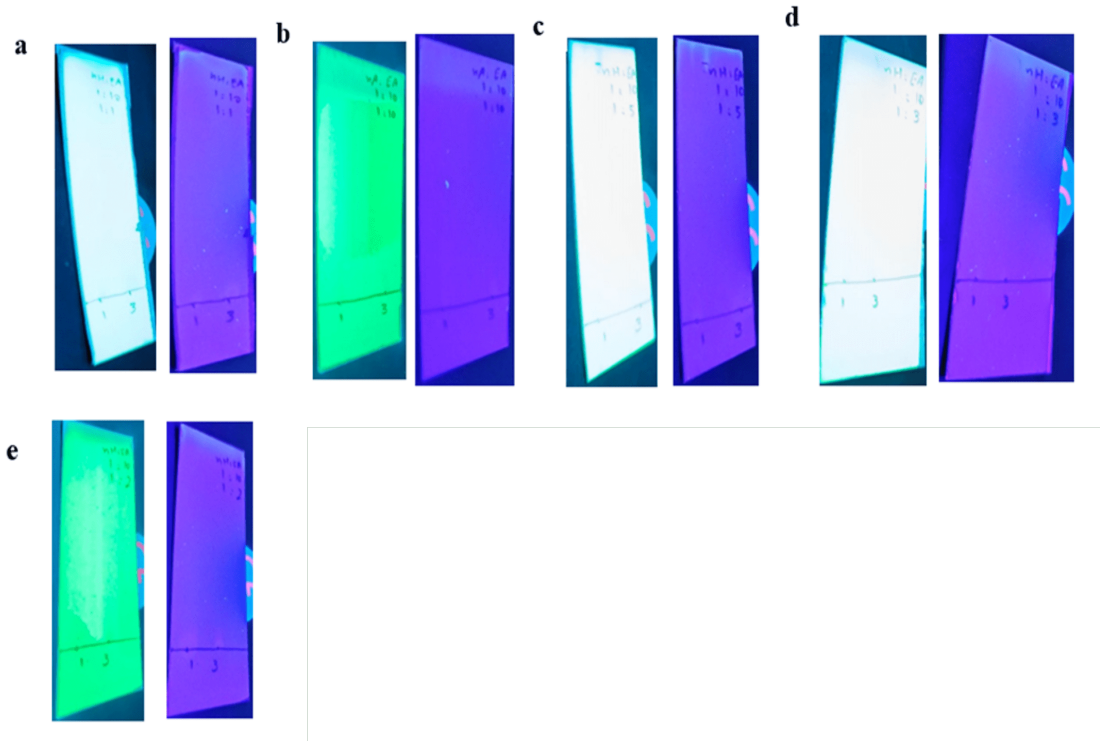

FIGURE 4.15: Chromoplates of no. of fractions collected after passing the eluent of n-hexane/ethyl acetate (1:5) in different n-hexane/ethyl acetate proportions a. 1:1, b. 1:10, c. 1:5, d. 1:3, e. 1:2

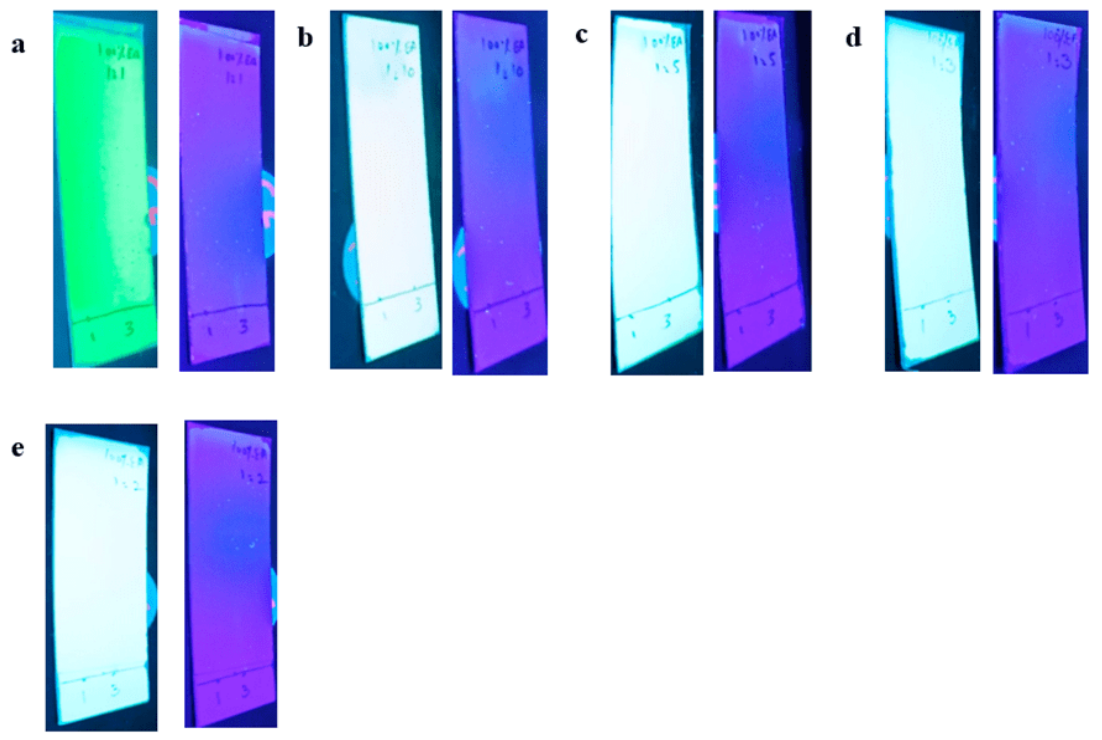

FIGURE 4.16: Chromoplates of no. of fractions collected after passing the eluent of n-hexane/ethyl acetate (1:10) in different n-hexane/ethyl acetate proportions a. 1:1, b. 1:10, c. 1:5, d. 1:3, e. 1:2

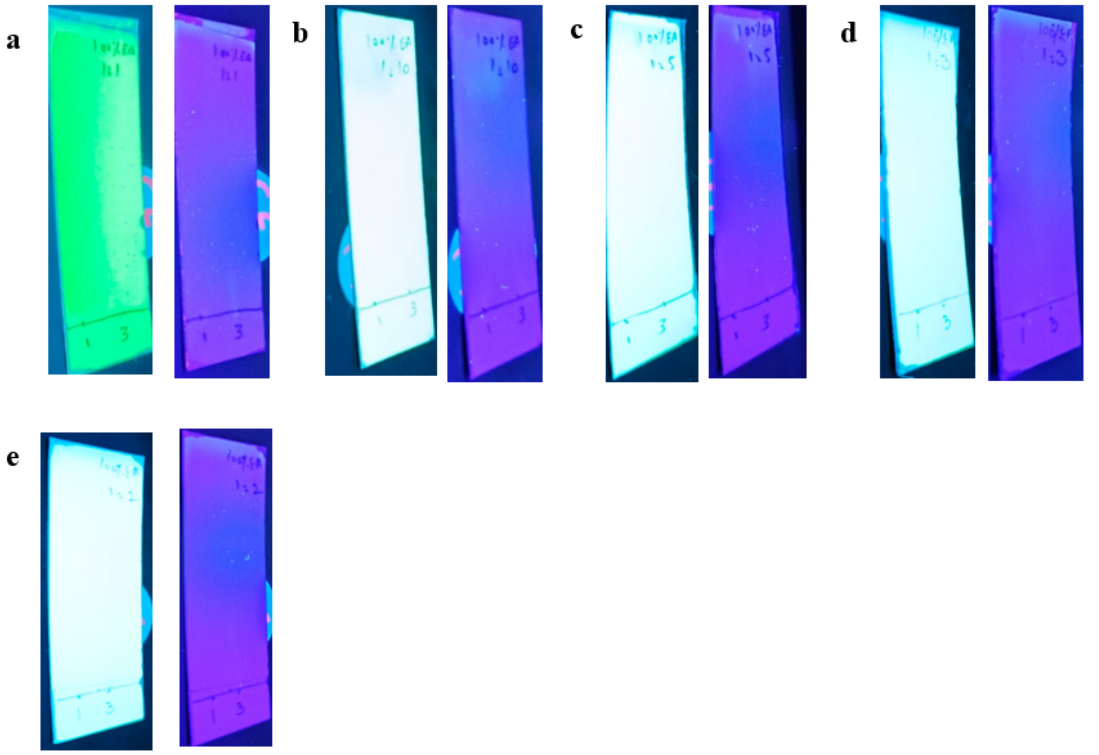

FIGURE 4.17: Chromoplates of no. of fractions collected after passing the eluent of 100% ethyl acetate in different n-hexane/ethyl acetate proportions a. 1:1, b. 1:10, c. 1:5, d. 1:3, e. 1:2

The TLCs were monitored to determine which fractions had bands that traveled similarly. Subsequently, all fractions collected from each eluent were combined and designated as F1, F2, F3, F4, F5, F6, F7, F8, F9, F10, and F11, as detailed in the table 4.3.

TABLE 4.3: Major fractions formation after mixing

Sr.	**Mobile Phase Eluent**	**Collected Fractions number**	**Formation of fractions after mixing**
a.	100% n-hexane	0:00	F1
b.	n-hexane/ethyl acetate (10:1)	5	F2
c.	n-hexane/ethyl acetate (5:1)	0:00	F3
d.	n-hexane/ethyl acetate (3:1)	4	F4
e.	n-hexane/ethyl acetate (2:1)	4	F5
f.	n-hexane/ethyl acetate (1:1)	3	F6
g.	n-hexane/ethyl acetate (1:2)	4	F7
h.	n-hexane/ethyl acetate (1:3)	4	F8

Table 4.3 continued from previous page

Sr.	Mobile Phase Eluent	Collected Fractions number	Formation of fractions after mixing
i.	n-hexane/ethyl acetate (1:5)	4	F9
j.	n-hexane/ethyl acetate (1:10)	4	F10
h.	100% ethyl acetate	4	F11

4.2.2 TLCs of Fractions Collected

Additionally, we conducted thin layer chromatography (TLC) for each eluent, followed by combining the collected fractions to create the major fractions. We then performed TLC again on the major fractions F2 to F11, using a solvent system of n-hexane and ethyl acetate in various ratios, including 10:1 and 5:1, as illustrated in the figure below.

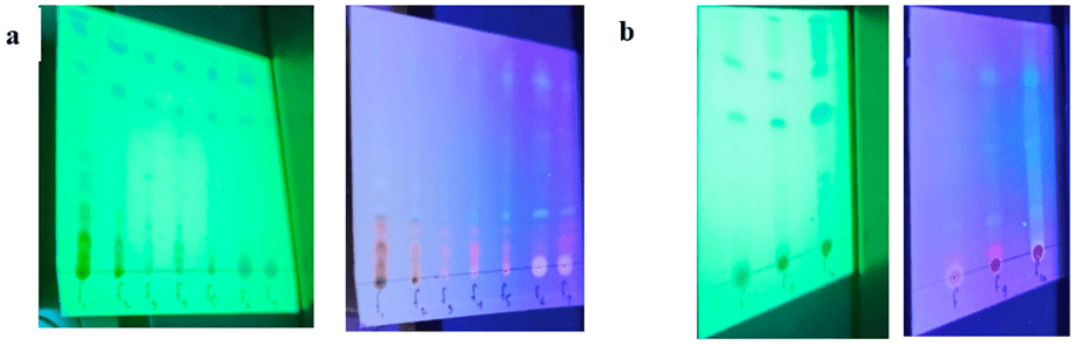

FIGURE 4.18: Chromoplates of fractions (F2-F11) in n-hexane/ ethyl acetate (5:1) a. F2-F8, b. F9-F11

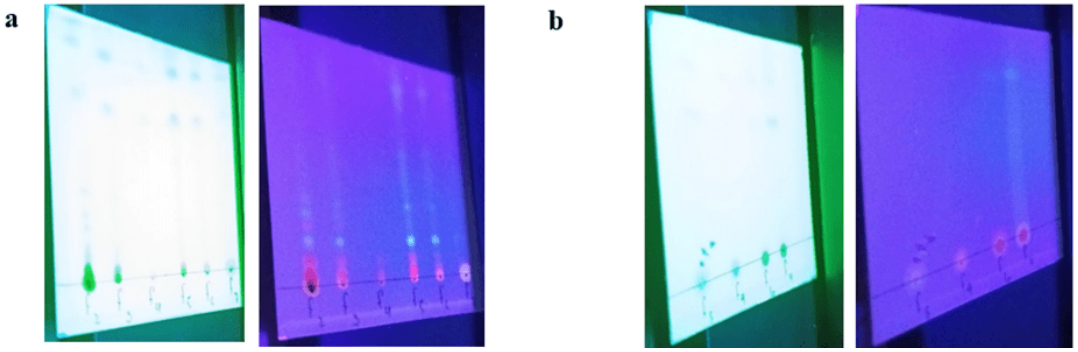

FIGURE 4.19: Chromoplates of fractions (F2-F11) in n-hexane/ ethyl acetate (10:1) a. F2-F7, b. F8-F11

4.2.3 Formation of Super Fractions

The investigation process for the fractions that covered the same distance was repeated. This step was essential to combine all fractions that exhibited similar distances traveled. This is important for obtaining super fractions, which will be used for the subsequent application of antidiabetic and antioxidant assays, as indicated in the table 4.4.

TABLE 4.4: Formation super fractions by mixing major fractions

Sr.	**Major Fractions**	**Eluents**	**Super Fraction**	**Fraction Proceeded for Assays**
a.	F1	n-hexane 100%	F1	Yes
b.	F2, F3, F4	n-hexane/ ethyl acetate (10:1, 5:1, 3:1)	F2	Yes
c.	F5, F6, F7	n-hexane/ ethyl acetate (2:1, 1:1, 1:2)	F3	Extremely low amount so could not proceed further
d.	F8, F9, F10, F11	n-hexane/ ethyl acetate (1:3,1:5, 1:10) and ethyl acetate100%	F4	Yes

4.3 Antioxidant Assays

4.3.1 2, 2 - Diphenyl - 1 - Picrylhydrazyl Radical Scavenging Assay

The established mechanism by which antioxidants prevent oxidation is through the scavenging of free radicals. Rapid investigation of the anti-oxidant capacity of particular compounds or extracts can be accomplished by the scavenging of stable DPPH free radicals' technique [150]. The technique used to measure the anti-oxidant activity of the methanolic leaf extract of okra is called the DPPHH (2, 2 diphenyl-1-1 picrylhydrazyl) test. DPPH was used as control. Methanolic okra leaf extract revealed the capability to scavenge free radicals. Methanolic leaf extract demonstrated the ability to scavenge free radicals.

A straightforward, quick, and highly-sensitive technique to assess the anti-oxidant ability of a particular drug or plant extract is to use the DPPH stable free radical assay [151]. The strongest absorption occurs when free-radical DPPH interacts with an odd electron at 517 nm (purple hue). DPPHH, which has less hydrogen than DPPH and is hence less absorbent, is produced when DPPH and an antioxidant that scavengers' free radicals unite. Unlike the DPPH-H state, this radical form decolorizes (becomes yellow) as the number of electrons it gathers increases (Figure 4.20)

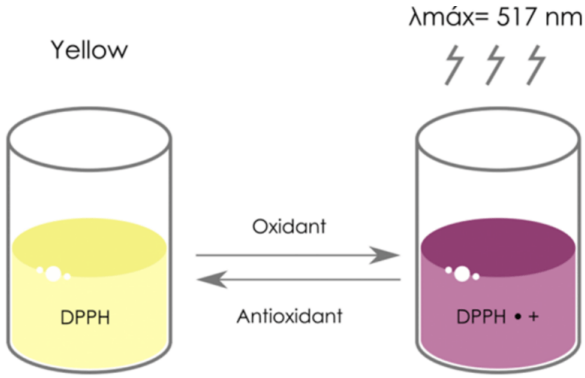

FIGURE 4.20: How an antioxidant and free-radical scavenger combine to produce DPPHH from DPPH

The reduction of DPPH's purple color in test samples indicates the antioxidant action. Hence, by donating electrons or supplying a hydrogen atom, antioxidant molecules can neutralize DPPH free radicals. As a result, the color-less, stable molecule 2,2-diphenyl-1-hydrazine is produced, which decreases the absorbance of the sample at 517 nm.

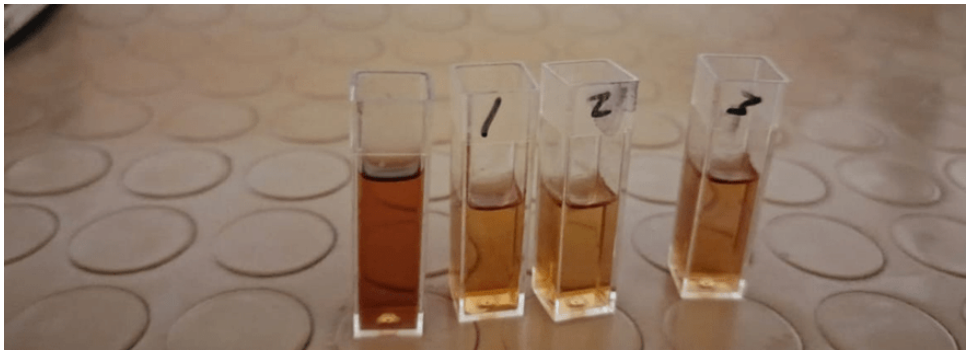

FIGURE 4.21: The DPPH assay of fraction along with the control

The DPPH solution was left undisturbed for thirty minutes in order to verify its stability. Throughout the experiment, the solution's color remained unchanged, indicating that DPPH's maximal stability had occurred.

At 517 nm, the absorption intensity was measured. The methanolic leaf extract of okra was gradually added to the DPPH solution, resulting in a steady drop in the absorption peak strength at 517 nm and a gradual shift in the solution's color from deep violet to pale yellow.

The anti-oxidant ability of the methanolic leaf of okra was calculated using DPPH. The antioxidant activity percentage was calculated as [(Ac - As) / Ac] × 100.

TABLE 4.5: Scavenging activity of fractions collected from Column Chromatography

Fractions	**Average**	**A control**		**DPPH Scavenging Percentage**		**Average**	**SD**
F1	0.5	20:54	43.97245	41.44661	42.3651	42.59472	1.278476
F2	0.418333	0.857	49.94166	52.27538	51.34189	51.18631	1.174614
F4	0.464333	20:45	44.73988	47.86127	46.35838	46.31985	1.56105

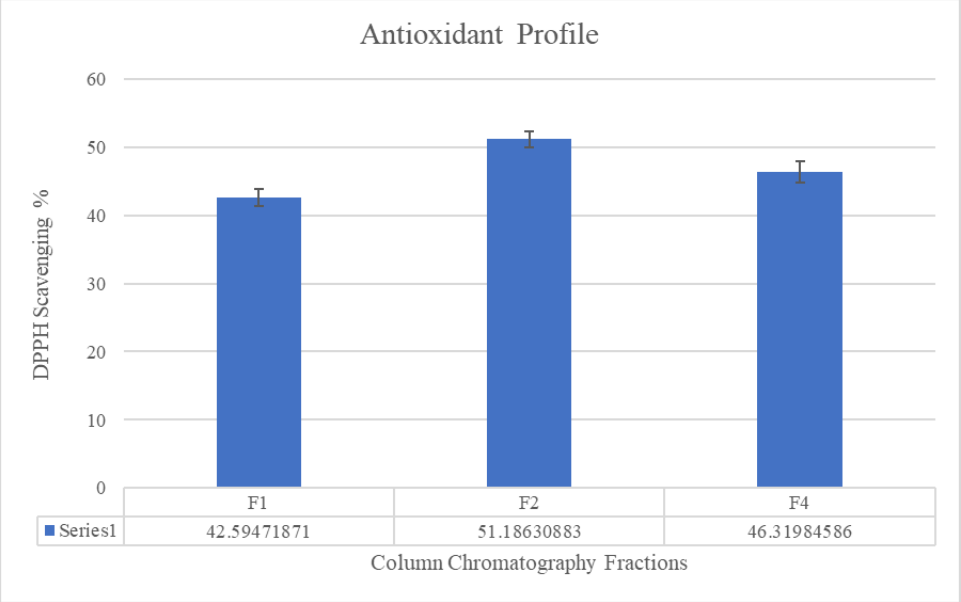

FIGURE 4.22: The scavenging activity of fractions collected from Column Chromatography

The antioxidant activity of different column chromatography fractions (F1, F2, F4) of okra (Abelmoschus esculentus) leaf extract was evaluated using the DPPH

free radical scavenging assay (Figure 4.21). Among the tested fractions, F2 exhibited the highest DPPH scavenging activity, with an average inhibition of 51.19 ± 1.17%, followed by F4 (46.32 ± 1.56%) and F1 (42.59 ± 1.28%). The relatively low standard deviations suggest that the results are reproducible and reliable. The superior anti-oxidant activity of fraction F2 may be attributed to the presence of a higher concentration or more potent polyphenolic. The chromatographic separation likely facilitated the enrichment of bioactive compounds in F2, explaining its enhanced scavenging capacity.

Overall, these results are consistent with former literature reporting the antioxidant potential of okra leaves [152, 153] and support their possible application as a natural source of antioxidants for use in functional foods, pharmaceuticals, or nutraceuticals. Further phytochemical characterization of the active fractions is recommended to detect the specific compounds having the observed anti-oxidant activity.

4.3.2 Total Phenolic Concentration

The study discovered a high correlation between the number of phenolic compounds in plant materials and their antioxidant activity [154]. Therefore, it is crucial to take into account how the overall phenolic content affects the antioxidant activity of extracts from plants.

It has been suggested that polyphenols are significant phytochemicals with strong antioxidant properties as well as other powerful therapeutic properties. It has been shown that the main plant chemicals with antioxidant activity are phenolic compounds, and that their redox characteristics are what give them this action. One family of antioxidant agents that may both adsorb and neutralize free radicals are phenolic compounds [155].

The FC method was utilized to observe the total phenolic content of the plant extract, and a calibration curve was created using gallic acid. The standard curve was used to create a regression equation, which was then used to quantify the

amount of gallic acid in the okra methanol extract: y= 0.0632x + 0.2211, R2 = 0.8958, where x is the equivalent gallic acid (mg/ml) and y is the absorbance.

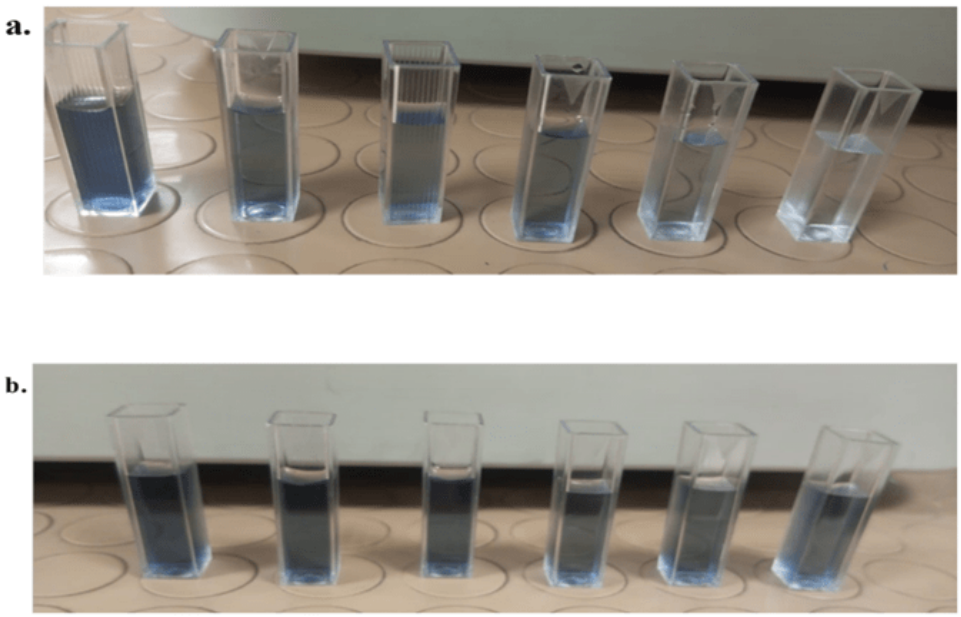

FIGURE 4.23: a, b shows the Gallic Acid concentration

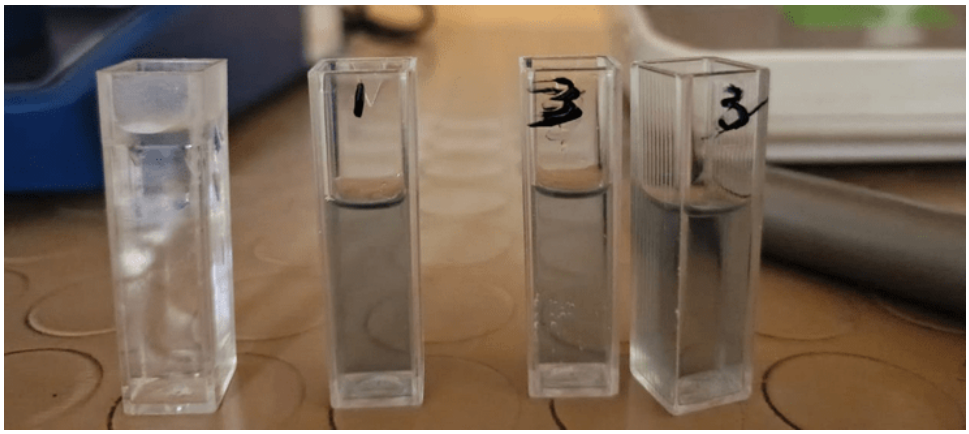

FIGURE 4.24: Fractions proceeded for TPC assay

The absorbance values (0.189, 0.321, 0.592, 0.489, 0.479, 0.653, 0.691, 0.654, 0.778, 0.784, 0.896, 1.057) increase as the concentration of Gallic acid increases (0 to 12 mg/ml). This implied that the amount of light absorbed at 765 nm and the concentration of gallic acid in the solution were directly correlated. Gallic acid curve shown in figure 4.24.

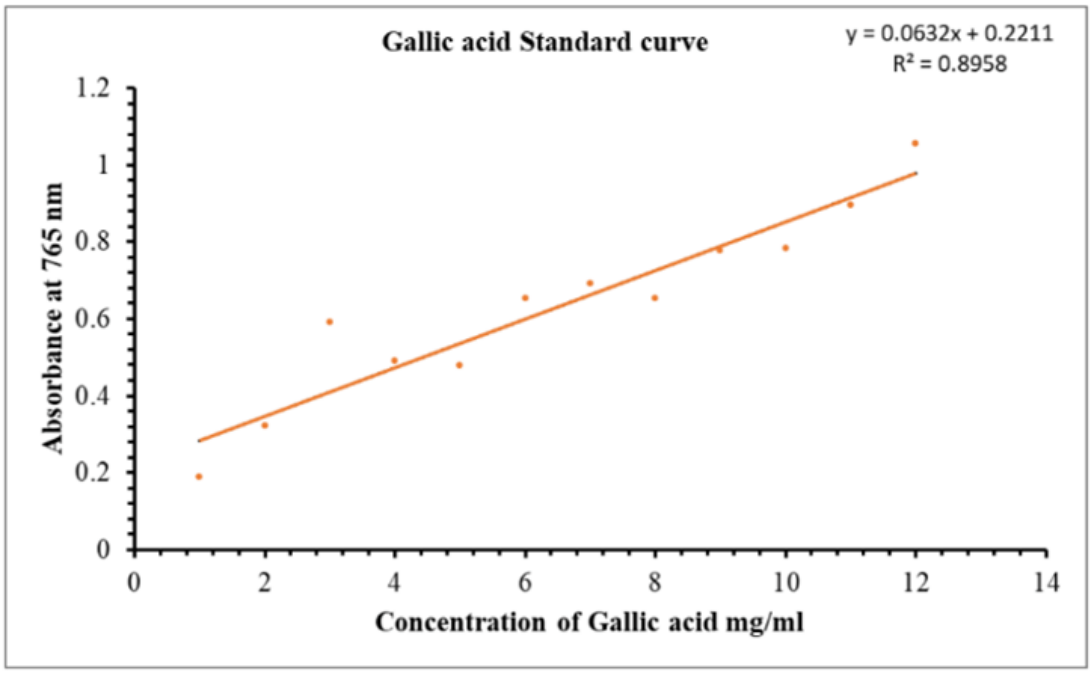

FIGURE 4.25: Graph plot for Gallic Acid results

Phenolic concentrations were observed in the methanolic leaf extract of okra that was being studied (figure 4.22 a, b). The kind of extract that is, the polari-nature of the solvent used in extraction, determines the overall phenolic levels of okra plant extracts.

When phenols are extracted using polar solvents, the resulting extracts contain high concentrations of these compounds due to their high solubility in these solvents [156].

TABLE 4.6: Absorbance of fractions collected from column chromatography at 765nm

Sample	**Absorbance of Fractions Collected from Column Chromatography at 765 nm**		
Methanolic Okra	**F1**	**F3**	**F4**
Leaf Extract	0.398	0.47	0.4

This implied a favorable relationship between the extract's phenolic component concentration and absorbance measured at the specific wavelength used (typically around 765 nm for phenolic compounds).

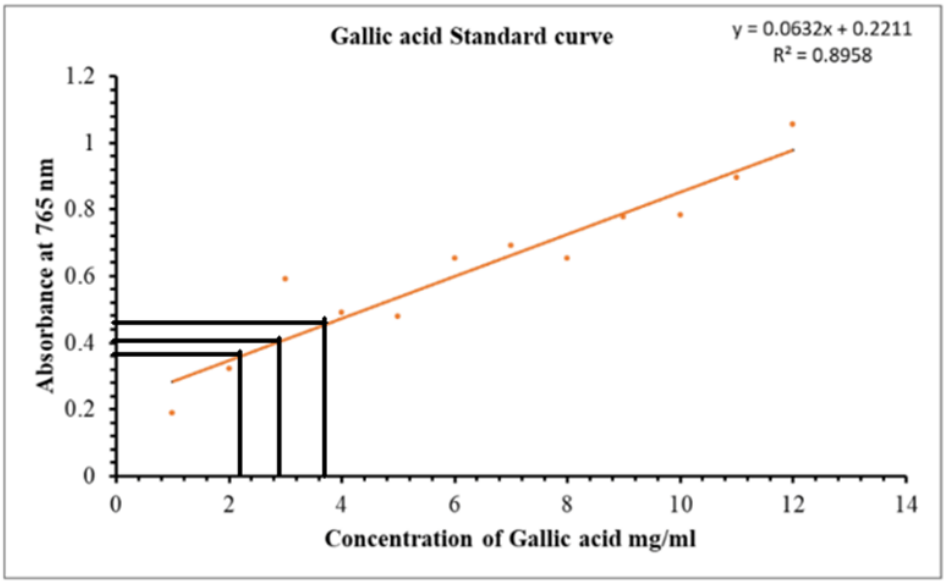

FIGURE 4.26: Phenolic concentration in Okra's methanolic leaf extract

4.4 Anti-diabetic Activity

4.4.1 Inhibition of Alpha Amylase

The enzyme alpha-amylase breaks down starch molecules to produce reducing sugars like maltose. The addition of DNSA, which is converted into 3-amino-5-nitrosalicylic acid (ANSA) in the presence of maltose, can identify these reducing sugars (Figure 4.26). Spectrophotometric identification of the bright orange-red molecule ANSA is possible at 540 nm [157]. The amount of ANSA generated will decrease when α-amylase activity is inhibited.

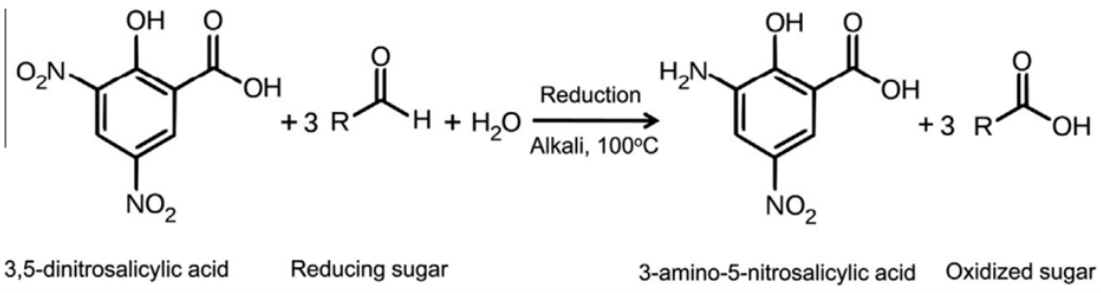

FIGURE 4.27: Conversion of an orange red ANSA to yellow DNSA in the presence of a reducing sugar

One of the critical enzymes involved in the destruction of starch, glycogen, and the metabolism of carbohydrates is alpha amylase. One method for treating problems involving the absorption of carbohydrates, such as diabetes and obesity, is to inhibit it. Because it is involved in the metabolism of carbohydrates, blocking it will lower blood sugar levels after meals [158]. Many medicinal plants and their preparations are utilized in both traditional medicine and ethnomedicine to cure diabetes because their main bioactive ingredients have strong antioxidant and alpha amylase inhibitory qualities [159]. Alpha-amylase is involved in starch digestion, and its inhibition can have significant implications for various applications, including diabetes management and food processing. We investigated into the inhibitory effects in this study, of okra methanolic leaf extract against alpha-amylase activity.

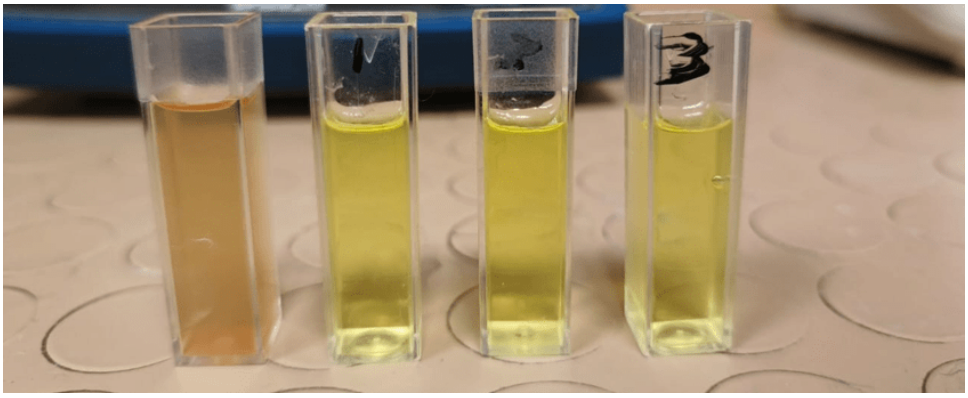

FIGURE 4.28: Sample for alpha-amylase assay

The following formula was used to get the inhibition percentage:

$$Alphaamylaseinhibitionpercentange = \frac{A_{control} - A_{treatement}}{A_{control}} \times 100\%$$

4.4.2 Alpha Amylase and Alpha Glucosidase Enzyme Inhibition Activity

The results of alpha-amylase and alpha-glucosidase inhibitory activity, as shown in the table 4.7 and graph, reveal a remarkable display of enzymatic control and

inhibition potential. The data practically exhibits the biochemical prowess of the analyzed fractions, showing prominent evidence about their inhibitory dominance.

TABLE 4.7: Enzyme inhibition profile of fraction of methanolic leaf extract of Okra

Fractions	**Alpha Amylase Inhibitory %**	**S.D**	**Glucosidase Inhibitory %**	**S.D**
F1	77.6	6:00	88	2.01
F2	78.4	1.53	89.1	2.09
F4	60.2	0:14	86.2	1.5

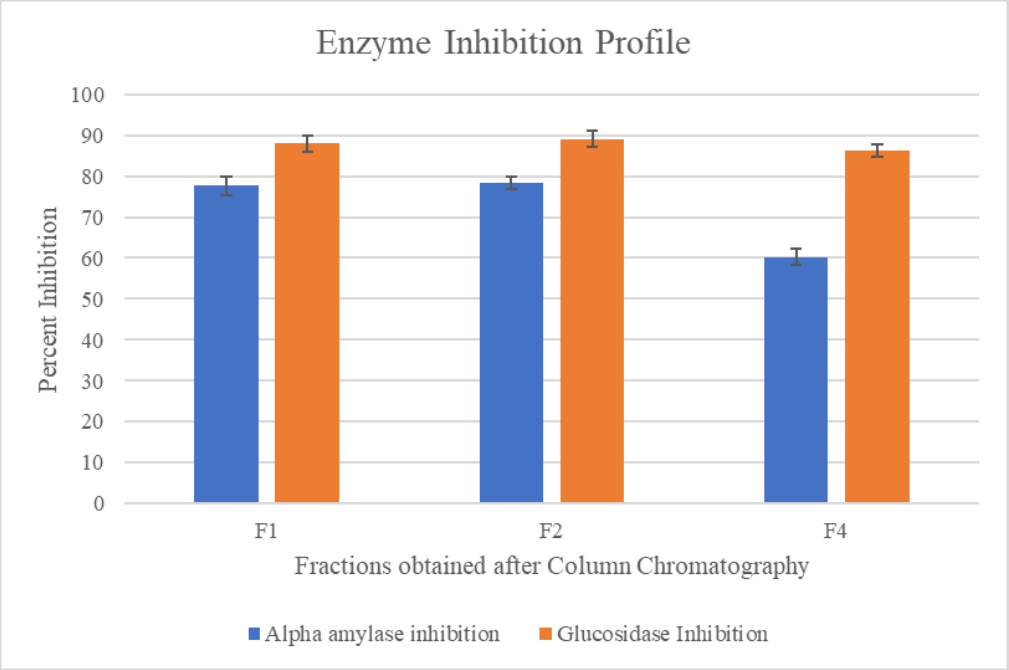

FIGURE 4.29: The graphical representation of enzyme inhibitory profile of the fraction of methanolic leaf extract of Okra

4.4.3 Alpha-Amylase Inhibition

Fraction F2 emerges as the uncontested champion of alpha-amylase inhibition, boasting a staggering 78.4% inhibitory activity with a low standard deviation of 1.53. This fraction towers above other fractions, showcasing a level of enzymatic suppression that borders on the extraordinary. Fraction F1 follows closely, flexing its inhibitory activity at 77.6%, F2. However, F4 stumbles in comparison, delivering a modest 60.2% inhibition.

4.4.4 Alpha-Glucosidase Inhibition

The alpha-glucosidase inhibitory activity observed among the tested fractions is particularly notable, with fraction F2 exhibiting the highest inhibition at 89.1% (±2.09). Fraction F1 follows closely with an inhibition rate of 88.0%, demonstrating comparable potency. Fraction F4, while slightly lower at 86.2%, still presents a significant level of enzymatic inhibition, underscoring its biological relevance.

4.4.5 Comparative Analysis of Enzyme Inhibition Assays

A comparative analysis revealed a consistent and noteworthy pattern across the fractions. Fraction F2 emerges as the most potent dual inhibitor, achieving the highest efficacy in both enzymatic assays. Fraction F1, though marginally less effective than F2, also exhibits robust inhibition against both enzymes. Fraction F4, while showing relatively lower alpha-amylase inhibition, maintains substantial alpha-glucosidase inhibitory potential.

Collectively, these findings highlight the strong enzymatic inhibitory capabilities of the studied fractions, with F2 clearly standing out as the most effective. The low standard deviations across replicates reflect the reliability and reproducibility of the data. These results not only emphasize the therapeutic promise of these fractions but also open avenues for further exploration in biochemical and pharmaceutical applications, particularly in the context of enzyme-targeted interventions for metabolic disorders.

4.5 Analysis and Interpretation of HPLC Results for Methanolic Okra Leaf Extract

This section presents the High-Performance Liquid Chromatography (HPLC) analysis of fractions (F1, F2, F3) obtained from the column chromatography of methanolic okra leaf extract. The HPLC analysis was conducted to characterize the chemical profiles of these fractions and identify major components.

4.5.1 HPLC Analysis of Fraction F-1

The chromatogram for Fraction F-1 reveals the presence of several peaks, indicating a mixture of compounds. The integration results (Table 4.8) provide quantitative data for each detected peak.

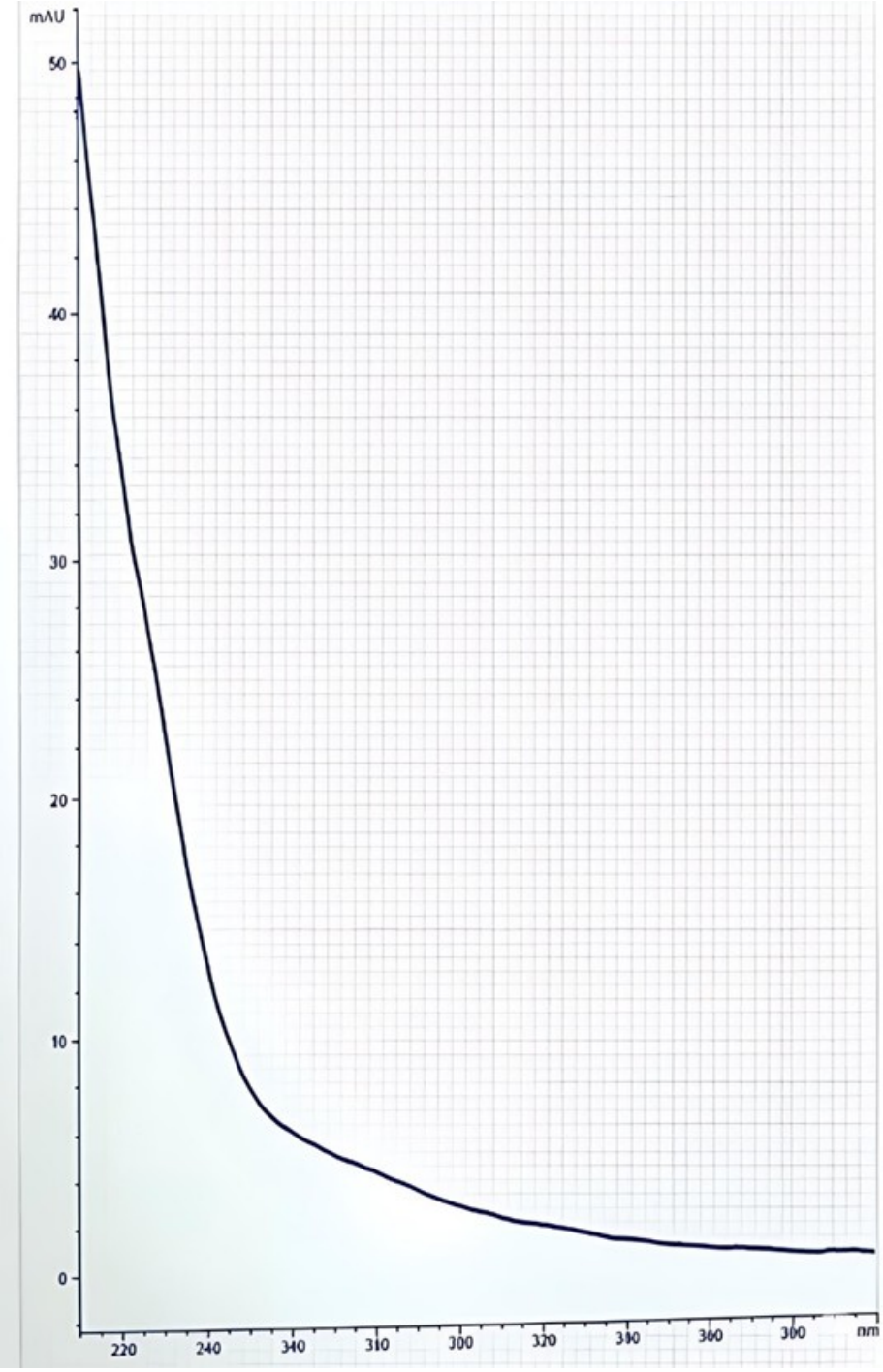

FIGURE 4.30: UV absorbance spectrum for the peak at a retention time of 2.948 minutes. The spectrum provides information about the chromophores present in this specific compound.

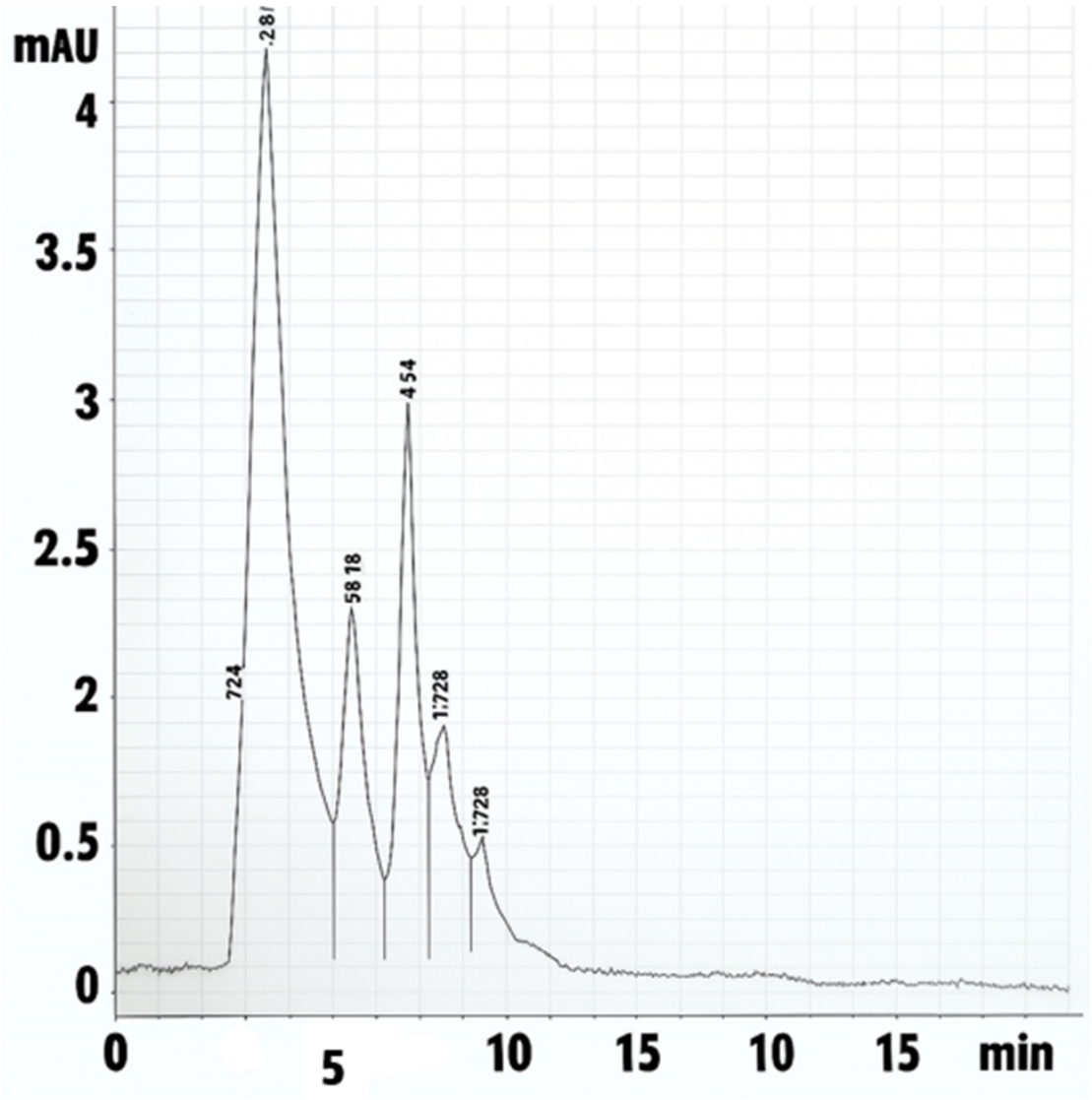

FIGURE 4.31: Chromatogram presented in Figure 4.30 illustrates the elution profile of compounds in Fraction F-1, with absorbance recorded at 254.4 nm. Significant peaks are identified at retention times of approximately 2.378, 2.488, 2.948, 5.012, and 6.118 minutes

TABLE 4.8: Integration results for fraction F-1

Peak #	**Type**	**Time [min]**	**Area [mAU*s]**	**Height [mAU]**	**Width [min]**	**Start [min]**	**End [min]**
1	BV	9:04	7.01549	1.18818	0.0829	2.201	2.437
2	VV	2.488	9.05847	0.841814	0.1395	2.437	2.717
3	VB	22:45	142.99446	2.71922	0.6595	2.717	4.424
4	BB	5.012	3.86467	0.210665	0.224	4.788	5.401
5	BV	6.116	11.00994	0.443554	0.2996	5.768	6.614

In table 4.8, the peak at 2.948 minutes exhibits the largest area (142.99446 mAU*s) and height (2.71922 mAU), suggesting it is the most abundant compound in Fraction F-1.

4.5.2 HPLC Analysis of Fraction F-2

The HPLC chromatogram for Fraction F-2 shows a different profile compared to F-1, with distinct major peaks.

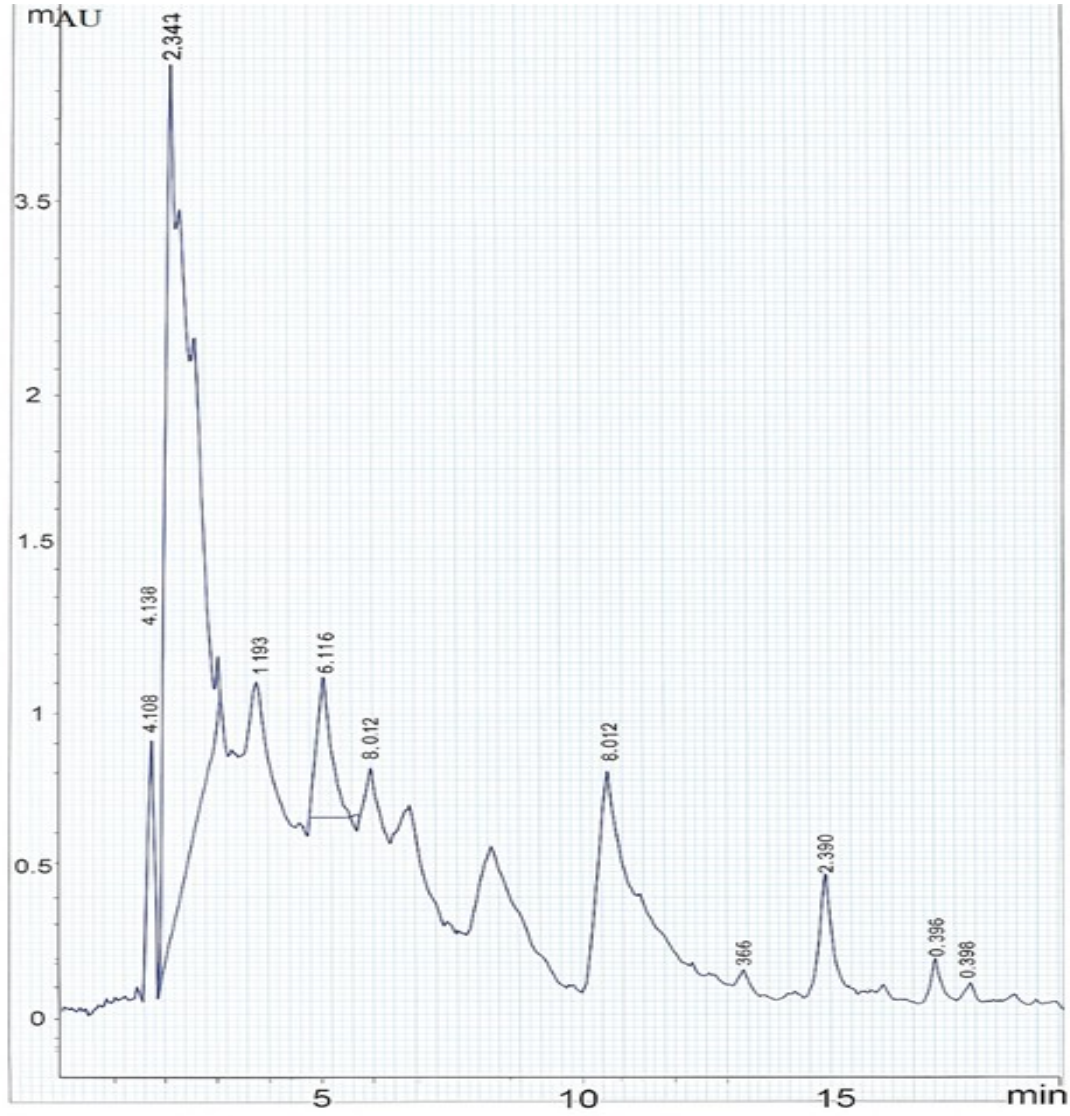

FIGURE 4.32: Chromatogram shows the elution profile of compounds in Fraction F-2. Prominent peaks are observed at approximately 2.334, 2.949, 4.878, 5.924, 6.572, and 7.228 minutes.

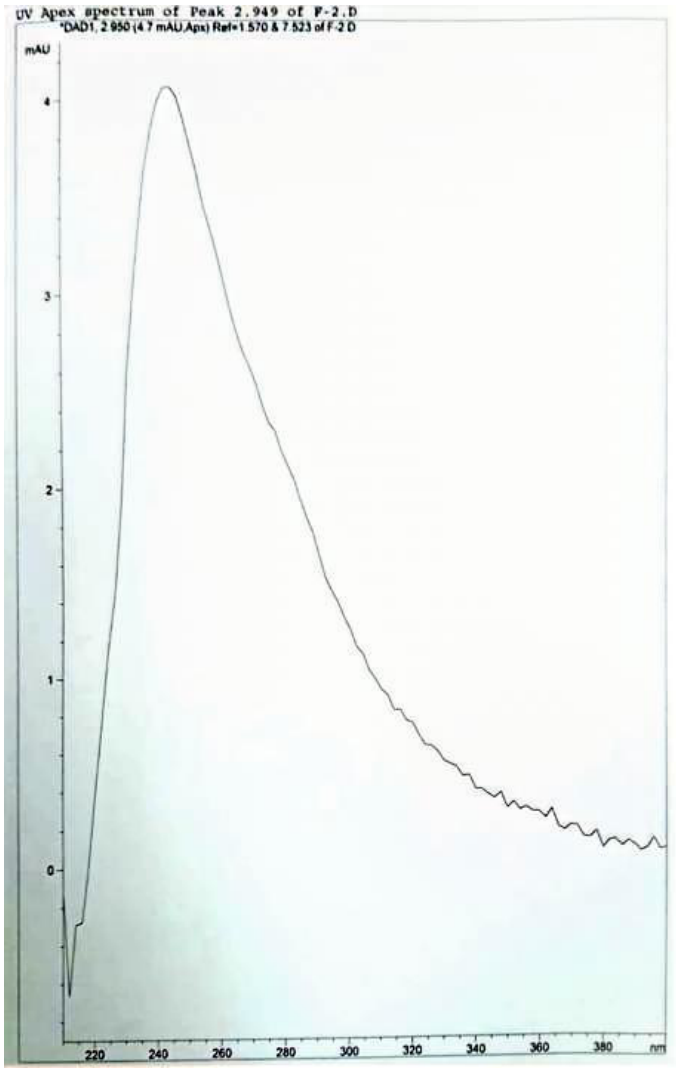

FIGURE 4.33: UV Apex Spectrum of Peak 2.949 of F-2

This figure displays the UV absorbance spectrum for the peak at a retention time of 2.949 minutes, similar to the major peak in F-1.

TABLE 4.9: Integration Results for Fraction F-2

Peak #	**Type**	**Time [min]**	**Area [mAU*s]**	**Height [mAU]**	**Width [min]**	**Start [min]**	**End [min]**
1	BV	8:00	5.22219	1.08868	0.072	1.573	2.381
2	VV	2.949	266.44955	3.5712	0.8865	2.381	4.598
3	VV	21:04	48.42618	1.30215	0.4659	4.598	5.569
4	VV	5.924	64.83658	2.04109	0.4226	5.569	6.429
5	VV	6.572	26.51945	0.827159	0.386	6.429	7.124
6	VB	7.228	8.57414	0.42336	0.2443	7.124	7.52

Similar to F-1, the peak at 2.949 minutes in F-2 is the most prominent, with a significantly larger area (266.44955 mAU*s) and height (3.57120 mAU) than other peaks in this fraction, indicating its high abundance

4.5.3 HPLC Analysis of Fraction F-4

The HPLC chromatogram for Fraction F-4 shows a distinct profile, with a very dominant peak

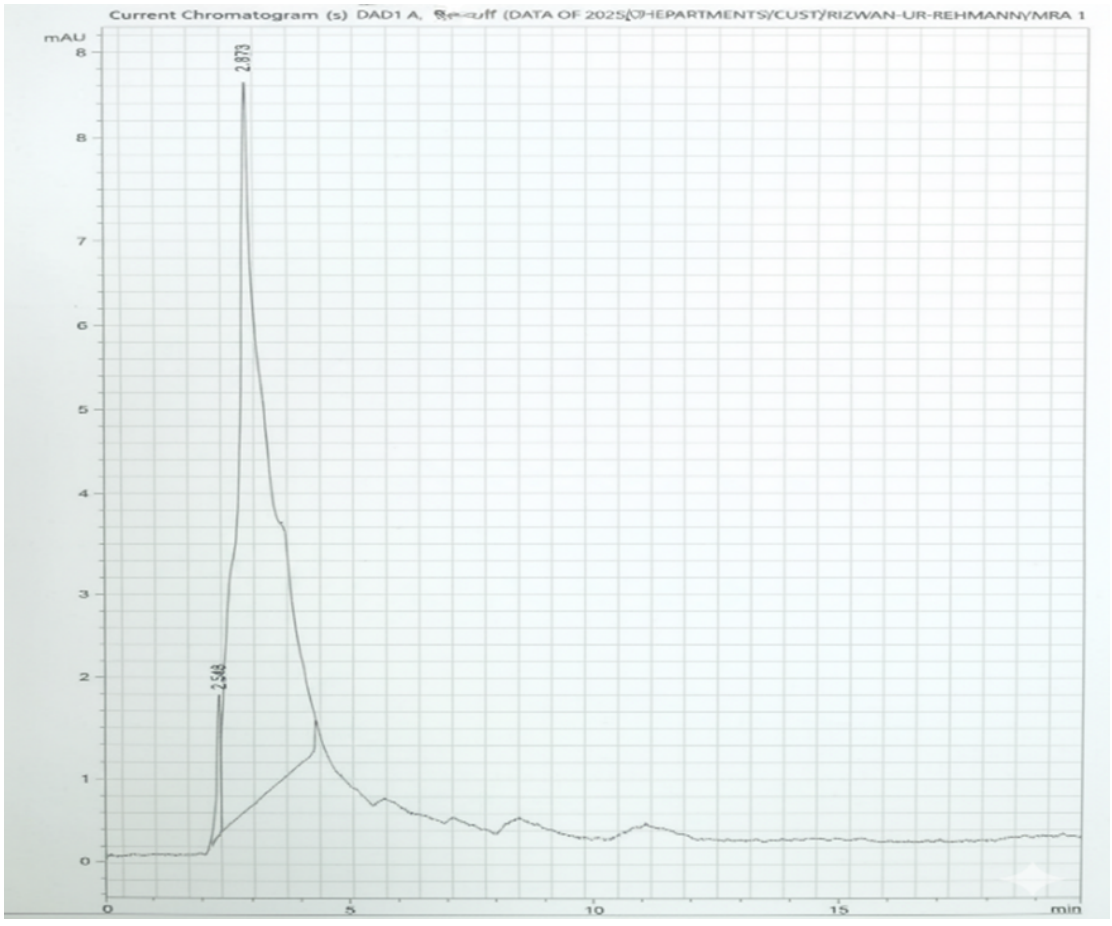

FIGURE 4.34: Chromatogram of Fraction F-4

This chromatogram (in figure 4.33) shows the elution profile of compounds in Fraction F-4. A highly dominant peak is observed at approximately 2.873 minutes, with a smaller peak at 2.348 minutes.

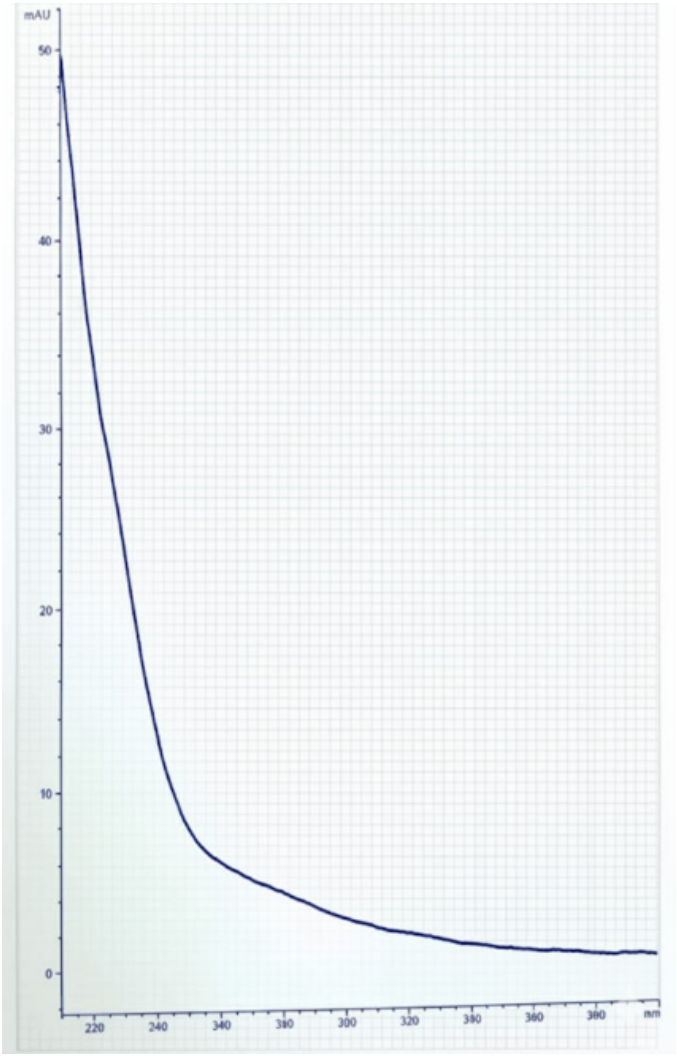

FIGURE 4.35: Chromatogram of Fraction F-4

This figure (see fig 4.35) displays the UV absorbance spectrum for the major peak at a retention time of 2.873 minutes.

TABLE 4.10: Integration Results for Fraction F-4

Peak #	**Type**	**Time [min]**	**Area [mAU*s]**	**Height [mAU]**	**Width [min]**	**Start [min]**	**End [min]**
1	BV	8:21	9.88627	1.66149	0.0834	2.138	2.383
2	VV	2.873	411.34369	8.32308	0.6206	2.383	4.418

Based on the visual representation of the chromatogram, the peak at 2.873 minutes is by far the most abundant compound in Fraction F-4, suggesting a high degree of purification for this specific compound in this fraction

4.5.4 Discussion of HPLC Results

The HPLC analysis demonstrates that the column chromatography successfully separated various compounds from the crude methanolic okra leaf extract into different fractions.

- Fraction F-1 contains a mix of compounds, with a significant component eluting at approximately 2.948 minutes.
- Fraction F-2 also shows multiple peaks, and notably, the peak at 2.949 minutes is the most abundant, suggesting that the compound corresponding to this retention time is concentrated in both F-1 and F-2, but more so in F-2. The slight shift in retention time (2.948 min in F-1 vs. 2.949 min in F-2) could be due to minor variations in chromatographic conditions or peak integration.
- Fraction F-4 exhibits a highly enriched profile for the compound eluting at 2.873 minutes. The dominance of this single peak indicates that this fraction contains a substantially purified compound. The slight difference in retention time (2.873 min) compared to the major peak in F-1 and F-2 (2.948/2.949 min) suggests that while they are closely related or perhaps even the same compound, further investigation would be needed to confirm this definitively. It is possible that the major compound is more concentrated and appears sharper in F-4, leading to a slightly different reported retention time due to the automated integration.

The differences in the chromatographic profiles across the fractions highlight the effectiveness of column chromatography in separating the complex mixture present in the methanolic okra leaf extract.

The presence of a highly concentrated peak in Fraction F-4 suggests that this fraction is a promising candidate for further structural elucidation and biological activity testing of the isolated compound.

4.6 Selection of Lead Compound

A study by M. Suzery *et al.*, [160] of flavonoid analysis (quercetin and rutin) in Alpinia purpurata and Alpinia galanga rhizomes using HPLC technique was conducted. This investigation was performed to assess the presence of rutin and quercetin compounds in Alpinia purpurata and Alpinia galanga rhizomes qualitatively and quantitatively.

The results inferred from the study where quercetin was identified at retention time of 2.66 minutes, while rutin was identified at 2.94 minutes at 254 nm.

The highest peak observed in all three fractions collected from column chromatography, followed by HPLC detection, can tentatively be identified as rutin, with a retention time of 2.94 minutes at 254 nm [160].

4.7 Selection and Preparation of Protein

4.7.1 Structure of Protein

Different experimental techniques exist to determine the structure of target protein. These include X-ray crystallography, cryogenic electron microscopy or nuclear magnetic resonance (NMR). These structures can be accessed from Protein data bank (PDB) [161]. The protein data bank (PDB) provided the 3D structure of the protein.

4.7.2 Protein Purification

The protein crystal structure acquired from PDB were refined to prepare it for docking (Fig 4.35 a, b, c). For this purpose, PyMol software was used to remove heteroatoms and water molecules. After purification EGFR structure was saved in PDB format [162].

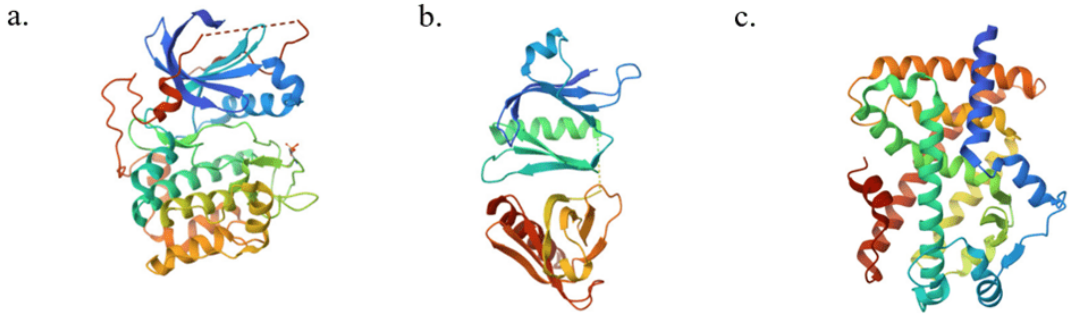

FIGURE 4.36: 3D refined structure of the target proteins a. AkT, b. IRS1, c. PPARG

4.7.3 Determination of Physiochemical Properties of Protein

The chemical and physical characteristics of target protein sequence, were assessed using ExPASy's ProtParam tool. These properties included molecular weight, extinction coefficient, theoretical pI, atomic composition, instability index, estimated half-life, amino acid composition, total No. of residues with positive charge (Arg + Lys), total No. of residues with negative charge (Asp + Glu), grand average of hydropathicity (GRAVY) and aliphatic index [163].

A pH value at which molecule carried no electric charge is designated as isoelectric point (pI). This notion finds its significance in zwitterionic molecules (like proteins, peptides and amino acids). This value indicates the global basic or acidic nature of zwitterionic molecule. Compounds having pI > 7 are basic, and the ones with pI < 7 are acidic [164]. In order to predict stability of protein in vivo, a primary structure dependent method available is dipeptide composition-based Instability Index (II). According to this method proteins are stable if they have II value below 40 [165]. Aliphatic index (AI) is the relative vol. of protein's aliphatic side chains. This serves a crucial role in thermal stability of protein. Higher the Aliphatic index, more thermally stable the protein is [166].

The average hydropathy value of peptide/ protein is represented by GRAVY (Grand Average of Hydropathy) [167]. Hydropathy index of amino acid shows

whether the side chains are hydrophobic or hydrophilic. This idea was first proposed by Jack Kyte and Russell F. Doolittle in 1982. Greater the No., more hydrophobic amino acid is. Isoleucine (4.5) and valine (4.2) are the amino acids with the highest hydrophobicity. On the other hand, arginine (-4.5) and lysine (-3.9) are the amino acids with the highest hydrophilicity. This is very significant when considering the 3D structure of protein as hydrophilic amino acids are commonly present on surface, while hydrophobic ones are buried inside [168].

The extinction coefficient of protein is usually accurate at wavelength of 280nm. In order to determine this, a common approach used is amino acid sequence based theoretical prediction. These theoretical predictions are made based on molar UV absorption (280nm) of tryptophan, tyrosine, and cystine residues [169]. Lys and Arg are cationic with positive charge while glutamic acid and aspartic acid are anionic with negative charge [170].

TABLE 4.11: The physicochemical properties of PPARγ, AkT and IRS1 acquired Protparam tool

Sr.	**Target Proteins**	**MW**	**PI**	**NR**	**PR**	**Ext Co1**	**Ext Co2**	**Instability Index**	**Aliphatic Index**	**GRAVY**
A	PPARγ	5:16	6.87	39	38	12045	11920	45.96	101.03	-0.151
B	AkT/PKB	11:16	5.86	58	49	42205	41830	30.98	76.84	-0.428
C	IRS1	41541.43	9.17	44	53	40130	39880	46.14	76.22	-0.408

4.7.4 Identification of Protein Functional Domains

The globular protein's smallest functional unit is protein domain. A plethora of structural domains have been identified. Every one of them is responsible for a particular function in cell. The protein-protein interactions are mediated by many such domains, by binding to ligand molecules' structural features or motifs [171].

The InterPro database brings together various presumptive models, called signatures, which represent different protein domains, families, and functional sites. It combines data from many sources to give a more complete picture of how proteins work and their roles in organisms [172].

The UniProtKB database freely accessible at www.uniprot.orgw is the most comprehensive high-quality resource for sequence of proteins and their respective functional information.

It gives a summary of computationally predicted or experimentally verified information. This information is provided by biocuration team [173]. From Uniprotkb, fasta format sequence of IRS1, AkT and PPARγ proteins were obtained and then used in Interpro.

Fig 4.36 shows that protein IRS1 had 2 functional domains and chain with 264 residues while figure 4.37 illustrates that protein AkT had 1 functional domain and chain with 276 residues and fig 4.38 shows that protein PPARγ had several functional domains and chain with 336 residues.

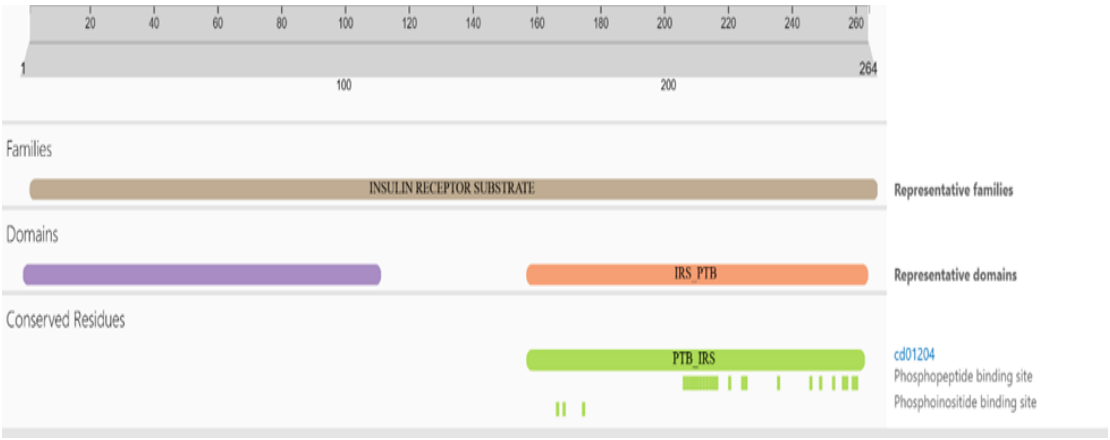

FIGURE 4.37: Functional domains of IRS1

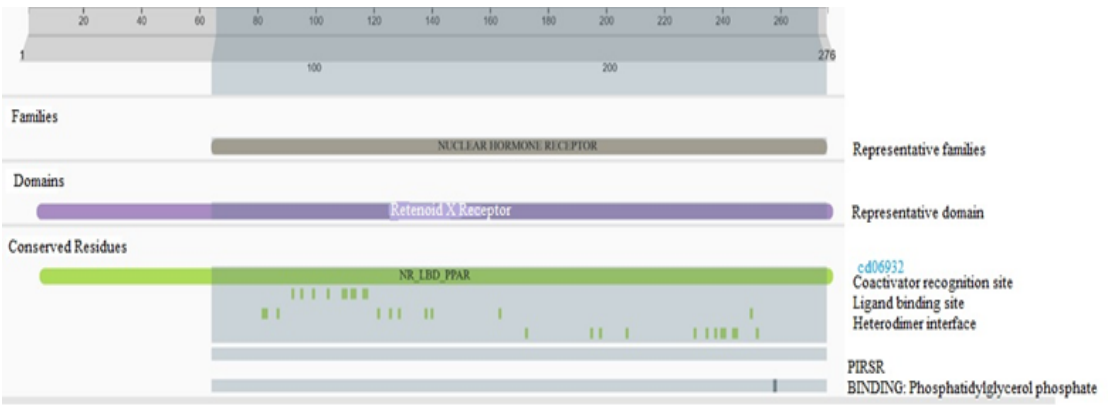

FIGURE 4.38: Functional domains of AkT

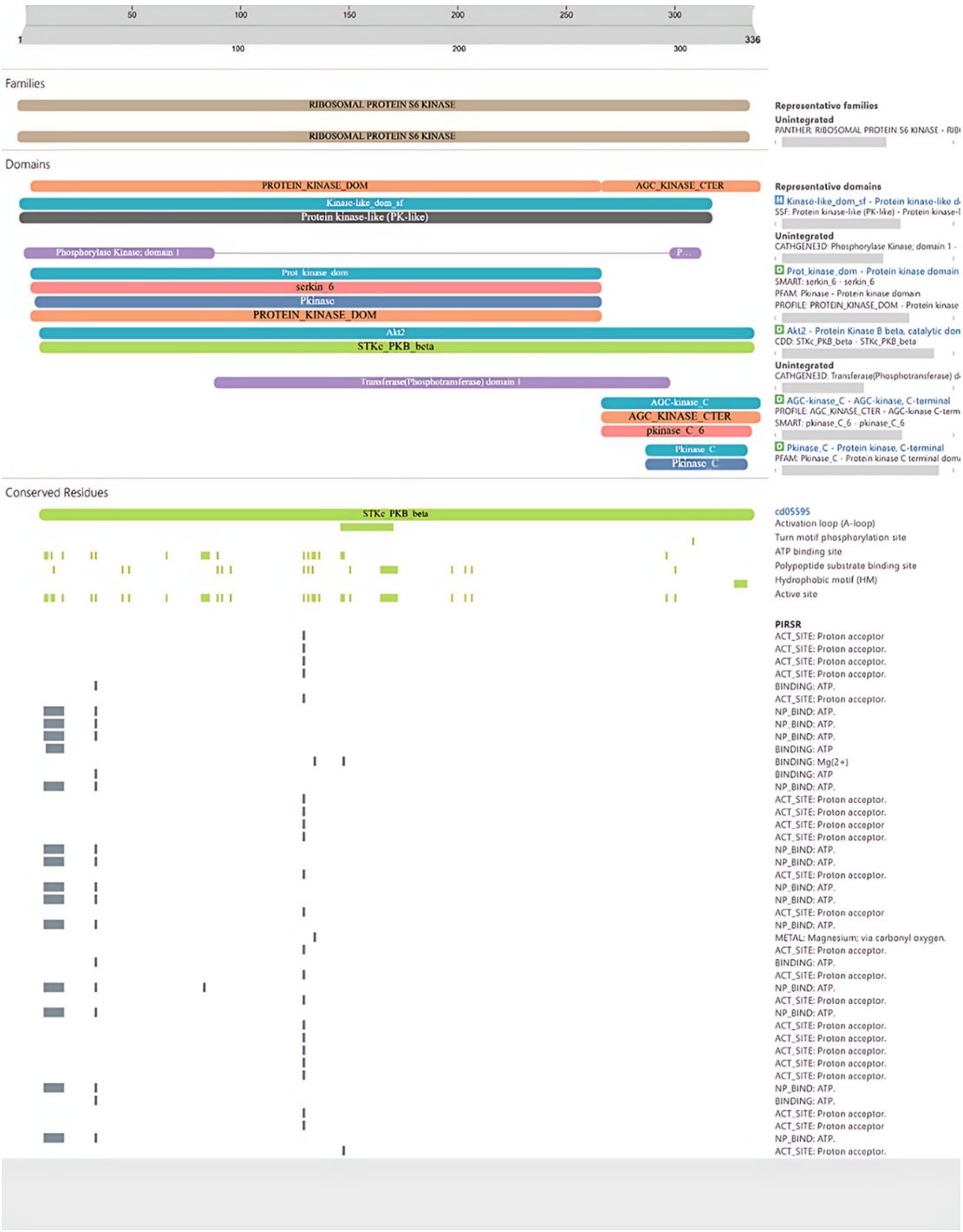

FIGURE 4.39: Functional domains of PPRARG

4.7.5 Binding Pockets Prediction

The capability to identify possible binding pockets and sub-pockets of a protein of interest is provided by DogSiteScorer. With the help of a support vector machine

(SVM), it then assesses draggability by examining the geometrical and physico-chemical characteristics of these pockets [174].

TABLE 4.12: Binding pockets of the target proteins

Sr.	Protein Name	Binding Pockets	Pockets Name	Volume	Surface Area
a	AkT	0:00	P-1	1217.92	1283.86
			P-2	279.42	355.8
			P-3	272.58	355.8
			P-4	237.18	454.46
			P-5	216.51	217.81
			P-6	194.43	307.95
			P-7	172.93	483.02
			P-8	161.02	260.72
			P-9	146.3	253
			P-10	131.97	252.45
			P-11	121.47	253.9
			P-12	113.86	222.55
			P-13	112.58	318.81
			P-14	111.49	282.18
b	IRS1	11	P-1	848.9	994.36
			P-2	778.37	1089.66
			P-3	707.78	951.55
			P-4	239.81	431.22
			P-5	237.57	463.06
			P-6	232.77	431.62
			P-7	211.65	343.03
			P-8	181.76	304.69
			P-9	131.46	312.92
			P-10	128.06	288.59
			P-11	122.24	249.17
c	PPARγ	9	P-1	1820.93	1975.02
			P-2	314.05	473.08
			P-3	172.67	298.38
			P-4	166.27	382.52
			P-5	164.86	368.84
			P-6	101.57	216.9
			P-7	100.93	282.91
			P-8	100.22	208.1

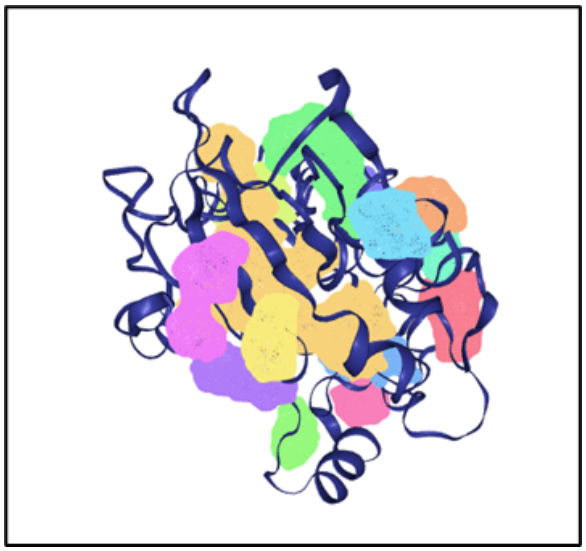

FIGURE 4.40: binding pockets of AkT

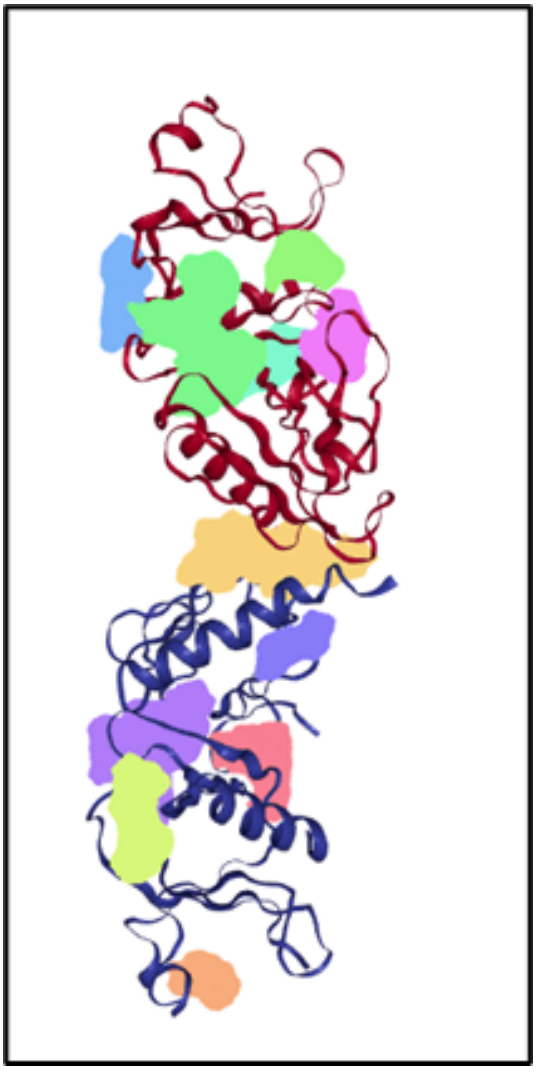

FIGURE 4.41: Functional domains of IRS1

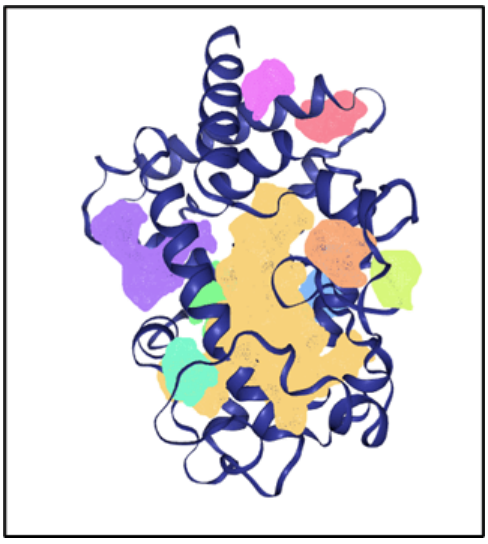

FIGURE 4.42: Functional domains of PPARG

4.8 Ligands Selection and Preparation

An open chemistry database called PubChem provided information about chemical properties, structures, and biological activities. It is managed by National Institutes of Health (NIH). It mainly focuses on small molecules but also have macromolecules like peptides, lipids, carbohydrate, nucleotides etc. [161]. Literature review and HPLC results revealed rutin as ligand compound, and their respective structure was procured from PubChem in SDF format. Table **??** shows molecular weight, formula and structure of the ligand obtained from PubChem. Using PyMol they were converted to PDB format. This was visualized in Discovery studio visualizer.

TABLE 4.13: Physicochemical properties of the ligand compound

Ligand	**Formula**	**Weight**	**Canonical smile**	**Molecular structure**
Rutin	$C_{27}H_{30}O_{16}$	610.5 g/mol	C[C@H]1[C@@H]([C@H]([C@H]([C@@H](O1)OC[C@@H]2[C@H]([C@@H]([C@H]([C@@H](O2)OC3=C(OC4=CC(=CC(=C4C3=O)O)O)C5=CC(=C(C=C5)O)O)O)O)O)O)O)O	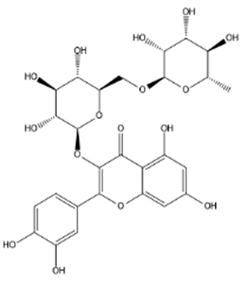

Energy minimization was done by Chem3D and then file was saved as PDB format as show on fig 4.43.

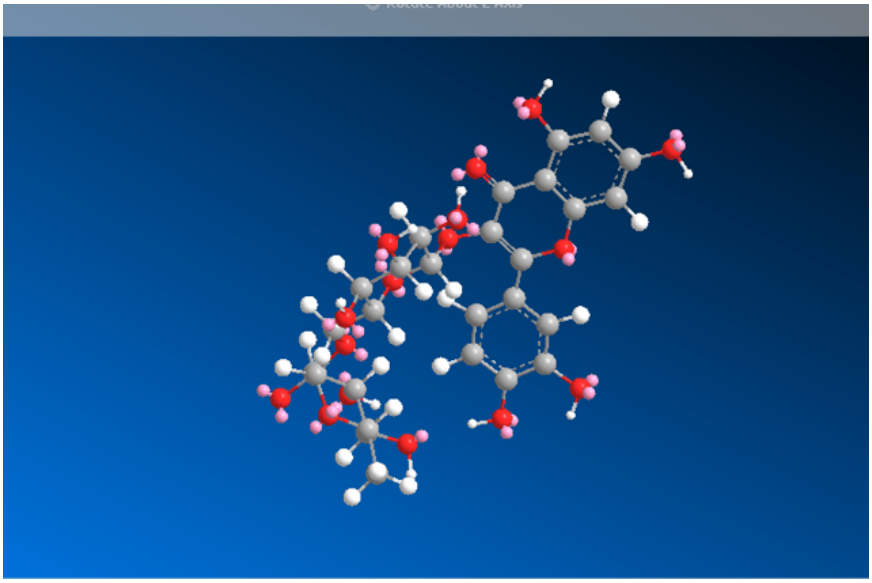

FIGURE 4.43: Structure of energy minimized of Rutin

4.9 Molecular Docking

The user-friendly and common computational structure-based drug design (SBDD) approach is molecular docking (MD). This is being widely used since 1980s. This is preferred to be used when 3D structure of protein is available. The immense rise in availability and power of computers has aided popularity of molecular docking, as they increased No. and accessibility to small molecules and proteinaceous models.

The goal of these *in silico* investigations is to comprehend and anticipate molecular identification. This is done at structural level by identifying potential binding styles, and energy level by prediction of affinity of binding.

Originally MD was developed for use on small molecules (ligand) and target large molecules (protein). There is however, growing interest in docking proteins with proteins, nucleic acid (DNA and RNA) with ligands, and nucleic acid, protein and ligands [161]. Table 4.14 shows docking scores of rutin with the target protein, revealing the highest docking score with AkT i.e., -10.4.

TABLE 4.14: Docking score of the Rutin with the target proteins

Target Protein	Vina Score	Cavity Size	Center			Size		
			x	y	z	x	y	z
AkT	-10.4	1491	43	31	172	24	24	24
IRS1	-9	662	8	37	37	24	24	24
PPARΓ	-9	587	-23	-18	5	24	24	24

4.10 Interactions of Ligands with Protein

A 2D schematic illustration is automatically generated by Discovery Studio program from PDB file input [175]. The output file gives pictorial information about intermolecular interactions between ligands and proteins.

It also shows the strength of interactions, H-bonds, hydrophobic inter-actions and availability of atoms. The software is quite generic and can be used for any ligand. It can also show what kind of interactions occur between protein and nucleic acids [176].

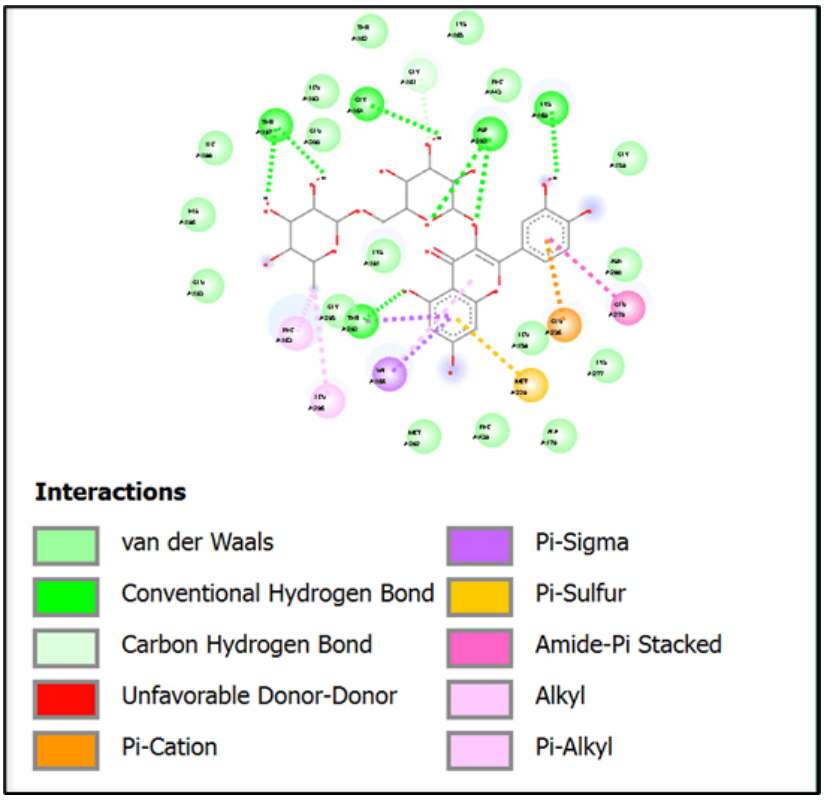

FIGURE 4.44: Docking of Rutin with AkT

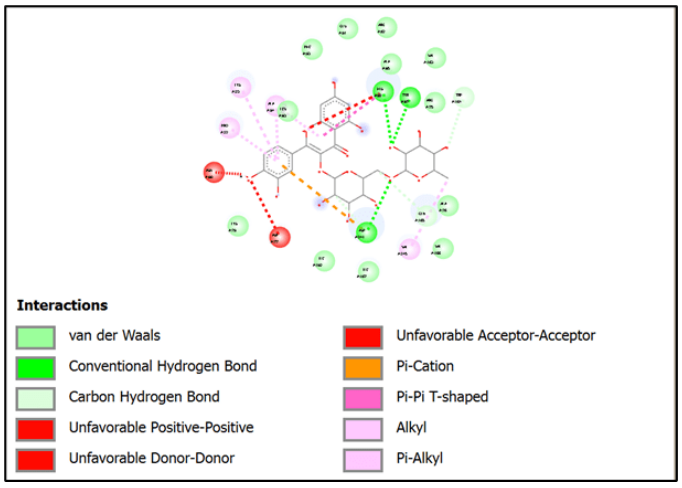

FIGURE 4.45: Docking of Rutin with IRS1

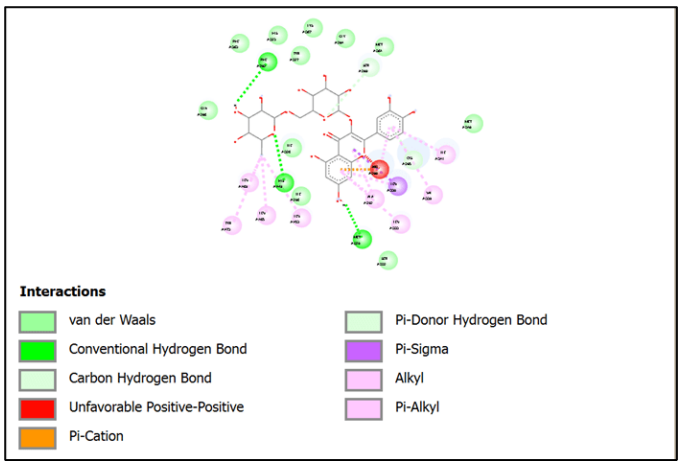

FIGURE 4.46: Docking of Rutin with PPARG

4.11 Virtual Screening through Lipinski Rule of Five

It shows experimental and computational approach to evaluate permeability, soluble nature and effectiveness in process of discovery and development of drug [167]. The five rules are:

1. H-bonds donors (OH, NH) < 5
2. H-bonds acceptors (N, O etc) < 10
3. LogP < 5 (LogP is the fat-water partition coefficient)

4. Mol. Wt. < 500 (5) No. of rotatable keys < 10 [177].
5. Rotatable bonds < 10

According to results in table 4.15, rutin is obeying all rules without violating any rule.

TABLE 4.15: Lipinski's Rule of Five applied to Rutin

Description	**Value**
Molecular Weight	490 g/mol
LogP	4.6871
#Rotatable Bonds	6
#Acceptors	9
#Donors	5
Surface Area	240.901

4.12 ADMET Properties

In early stages of drug development, significant role is played by ADMET properties. This is because high quality drug candidates have both significant efficacy against target molecule as well as proper ADMET traits at required dose [178].

4.12.1 Absorption

The rate and extent to which the drug moves from its point of administration to point of action (target site) is designated as drug absorption. It is a very crucial constituent in pharmacokinetics of drug. The drug must cross numerous barriers to reach its target site. The dose that should be administered is dictated by: 1) rate and extent of absorption, 2) time required by drug to produce a significant/ noticeable effect [179]. If the log Papp value of a chemical is higher than 0.90 cm/s, then it is believed to have high-level Caco-2 permeability (on pkCSM) [180]. After oral drug administration, water solubility is critical part in pharmacological reaction of drug. Increase in water solubility ensures good drug features like high absorption and bioavailability. These in turn increase conc. of drug in plasma at

target site, ensuring therapeutic effectiveness of drug [95]. A compound solubility ranges from -4 to -2; Soluble (-2 to 0), and extremely soluble (> 0).

The skin permeability value (recommended > -2.5cm/h) is an important feature to enhance effectiveness of drug. It is specifically important in development of drugs with transdermal route of administration [92]. P-glycoprotein (P-gp) is an ABC transporter (ATP-binding cassette). Its function to provide the biological hinderance by elimination of toxins and xenobiotics. P-gp I/II inhibitor is the ability of chemical to stop transportation of P-gp I and P-gp II. There is important pharmacokinetics outcome for P-gp substrates when P-gp mediated transport is modified [180].

The absorption properties of rutin, as predicted by pkCSM as illustrated by table 4.16, reveal notable limitations in its oral bioavailability. The compound shows moderate water solubility, with a log mol/L value of -2.892, implying that while not completely insoluble, its solubility may still present formulation challenges. Its Caco-2 permeability value of -0.949 (log Papp in 10^{-6} cm/s) categorizes it as having low permeability, reflecting its poor ability to passively diffuse across intestinal epithelial cells. Furthermore, the predicted human intestinal absorption is just 23.446%, significantly below the commonly accepted 30% threshold for good absorption, confirming its limited oral uptake. Rutin also displays low skin permeability, with a log Kp value of -2.735, indicating minimal ability for transdermal transmission. It is identified as a substrate of P-glycoprotein, a membrane transporter involved in drug efflux, which may further decrease its intracellular concentration and systemic absorption. However, it does not inhibit P-glycoprotein I or II, suggesting it is unlikely to interfere with the transport of other substances. These findings align with existing knowledge of rutin's poor bioavailability and underscore the need for advanced formulation strategies to improve its pharmacokinetic properties.

TABLE 4.16: Rutin(ligand) with respective absorption properties

Model Name	**Predicted Value**	**Unit**
Water Solubility	-2.892	Numeric (log mol/L)
Caco2 permeability	-0.949	Numeric (log Papp in 10-6 cm/s)

Table 4.16 continued from previous page

Model Name	Predicted Value	Unit
Intestinal Absorption (human)	23.446	Numeric (% Absorbed)
Skin Permeability	-2.735	Numeric (Log Kp)
P-glycoprotein substrate	Yes	Categorical (Yes/No)
P-glycoprotein I inhibitor	No	Categorical (Yes/No)
P-glycoprotein II inhibitor	No	Categorical (Yes/No)

4.12.2 Distribution

The drug is distributed to interstitial and intracellular compartments when the drug reached the blood stream. Many drugs may bound to plasma protein in blood. This binding is reversible and the bound drug and unbound drug exist in dynamic equilibrium. Any change in conc. of one of them is always followed by change in conc. of other. Only unbound drug is considered pharmacologically active and have the ability to cross membranes and/ or interact with target sites. The volume of distribution (Vd) represents the vol. in which a drug needs to distribute to achieve the same conc. as that detected in the blood plasma. We can calculate Vd by division of amount of the drug in the body with the plasma conc. Vd gives an insight about how much drug is present in extravascular tissues. Vd is affected by lipid solubility, since more lipid soluble drugs have better cell penetration (and more Vd) [179].

The drug capacity to be dispersed in the body is determined by 2 important factors i.e. volume of supply at steady state (VDss) and the blood-brainbarrier (BBB). When a molecule has VDss higher than 0.45, it has good dispersion. When log BB is higher than 0.3, molecule can move quickly across BBB [180].

Table 4.17 shows the distribution characteristics of rutin, as predicted by pkCSM, providing insight into its pharmacokinetics within the human. The volume of distribution (VDss) is estimated at 1.663 log L/kg, equivalent to approximately 46 L/kg. This suggests that rutin has moderate to high tissue distribution, indicating it diffuses extensively into body tissues rather than remaining confined to plasma. The fraction unbound (Fu) in plasma is 0.187, meaning 18.7% of rutin is unbound

and pharmacologically active. This moderate plasma protein binding indicates that while a significant portion is bound, a considerable amount remains available for therapeutic action or clearance.

Regarding central nervous system (CNS) distribution, predictions indicate minimal potential. The blood-brain barrier (BBB) permeability is -1.899 (log BB), reflecting poor brain penetration. Similarly, the CNS permeability (log PS) is extremely low at -5.178, confirming negligible brain tissue permeability. These findings suggest that rutin is unsuitable for CNS disorder treatments due to its limited ability to cross into the brain. In conclusion, rutin demonstrates favorable peripheral tissue distribution but restricted CNS access, which is critical to consider in its therapeutic applications and formulation strategies.

TABLE 4.17: Distribution properties predicted of rutin

Model name	**Predicted value**	**Unit**
VDss (human)	1.63	Numeric (Log L/kg)
Fraction unbound (human)	0.187	Numeric (Fu)
BBB permeability	-1.899	Numeric (Log BB)
CNS permeability	-5.178	Numeric (Log PS)

4.12.3 Metabolism

After distribution of drug throughout the body, it is metabolized. It converts to polar inactive metabolites so that it can be eliminated from the body. Drugs which are lipophilic in nature can pass through biological membranes and reach target site with ease. This lipophilicity can hinder their excretion from the body [179]. An enzyme that is involved in detoxification in liver is cytochrome P450. It also plays role in drug metabolism. The pharmacokinetics of drugs is significantly impacted by P450 inhibitors. Therefore, it is important to evaluate if the molecule in question is substrate of CYP2D6/CYP3A4, and can be acted upon by P450. CYP 450 acts on xenobiotics, oxidizing them and allowing their excretion [180].

The metabolism profile of Rutin, as predicted in table 4.18 by pkCSM, indicates minimal interaction with the major cytochrome P450 (CYP450) enzyme system,

crucial for drug metabolism. Predictions suggest that Rutin is not a substrate for CYP2D6 or CYP3A4, two key enzymes involved in drug metabolism, implying it is unlikely to undergo significant hepatic metabolism via these isoenzymes, potentially influencing its metabolic stability and half-life.

Additionally, Rutin is not predicted to inhibit any major CYP450 isoforms, including CYP1A2, CYP2C19, CYP2C9, CYP2D6, and CYP3A4. This lack of inhibitory activity suggests a low risk of drug-drug interactions through CYP-mediated pathways, enhancing its safety profile when co-administered with other drugs relying on these enzymes for metabolism. The metabolic characteristics of Rutin indicate it is neither a substrate nor an inhibitor of key CYP450 enzymes, illustrating it may primarily undergo non-CYP metabolic pathways, such as phase II conjugation (e.g., glucuronidation or sulfation).

The metabolic characteristics of Rutin indicate it is neither a substrate nor an inhibitor of key CYP450 enzymes, illustrating it may primarily undergo non-CYP metabolic pathways, such as phase II conjugation (e.g., glucuronidation or sulfation). This profile highlights its low hepatotoxicity potential and minimal interference with common metabolic enzymes, favorable attributes for pharmacokinetics and safety.

Table 4.18: Metabolism characteristics of Rutin

Model Name	**Predicted Value**	**Unit**
CYP2D6 substrate	No	Categorical (Yes/No)
CYP3A4 substrate	No	Categorical (Yes/No)
CYP1A2 inhibitor	No	Categorical (Yes/No)
CYP2C19 inhibitor	No	Categorical (Yes/No)
CYP2C9 inhibitor	No	Categorical (Yes/No)
CYP2D6 inhibitor	No	Categorical (Yes/No)
CYP3A4 inhibitor	No	Categorical (Yes/No)

4.12.4 Excretion

Liver metabolism and renal excretion are two main ways via which drugs are excreted from the body. Some drugs may also be secreted in negligible amount

via sweat, tears and saliva. The elimination of drug via these routes depends on 1) pH od urine and 2) nonionized lipophilic diffusion of drug through glandular epithelial cells [179].

The excretion characteristics of rutin, as depicted in table 4.19, reveal a total clearance value of -0.369 (log ml/min/kg), indicating a relatively low clearance rate. This suggests that rutin may remain in the body for an extended duration, potentially witnessing in a longer shelf-life. Furthermore, rutin is not a substrate for the renal organic cation transporter 2 (OCT2), as classified under the "No" category. Consequently, its renal excretion is unlikely to be mediated by OCT2, which may affect its elimination pathway and overall pharmacokinetic profile.

Drugs with low clearance rates generally demonstrate prolonged systemic exposure, which can be beneficial for sustained therapeutic effects but may also pose risks of accumulation. The lack of OCT2-mediated renal excretion implies that rutin's elimination may depend on alternative mechanisms, such as hepatic metabolism or other transporters. These results are consistent with the established pharmacokinetic behavior of flavonoids, which are often extensively metabolized rather than eliminated via renal excretion.

TABLE 4.19: Excretion characteristics of Rutin

Model Name	**Predicted Value**	**Unit**
Total Clearance	-0.369	Numeric (log mil/min/kg)
Renal OCT2 substrate	No	Categorical (Yes/No)

4.12.5 Toxicity

LD50 is the toxic dose decided in mg/kg body weight. LD refers to the median lethal dose, indicating the amount of a compound resulting to leathality in 50% of test subjects. *T. pyroformis* toxicity values greater than -0.5 are considered non-toxic [181].

Using Salmonella typhimurium, AMES test is employed to analyze mutagenicity of a compound. The bacterial cells upon exposure to mutagenic materials undergo

several mutations, and allow bacteria to prosper in environment with no histidine. Positive results implicate that compound is mutagenic and may cause cancer. hERG I and II sheds light on cardiotoxicity as they lead to lethal arrythmias of ventricles by inhibiting potassium channels. Pharmacokinetics of drug is affected by hepatotoxicity. The oral rat chronic toxicity (dose 0.341 to 2.674) analyzes the impact of drug on body upon repeated ingestion, skin application or inhalation during a specific time period. This parameter allows evaluation of MRTD to start clinical trial on humans. MRTD estimates a threshold where substance becomes toxic to humans and is crucial in dose determination during clinical trials [182].

Minnow toxicology testing determines the amount/dose which causes 50% death in research animals (fathead minnows). Substances have acute toxicity when they have low LC50 (less than 0.5 mM or Log LC50 less than -0.3). Skin sensitization determines if the substance will cause allergic contact dermatitis [183].

The toxicity profile of rutin, as shown by table 4.20, indicates a relatively safe compound with some notable exceptions. Rutin is predicted to be non-mutagenic (AMES toxicity: No) and non-hepatotoxic (Hepatotoxicity: No), consistent with its established safety as a natural flavonoid.

The highest tolerated dosage (0.452 log mg/kg/day) and oral rat acute toxicity (LD50: 2491 mol/kg) suggest low acute toxicity, typical of flavonoids. However, the prediction of hERG I channel inhibition (hERG I inhibitor: Yes) raises concerns about potential cardiotoxicity and QT interval prolongation, a known risk for certain drugs. In contrast, it does not inhibit the hERG II channel (hERG II inhibitor: No), indicating a selective interaction.

The oral rat chronic toxicity (LOAEL: 3.673 log mg/kg_bw/day) indicates moderate safety for long-term use, while the absence of skin sensitization (Skin Sensitisation: No) supports its potential for topical applications. The low toxicity to T. Pyriformis (0.285 log µg/L) and minnows (7.677 log mM) suggests minimal environmental hazard, a favorable attribute for natural compounds.

Therefore, rutin's toxicity profile is generally benign, apart from the hERG I inhibition, which warrants further experimental validation to assess potential cardiac

risks. These predictions align with existing literature on rutin's safety but emphasize caution regarding possible cardiovascular effects.

TABLE 4.20: Toxicity features of Rutin

Model Name	Predicted Value	Unit
AMES toxicity	No	Categorical (Yes/No)
Max. tolerated dose	0.452	Numeric (log mg/kg/day)
hERG I inhibitor	Yes	Categorical (Yes/No)
hERG II inhibitor	No	Categorical (Yes/No)
Oral Rat Acute Toxicity (LD50)	2491	Numeric (mol/kg)
Oral Rat Chronic Toxicity (LOAEL)	3.673	Numeric (log mg/kg _ bw/day)
Hepatotoxicity	No	Categorical (Yes/No)
Skin Sensitization	No	Categorical (Yes/No)
T. Pyriformis toxicity	0.285	Numeric (log ug/L)
Minnow toxicity	7.677	Numeric (log mM)

4.13 Discussion of Results

4.13.1 Systematic Development of a Chromatographic Protocol for the Isolation of Bioactive Constituents

The initial and critical stage of the phytochemical investigation involved the establishment of an efficient separation protocol to isolate the active principles from the complex crude extract. To this end, Thin-Layer Chromatography (TLC) was employed as an analytical screening technique to evaluate a matrix of solvent systems of varying polarities and compositions. The efficacy of each mobile phase was rigorously assessed based on key chromatographic parameters, including the resolution of constituent bands, optimal retardation factor (Rf) values, and the absence of tailing. This systematic optimization was paramount to achieving high-resolution separation on a preparative scale.

Guided by the analytical TLC results, a refined and isocratically-run gravity column chromatography system was employed. The stationary phase was meticulously packed to ensure uniformity, and the optimized mobile phase was applied

to facilitate the differential migration of chemical constituents through the column based on their distinct adsorption affinities. This process successfully yielded three primary fractions (F-A, F-B, and F-C), which were collected based on their elution profiles.

Subsequent in vitro pharmacological screening revealed that these fractions possessed significant antidiabetic (e.g., α-amylase & α-glucosidase inhibition) and antioxidant (e.g., DPPH radical scavenging, FRAP assay) activities, confirming the success of the bioactivity-guided fractionation approach. These bioactive fractions were then concentrated and subjected to advanced analytical techniques for detailed phytochemical profiling.

4.13.2 Structural Elucidation of Rutin via High-Performance Liquid Chromatography

To definitively characterize the chemical identity of the bioactive compounds within the active fractions, High-Performance Liquid Chromatography (HPLC) was employed under rigorously optimized conditions. The HPLC analysis of the most potent fraction revealed a dominant, sharp, and symmetrical peak, indicating a high purity compound within that fraction. The initial identification strategy was a comparative analysis: the retention time and the full UV-Vis absorption spectrum (200-400 nm) of this unknown peak were meticulously compared to those of an authentic rutin standard analyzed under identical instrumental parameters.

The observed chromatographic and spectral congruence provided strong preliminary evidence for the identity of the compound. To solidify this identification, an extensive review of the scientific literature was conducted, cross-referencing the obtained HPLC data with published chromatographic fingerprints of rutin from similar matrices. This conclusive multi-point comparison confirmed the major bioactive compound as rutin (quercetin-3-O-rutinoside), a prominent flavonoid glycoside extensively documented in the scientific literature for its potent dual antidiabetic and antioxidant properties, thereby establishing a clear phytochemical basis for the observed biological activities of the fraction.

4.13.3 Computational Validation of Mechanism: Molecular Docking Studies with IRS Signaling Pathway Proteins

To transcend mere correlation and propose a mechanistic rationale for the antidiabetic effects of rutin, sophisticated *in silico* molecular docking simulations were conducted. This computational approach predicts the preferred orientation and binding affinity of a small molecule (ligand) when bound to a target protein's active site. Rutin, identified as the key bioactive, was docked against three critically important protein targets intricately involved in the Insulin Receptor Substrate (IRS) signaling pathway, a master regulatory cascade for glucose metabolism and insulin sensitivity:

- IRS1 (Insulin Receptor Substrate 1): The primary docking platform that transmits signals from the activated insulin receptor to downstream effectors, essential for initiating metabolic actions.
- Akt (Protein Kinase B): A serine/threonine kinase that acts as a central signaling node, critically regulating insulin-mediated glucose uptake via GLUT4 translocation and influencing cell survival and proliferation.
- PPARγ (Peroxisome Proliferator-Activated Receptor Gamma): A ligand-activated nuclear transcription factor that regulates genes involved in adipogenesis, lipid metabolism, and systemic insulin sensitization.

The docking analysis yielded quantitatively robust results, demonstrating that rutin possesses remarkably strong binding affinities for all three targeted proteins. The most thermodynamically favorable and stable interaction was observed with Akt, as evidenced by an exceptional docking score of -10.0 kcal/mol (using AutoDock Vina), which signifies a highly spontaneous and stable binding interaction. These computational findings propose a compelling putative mechanism of action: rutin may exert its potent antidiabetic effects by directly binding to and modulating the activity of key proteins in the IRS pathway. Its pronounced

affinity for Akt suggests a primary role in potentiating the insulin signal downstream, thereby enhancing glucose uptake and metabolism. This modulation of the IRS1/Akt/PPARγ axis presents a rational, multi-target molecular explanation for the observed improvement in insulin sensitivity and glucose homeostasis.

Chapter 5

Conclusion

This text investigated the anti-diabetic and antioxidant attributes of okra (*Abelmoschus esculentus*) through a comprehensive lab-driven and computational tools-based approach. The research involved the preparation of plant extracts, followed by fractionation using thin layer chromatography and column chromatography. Three activated fractions were obtained based on anti-diabetic (α-amylase and α-glucosidase inhibition) and anti-oxidant assays. Subsequent High-Performance Liquid Chromatography analysis identified Rutin as a prominent bioactive compound within these fractions, based on retention time comparison with literature data.

Furthermore, in silico docking was conducted to assess the interaction of Rutin with proteins of the insulin receptor substrate signaling pathway, specifically IRS1, Akt, and PPARγ, all critical in glucose metabolism and insulin sensitivity. Among these, Rutin exhibited a high binding affinity for Akt (vina score of -10), suggesting a potential mechanism for its anti-diabetic effects through modulation of Akt-mediated signaling.

To summarize, this research provides evidence for the capability of okra extracts, particularly Rutin, as a source of anti-diabetic and antioxidant compounds. The in vitro and in silico findings warrant further investigation into the bioavailability, in vivo efficacy, and clinical potential of okra-derived compounds for the containment of T2DM.

5.1 Recommendations

- Further studies, including animal model-based studies and clinical trials, is warranted to fully elucidate the therapeutic capability of okra and its isolated compounds in the containment of T2DM
- Further studies should emphasize on bioavailability enhancement strategies, to completely elucidate the pharmaceutical and nutraceutical potential of okra and its bioactive constituents by up-scaling.
- The results of this investigation may pave the way for the formulation of novel, okra-based therapeutic interventions for diabetic patients.

Bibliography

[1] "National diabetes statistics report," May 2024. [Online]. Available: https://www.cdc.gov/diabetes/php/data-research/index.html

[2] N. A. ElSayed *et al.*, "Classification and diagnosis of diabetes: Standards of care in diabetes—2023," *Diabetes Care*, vol. 46, no. Supplement, pp. S19–S40, Dec 2022.

[3] V. Bojkovska, "90+ important diabetes statistics in 2024," Apr 2022. [Online]. Available: https://www.myshortlister.com/insights/diabetes-statistics

[4] "Diagnosis and classification of diabetes mellitus," *Diabetes Care*, vol. 37, no. Supplement, pp. S81–S90, Dec 2013.

[5] F. B. Hu *et al.*, "Diet, lifestyle, and the risk of type 2 diabetes mellitus in women," *New England Journal of Medicine*, vol. 345, no. 11, pp. 790–797, 2001.

[6] C. O'Donnell, "Diabetes," in *Contact Lens Practice*. Elsevier, 2024, pp. 344–350.e2.

[7] "Diabetes, heart disease, & stroke," Apr 2025. [Online]. Available: https://www.niddk.nih.gov/health-information/diabetes/overview/preventing-problems/heart-disease-stroke

[8] A. Sharma, S. Mittal, R. Aggarwal, and M. K. Chauhan, "Diabetes and cardiovascular disease: inter-relation of risk factors and treatment," *Future Journal of Pharmaceutical Sciences*, vol. 6, pp. 1–19, 2020.

[9] A. S. M. Sayem, A. Arya, H. Karimian, N. Krishnasamy, A. Ashok Hasamnis, and C. F. Hossain, "Action of phytochemicals on insulin signaling pathways accelerating glucose transporter (glut4) protein translocation," *Molecules*, vol. 23, no. 2, p. 258, 2018.

[10] J. J. Marín-Peñalver, I. Martín-Timón, C. Sevillano-Collantes, and F. J. del Cañizo-Gómez, "Update on the treatment of type 2 diabetes mellitus," *World Journal of Diabetes*, vol. 7, no. 17, p. 354, 2016.

[11] T. Sivakumar and B. Deepa, "A critical review on antidiabetic potential of herbal plants and its their bioactive components," *Journal of University of Shanghai for Science and Technology*, vol. 25, no. 01, pp. 303–314, 2023.

[12] O. Matthew, U. O. Ohwo, and M. E. Osawaru, "Morphological characterization of okra (abelmoschus) accessions," *Makara Journal of Science*, pp. 67–76, 2018.

[13] Q. Ayub *et al.*, "Responses of different okra (abelmoschus esculentus) cultivars to water deficit conditions," *Journal of Horticultural Sciences*, vol. 16, no. 1, pp. 53–63, 2021.

[14] N. Temam, W. Mohammed, and S. Aklilu, "Variability assessment of okra (abelmoschus esculentus (l.) moench) genotypes based on their qualitative traits," *International Journal of Agronomy*, vol. 2021, no. 1, p. 6678561, 2021.

[15] W. Tongjaroenbuangam, N. Ruksee, P. Chantiratikul, N. Pakdeenarong, W. Kongbuntad, and P. Govitrapong, "Neuroprotective effects of quercetin, rutin and okra (abelmoschus esculentus linn.) in dexamethasone-treated mice," *Neurochemistry International*, vol. 59, no. 5, pp. 677–685, 2011.

[16] S. Fan *et al.*, "Extract of okra lowers blood glucose and serum lipids in high-fat diet-induced obese c57bl/6 mice," *The Journal of Nutritional Biochemistry*, vol. 25, no. 7, pp. 702–709, 2014.

[17] H. Wang, G. Chen, D. Ren, and S. T. Yang, "Hypolipidemic activity of okra is mediated through inhibition of lipogenesis and upregulation of cholesterol degradation," *Phytotherapy Research*, vol. 28, no. 2, pp. 268–273, 2014.

[18] L. Hu, W. Yu, Y. Li, N. Prasad, and Z. Tang, "Antioxidant activity of extract and its major constituents from okra seed on rat hepatocytes injured by carbon tetrachloride," *BioMed Research International*, vol. 2014, no. 1, p. 341291, 2014.

[19] Y. Yang, Z. Jin, P. Mao, J. Jin, J. Huang, and M. Yang, "Study on anti-fatigue effect of okra extracts," *Chinese Journal of Modern Applied Pharmacy*, vol. 29, no. 4, 2012.

[20] S. Alqasoumi, "'okra' hibiscus esculentus l.: A study of its hepatoprotective activity," *Saudi Pharmaceutical Journal*, vol. 20, no. 2, pp. 135–141, 2012.

[21] B. Xiong *et al.*, "Okra pectin relieves inflammatory response and protects damaged intestinal barrier in caerulein-induced acute pancreatic model," *Journal of the Science of Food and Agriculture*, vol. 101, no. 3, pp. 863–870, 2021.

[22] B. K. Shoichet, S. L. McGovern, B. Wei, and J. J. Irwin, "Lead discovery using molecular docking," *Current Opinion in Chemical Biology*, vol. 6, no. 4, pp. 439–446, 2002.

[23] W. Consultation, "Definition, diagnosis and classification of diabetes mellitus and its complications," 1999, part.

[24] P. Zimmet *et al.*, "Latent autoimmune diabetes mellitus in adults (lada): the role of antibodies to glutamic acid decarboxylase in diagnosis and prediction of insulin dependency," *Diabetic Medicine*, vol. 11, no. 3, pp. 299–303, 1994.

[25] A. Humphrey, D. McCarty, I. R. Mackay, M. J. Rowley, T. Dwyer, and P. Zimmet, "Autoantibodies to glutamic acid decarboxylase and phenotypic features associated with early insulin treatment in individuals with adult-onset diabetes mellitus," *Diabetic Medicine*, vol. 15, no. 2, pp. 113–119, 1998.

[26] Japan and P. C. D. R. Groups, "Coma at the onset of young insulin-dependent diabetes in japan: The results of a nationwide survey," *Diabetes*, vol. 34, no. 12, pp. 1241–1246, 1985.

[27] P. Z. Zimmet, "The pathogenesis and prevention of diabetes in adults: genes, autoimmunity, and demography," *Diabetes Care*, vol. 18, no. 7, pp. 1050–1064, 1995.

[28] J. A. Willis *et al.*, "Islet cell antibodies and antibodies against glutamic acid decarboxylase in newly diagnosed adult-onset diabetes mellitus," *Diabetes Research and Clinical Practice*, vol. 33, no. 2, pp. 89–97, 1996.

[29] O. Hother-Nielsen, O. Faber, N. S. Sørensen, and H. Beck-Nielsen, "Classification of newly diagnosed diabetic patients as insulin-requiring or non-insulin-requiring based on clinical and biochemical variables," *Diabetes Care*, vol. 11, no. 7, pp. 531–537, 1988.

[30] C. F. Verge *et al.*, "Prediction of type i diabetes in first-degree relatives using a combination of insulin, gad, and ica512bdc/ia-2 autoantibodies," *Diabetes*, vol. 45, no. 7, pp. 926–933, 1996.

[31] A. Mølbak, B. Christau, B. Marner, K. Borch-Johnsen, and J. Nerup, "Incidence of insulin-dependent diabetes mellitus in age groups over 30 years in denmark," *Diabetic Medicine*, vol. 11, no. 7, pp. 650–655, 1994.

[32] C. Betterle *et al.*, "Clinical and subclinical organ-specific autoimmune manifestations in type 1 (insulin-dependent) diabetic patients and their first-degree relatives," *Diabetologia*, vol. 26, pp. 431–436, 1984.

[33] D. McLarty, I. Athaide, G. Bottazzo, A. Swai, and K. Alberti, "Islet cell antibodies are not specifically associated with insulin-dependent diabetes in tanzanian africans," *Diabetes Research and Clinical Practice*, vol. 9, no. 3, pp. 219–224, 1990.

[34] B. Ahren and C. Corrigan, "Intermittent need for insulin in a subgroup of diabetic patients in tanzania," *Diabetic Medicine*, vol. 2, no. 4, pp. 262–264, 1985.

[35] M. Harris, P. Zimmet, and K. Alberti, "Classification of diabetes mellitus and other categories of glucose intolerance," in *International Textbook of Diabetes Mellitus*, 1997, pp. 3–18.

[36] S. Lillioja *et al.*, "Insulin resistance and insulin secretory dysfunction as precursors of non-insulin-dependent diabetes mellitus: prospective studies of pima indians," *New England Journal of Medicine*, vol. 329, no. 27, pp. 1988–1992, 1993.

[37] J. M. Mooy *et al.*, "Prevalence and determinants of glucose intolerance in a dutch caucasian population: the hoorn study," *Diabetes Care*, vol. 18, no. 9, pp. 1270–1273, 1995.

[38] P. J. Campbell and M. G. Carlson, "Impact of obesity on insulin action in niddm," *Diabetes*, vol. 42, no. 3, pp. 405–410, 1993.

[39] C. Bogardus, S. Lillioja, D. Mott, C. Hollenbeck, and G. Reaven, "Relationship between degree of obesity and in vivo insulin action in man," *American Journal of Physiology-Endocrinology and Metabolism*, vol. 248, no. 3, pp. E286–E291, 1985.

[40] A. H. Kissebah, N. Vydelingum, R. Murray, D. J. Evans, R. K. Kalkhoff, and P. W. Adams, "Relation of body fat distribution to metabolic complications of obesity," *The Journal of Clinical Endocrinology & Metabolism*, vol. 54, no. 2, pp. 254–260, 1982.

[41] M. A. Banerji *et al.*, "Gad antibody negative niddm in adult black subjects with diabetic ketoacidosis and increased frequency of human leukocyte antigen dr3 and dr4: Flatbush diabetes," *Diabetes*, vol. 43, no. 6, pp. 741–745, 1994.

[42] G. Umpierrez, M. M. Casals, S. S. Gebhart, P. S. Mixon, W. S. Clark, and L. Phillips, "Diabetic ketoacidosis in obese african-americans," *Diabetes*, vol. 44, no. 7, pp. 790–795, 1995.

[43] K. S. Polonsky, J. Sturis, and G. I. Bell, "Non-insulin-dependent diabetes mellitus—a genetically programmed failure of the beta cell to compensate

for insulin resistance," *New England Journal of Medicine*, vol. 334, no. 12, pp. 777–783, 1996.

[44] D. C. Simonson *et al.*, "Mechanism of improvement in glucose metabolism after chronic glyburide therapy," *Diabetes*, vol. 33, no. 9, pp. 838–845, 1984.

[45] R. R. Wing, E. H. Blair, P. Bononi, M. D. Marcus, R. Watanabe, and R. N. Bergman, "Caloric restriction per se is a significant factor in improvements in glycemic control and insulin sensitivity during weight loss in obese niddm patients," *Diabetes Care*, vol. 17, no. 1, pp. 30–36, 1994.

[46] P. Z. Zimmet, "Kelly west lecture 1991 challenges in diabetes epidemiology—from west to the rest," *Diabetes Care*, vol. 15, no. 2, pp. 232–252, 1992.

[47] T. Songer, "Disability in diabetes," in *Diabetes in America*, 2nd ed., M. I. Harris, C. C. Cowie, M. P. Stern, E. J. Boyko, G. E. Reiber, and P. H. Bennett, Eds. Scientific Research Publishing, 1995, pp. 429–448. [Online]. Available: https://scirp.org/reference/referencespapers?referenceid=689917

[48] T. Valle, J. Tuomilehto, and J. Eriksson, "Epidemiology of niddm in europids," in *International Textbook of Diabetes Mellitus*, 1997.

[49] M. de Courten, P. H. Bennet, J. Tuomilehto, and P. Zimmet, "Epidemiology of niddm in non-europids," in *International Textbook of Diabetes Mellitus*, 1997.

[50] W. C. Knowler, M. F. Saad, D. J. Pettitt, R. G. Nelson, and P. H. Bennett, "Determinants of diabetes mellitus in the pima indians," *Diabetes Care*, vol. 16, no. 1, pp. 216–227, 1993.

[51] M. M. Byrne *et al.*, "Altered insulin secretory responses to glucose in diabetic and nondiabetic subjects with mutations in the diabetes susceptibility gene mody3 on chromosome 12," *Diabetes*, vol. 45, no. 11, pp. 1503–1510, 1996.

[52] K. Clement *et al.*, "Assessment of insulin sensitivity in glucokinase-deficient subjects," *Diabetologia*, vol. 39, pp. 82–90, 1996.

[53] K. Yamagata *et al.*, "Mutations in the hepatocyte nuclear factor-1α gene in maturity-onset diabetes of the young (mody3)," *Nature*, vol. 384, no. 6608, pp. 455–458, 1996.

[54] P. Froguel *et al.*, "Close linkage of glucokinase locus on chromosome 7p to early-onset non-insulin-dependent diabetes mellitus," *Nature*, vol. 356, no. 6365, pp. 162–164, 1992.

[55] N. Vionnet *et al.*, "Nonsense mutation in the glucokinase gene causes early-onset non-insulin-dependent diabetes mellitus," *Nature*, vol. 356, no. 6371, pp. 721–722, 1992.

[56] K. Yamagata *et al.*, "Mutations in the hepatocyte nuclear factor-1α gene in maturity-onset diabetes of the young (mody3)," *Nature*, vol. 384, no. 6608, pp. 455–458, 1996.

[57] D. A. Staffers, J. Ferrer, W. L. Clarke, and J. F. Habener, "Early-onset type-ii diabetes mellitus (mody4) linked to ipf1," *Nature Genetics*, vol. 17, no. 2, pp. 138–139, 1997.

[58] M. Walker and D. Turnbull, "Mitochondrial related diabetes: a clinical perspective," *Diabetic Medicine*, vol. 14, no. 12, pp. 1007–1009, 1997.

[59] D. R. Johns, "Mitochondrial dna and disease," *New England Journal of Medicine*, vol. 333, no. 10, pp. 638–644, 1995.

[60] P. A. Gruppuso, P. Gorden, C. R. Kahn, M. Cornblath, W. P. Zeller, and R. Schwartz, "Familial hyperproinsulinemia due to a proposed defect in conversion of proinsulin to insulin," *New England Journal of Medicine*, vol. 311, no. 10, pp. 629–634, 1984.

[61] D. Robbins, S. Shoelson, A. Rubenstein, and H. Tager, "Familial hyperproinsulinemia. two cohorts secreting indistinguishable type ii intermediates of proinsulin conversion," *The Journal of Clinical Investigation*, vol. 73, no. 3, pp. 714–719, 1984.

[62] M. Haneda *et al.*, "Familial hyperinsulinemia due to a structurally abnormal insulin: definition of an emerging new clinical syndrome," *New England Journal of Medicine*, vol. 310, no. 20, pp. 1288–1294, 1984.

[63] N. Sanz, J. Karam, S. Horita, and G. Bell, "Prevalence of insulin-gene mutations in non-insulin-dependent diabetes mellitus," *The New England Journal of Medicine*, vol. 314, no. 20, pp. 1322–1323, 1986.

[64] C. R. Kahn *et al.*, "The syndromes of insulin resistance and acanthosis nigricans: insulin-receptor disorders in man," *New England Journal of Medicine*, vol. 294, no. 14, pp. 739–745, 1976.

[65] S. I. Taylor, "Lilly lecture: molecular mechanisms of insulin resistance: lessons from patients with mutations in the insulin-receptor gene," *Diabetes*, vol. 41, no. 11, pp. 1473–1490, 1992.

[66] L. Gullo, R. Pezzilli, A. M. Morselli-Labate, and I. P. C. S. Group, "Diabetes and the risk of pancreatic cancer," *New England Journal of Medicine*, vol. 331, no. 2, pp. 81–84, 1994.

[67] S. Larsen, J. Hilsted, B. Tronier, and H. Worning, "Metabolic control and b cell function in patients with insulin-dependent diabetes mellitus secondary to chronic pancreatitis," *Metabolism*, vol. 36, no. 10, pp. 964–967, 1987.

[68] J. Permert *et al.*, "Islet amyloid polypeptide in patients with pancreatic cancer and diabetes," *New England Journal of Medicine*, vol. 330, no. 5, pp. 313–318, 1994.

[69] A. Moran *et al.*, "Insulin sensitivity in cystic fibrosis," *Diabetes*, vol. 43, no. 8, pp. 1020–1026, 1994.

[70] G. Phelps, P. Hall, I. Chapman, W. Braund, and M. Mackinnon, "Prevalence of genetic haemochromatosis among diabetic patients," *The Lancet*, vol. 334, no. 8657, pp. 233–234, 1989.

[71] C. Yajnik *et al.*, "The ketosis-resistance in fibro-calculous-pancreatic-diabetes. 1. clinical observations and endocrine-metabolic measurements

during oral glucose tolerance test," *Diabetes Research and Clinical Practice*, vol. 15, no. 2, pp. 149–156, 1992.

[72] I. MacFarlane, "Endocrine diseases and diabetes mellitus," in *Textbook of Diabetes*, 1997, pp. 64.1–64.17.

[73] G. J. Krejs *et al.*, "Somatostatinoma syndrome: biochemical, morphologic and clinical features," *New England Journal of Medicine*, vol. 301, no. 6, pp. 285–292, 1979.

[74] J. W. Conn, "Hypertension, the potassium ion and impaired carbohydrate tolerance," *New England Journal of Medicine*, vol. 273, no. 21, pp. 1135–1143, 1965.

[75] ——, "Hypertension, the potassium ion and impaired carbohydrate tolerance," *New England Journal of Medicine*, vol. 273, no. 21, pp. 1135–1143, 1965.

[76] S. O'Byrne and J. Feely, "Effects of drugs on glucose tolerance in non-insulin-dependent diabetics (part ii)," *Drugs*, vol. 40, no. 2, pp. 203–219, 1990.

[77] A. Gallanosa, D. Spyker, and R. Curnow, "Diabetes mellitus associated with autonomic and peripheral neuropathy after vacor rodenticide poisoning: a review," *Clinical Toxicology*, vol. 18, no. 4, pp. 441–449, 1981.

[78] M. D. Esposti, A. Ngo, and M. A. Myers, "Inhibition of mitochondrial complex i may account for iddm induced by intoxication with the rodenticide vacor," *Diabetes*, vol. 45, no. 11, pp. 1531–1534, 1996.

[79] R. Assan *et al.*, "Pentamidine-induced derangements of glucose homeostasis: determinant roles of renal failure and drug accumulation: a study of 128 patients," *Diabetes Care*, vol. 18, no. 1, pp. 47–55, 1995.

[80] V. Bojkovska, "90+ important diabetes statistics in 2024," Apr 2022. [Online]. Available: https://www.myshortlister.com/insights/diabetes-statistics

[81] S. Azeem, U. Khan, and A. Liaquat, "The increasing rate of diabetes in pakistan: A silent killer," *Annals of Medicine and Surgery*, vol. 79, 2022.

[82] Diabetes Atlas, "IDF Diabetes Atlas 2025 — Global Diabetes Data and Insights," Apr. 2025.

[83] World Health Organization, "Diabetes," Nov. 2024.

[84] A. Basit, S. Askari, J. Zafar, M. Riaz, A. Fawwad, and N. Members, "NDSP 06: Prevalence and risk factors for obesity in urban and rural areas of Pakistan: A study from second National Diabetes Survey of Pakistan (NDSP), 2016–2017," *Obesity Research and Clinical Practice*, vol. 15, no. 1, pp. 19–25, 2021.

[85] M. Adnan and M. Aasim, "Prevalence of type 2 diabetes mellitus in adult population of Pakistan: a meta-analysis of prospective cross-sectional surveys," *Annals of Global Health*, vol. 86, no. 1, p. 7, 2020.

[86] M. M. Rahman *et al.*, "Exploring the plant-derived bioactive substances as antidiabetic agent: an extensive review," *Biomedicine & Pharmacotherapy*, vol. 152, p. 113217, 2022.

[87] S. Letourneau, "Healing type 2 diabetes without medication: A cure that has a 100," n.d.

[88] J. J. Marín-Peñalver, I. Martín-Timón, C. Sevillano-Collantes, and F. J. del Cañizo-Gómez, "Update on the treatment of type 2 diabetes mellitus," *World Journal of Diabetes*, vol. 7, no. 17, p. 354, 2016.

[89] S. Bastaki, "Diabetes mellitus and its treatment," *International Journal of Diabetes and Metabolism*, vol. 13, no. 3, pp. 111–134, 2005.

[90] M. S. Nolte and J. H. Karam, "Pancreatic hormones and anti-diabetic drugs," in *Lange Medical Books*. McGraw-Hill, 2001, pp. 711–734.

[91] S. Suh and M. K. Park, "Glucocorticoid-induced diabetes mellitus: an important but overlooked problem," *Endocrinology and Metabolism*, vol. 32, no. 2, p. 180, 2017.

[92] E. B. de Melo, A. da Silveira Gomes, and I. Carvalho, "α- and β-glucosidase inhibitors: chemical structure and biological activity," *Tetrahedron*, vol. 62, no. 44, pp. 10 277–10 302, 2006.

[93] S. L. Aronoff, K. Berkowitz, B. Shreiner, and L. Want, "Glucose metabolism and regulation: beyond insulin and glucagon," *Diabetes Spectrum*, vol. 17, no. 3, pp. 183–190, 2004.

[94] S. K. P. Mph, "Glucose: reference range, interpretation, collection and panels." [Online]. Available: https://emedicine.medscape.com/article/2087913-overview

[95] Y. Huang, S. Karuranga, B. Malanda, and D. Williams, "Call for data contribution to the idf diabetes atlas 9th edition 2019," *Diabetes Research and Clinical Practice*, vol. 140, pp. 351–352, 2018.

[96] Z. Fu, E. R. Gilbert, and D. Liu, "Regulation of insulin synthesis and secretion and pancreatic beta-cell dysfunction in diabetes," *Current Diabetes Reviews*, vol. 9, no. 1, pp. 25–53, 2013.

[97] O. Lavrynenko *et al.*, "The relationship between circulatory levels of fractalkine, omentin, and the mass of adipose tissue and their role in the pathogenesis of diabetes mellitus type 2," *Diabetes*, vol. 68, no. Supplement, 2019.

[98] R. P. Robertson, J. Harmon, P. O. Tran, Y. Tanaka, and H. Takahashi, "Glucose toxicity in β-cells: type 2 diabetes, good radicals gone bad, and the glutathione connection," *Diabetes*, vol. 52, no. 3, pp. 581–587, 2003.

[99] F. Eker, "Brief introduction of insulin resistance and its effects," Feb 2023. [Online]. Available: https://gencomugen.com/brief-introduction-of-insulin-resistance-and-its-effects

[100] L. H. Chamberlain, M. J. Shipston, and G. W. Gould, "Regulatory effects of protein s-acylation on insulin secretion and insulin action," *Open Biology*, vol. 11, no. 3, p. 210017, 2021.

[101] T. Rosenzweig and S. R. Sampson, "Activation of insulin signaling by botanical products," *International Journal of Molecular Sciences*, vol. 22, no. 8, p. 4193, 2021.

[102] L. J. Holm, M. O. Monsted, M. Haupt-Jorgensen, and K. Buschard, "Ppars and the development of type 1 diabetes," *PPAR Research*, vol. 2020, no. 1, p. 6198628, 2020.

[103] H. Rang, M. Dale, and J. Ritter, "The endocrine system pharmacology," in *Pharmacology*. UK: Longman Group Ltd., 1991, pp. 504–508.

[104] T. Javid, M. Adnan, A. Tariq, B. Akhtar, R. Ullah, and N. M. Abd El Salam, "Antimicrobial activity of three medicinal plants (artemisia indica, medicago falcate and tecoma stans)," *African Journal of Traditional, Complementary and Alternative Medicines*, vol. 12, no. 3, pp. 91–96, 2015.

[105] C. R. Kahn, "Insulin action, diabetogenes, and the cause of type ii diabetes," *Diabetes*, vol. 43, no. 8, pp. 1066–1085, 1994.

[106] A. H. Heald *et al.*, "Estimating life years lost to diabetes: outcomes from analysis of national diabetes audit and office of national statistics data," *Cardiovascular Endocrinology & Metabolism*, vol. 9, no. 4, pp. 183–185, 2020.

[107] K. Maedler *et al.*, "Aging correlates with decreased β-cell proliferative capacity and enhanced sensitivity to apoptosis: a potential role for fas and pancreatic duodenal homeobox-1," *Diabetes*, vol. 55, no. 9, pp. 2455–2462, 2006.

[108] D. Edgar and A. Trifunovic, "The mtdna mutator mouse: Dissecting mitochondrial involvement in aging," *Aging (Albany NY)*, vol. 1, no. 12, p. 1028, 2009.

[109] K. F. Petersen *et al.*, "Mitochondrial dysfunction in the elderly: possible role in insulin resistance," *Science*, vol. 300, no. 5622, pp. 1140–1142, 2003.

[110] Z. Gao *et al.*, "Age-associated telomere attrition in adipocyte progenitors predisposes to metabolic disease," *Nature Metabolism*, vol. 2, no. 12, pp. 1482–1497, 2020.

[111] J. Fabianová *et al.*, "Yield, antioxidant activity and total polyphenol content of okra fruits grown in slovak republic," *Horticulturae*, vol. 8, no. 10, p. 966, 2022.

[112] Y. Jin, Y. Zhang, and K. Yuan, "The study on antioxidant activity and content of total flavonoids and total phenolic in different parts of abelmoschus esculentus l," in *2011 IEEE International Symposium on IT in Medicine and Education*, vol. 1. IEEE, 2011, pp. 169–172.

[113] P. Cuatrecasas, M. Wilchek, and C. B. Anfinsen, "Selective enzyme purification by affinity chromatography," *Proceedings of the National Academy of Sciences*, vol. 61, no. 2, pp. 636–643, 1968.

[114] J. Porath, "From gel filtration to adsorptive size exclusion," *Journal of Protein Chemistry*, vol. 16, pp. 463–468, 1997.

[115] J. Sherma and B. Fried, *Handbook of Thin-Layer Chromatography*. CRC Press, 2003.

[116] D. L. Pavia, G. M. Lampman, G. S. Kritz, and R. G. Engel, *Introduction to Organic Laboratory Techniques*. Thomson Brooks/Cole, 2006.

[117] M. Das and D. Dasgupta, "Pseudo-affinity column chromatography based rapid purification procedure for t7 rna polymerase," *Preparative Biochemistry & Biotechnology*, vol. 28, no. 4, pp. 339–348, 1998.

[118] F. E. Regnier, "High-performance liquid chromatography of biopolymers," *Science*, vol. 222, no. 4621, pp. 245–252, 1983.

[119] K. K. Chaudhary and N. Mishra, "A review on molecular docking: novel tool for drug discovery," *Databases*, vol. 3, no. 4, p. 1029, 2016.

[120] Y. Liu, M. Grimm, W.-t. Dai, M.-c. Hou, Z.-X. Xiao, and Y. Cao, "Cb-dock: a web server for cavity detection-guided protein–ligand blind docking," *Acta Pharmacologica Sinica*, vol. 41, no. 1, pp. 138–144, 2020.

[121] P. D. Bank, "Protein data bank," *Nature New Biology*, vol. 233, no. 223, pp. 10–1038, 1971.

[122] W. L. DeLano, "Pymol: An open-source molecular graphics tool," *CCP4 Newsletter on Protein Crystallography*, vol. 40, no. 1, pp. 82–92, 2002.

[123] S. Hunter *et al.*, "Interpro: the integrative protein signature database," *Nucleic Acids Research*, vol. 37, no. suppl, pp. D211–D215, 2009.

[124] K. Dobbs *et al.*, "Inherited dock2 deficiency in patients with early-onset invasive infections," *New England Journal of Medicine*, vol. 372, no. 25, pp. 2409–2422, 2015.

[125] T. A. Binkowski, S. Naghibzadeh, and J. Liang, "Castp: computed atlas of surface topography of proteins," *Nucleic Acids Research*, vol. 31, no. 13, pp. 3352–3355, 2003.

[126] J. Dundas, Z. Ouyang, J. Tseng, A. Binkowski, Y. Turpaz, and J. Liang, "Castp: computed atlas of surface topography of proteins with structural and topographical mapping of functionally annotated residues," *Nucleic Acids Research*, vol. 34, no. suppl, pp. W116–W118, 2006.

[127] J. S. Richardson, D. C. Richardson, and D. S. Goodsell, "Seeing the pdb," *Journal of Biological Chemistry*, vol. 296, 2021.

[128] S. Revathy, S. Elumalai, and M. B. Antony, "Isolation, purification and identification of curcuminoids from turmeric (curcuma longa l.) by column chromatography," *Journal of Experimental Sciences*, vol. 2, no. 7, 2011.

[129] Y. Liu, M. Grimm, W.-t. Dai, M.-c. Hou, Z.-X. Xiao, and Y. Cao, "Cb-dock: a web server for cavity detection-guided protein–ligand blind docking," *Acta Pharmacologica Sinica*, vol. 41, no. 1, pp. 138–144, 2020.

[130] C. Hall, "Thin layer chromatography: A complete guide to tlc," Mar 2020. [Online]. Available: https://chemistryhall.com/thin-layer-chromatography/#:$\sim$:text=There%20are%20commercial%20options%2C%20as,phase%2C%20instead%20of%20silica%20gel

[131] A. Niroula, S. Khatri, D. Khadka, and R. Timilsina, "Total phenolic contents and antioxidant activity profile of selected cereal sprouts and grasses," *International Journal of Food Properties*, vol. 22, no. 1, pp. 427–437, 2019.

[132] M. Cuendet, K. Hostettmann, O. Potterat, and W. Dyatmiko, "Iridoid glucosides with free radical scavenging properties from fagraea blumei," *Helvetica Chimica Acta*, vol. 80, no. 4, pp. 1144–1152, 1997.

[133] S. Poovitha and M. Parani, "In vitro and in vivo α-amylase and α-glucosidase inhibiting activities of the protein extracts from two varieties of bitter gourd (momordica charantia l.)," *BMC Complementary and Alternative Medicine*, vol. 16, pp. 1–8, 2016.

[134] M. Kazeem, J. Adamson, and I. Ogunwande, "Modes of inhibition of α-amylase and α-glucosidase by aqueous extract of morinda lucida benth leaf," *BioMed Research International*, vol. 2013, no. 1, p. 527570, 2013.

[135] A. H. Laghari, S. Memon, A. Nelofar, K. M. Khan, and A. Yasmin, "Determination of free phenolic acids and antioxidant activity of methanolic extracts obtained from fruits and leaves of chenopodium album," *Food Chemistry*, vol. 126, no. 4, pp. 1850–1855, 2011.

[136] R. Santhoshkumar and A. Yusuf, "In silico structural modeling and analysis of physicochemical properties of curcumin synthase (curs1, curs2, and curs3) proteins of curcuma longa," *Journal of Genetic Engineering and Biotechnology*, vol. 18, no. 1, p. 24, 2020.

[137] M. Blum *et al.*, "The interpro protein families and domains database: 20 years on," *Nucleic Acids Research*, vol. 49, no. D1, pp. D344–D354, 2021.

[138] Y. Wang, J. Xiao, T. O. Suzek, J. Zhang, J. Wang, and S. H. Bryant, "Pubchem: a public information system for analyzing bioactivities of small molecules," *Nucleic Acids Research*, vol. 37, no. suppl, pp. W623–W633, 2009.

[139] S. Kim and E. E. Bolton, "Pubchem: A large-scale public chemical database for drug discovery," *Open Access Databases and Datasets for Drug Discovery*, pp. 39–66, 2024.

[140] K. Roy, S. Kar, and R. N. Das, "Computational chemistry," in *Elsevier eBooks*, 2015, pp. 151–189.

[141] T. I. Adelusi *et al.*, "Molecular modeling in drug discovery," *Informatics in Medicine Unlocked*, vol. 29, p. 100880, 2022.

[142] K. P. Baskaran, A. Arumugam, R. Kandasamy, and S. Alagarsamy, "In silico method for prediction of maximum binding affinity and ligand-protein interaction studies on alzheimer's disease," *International Journal of Research Granthaalayah*, vol. 8, no. 11, pp. 362–370, 2020.

[143] R. Patil, S. Das, A. Stanley, L. Yadav, A. Sudhakar, and A. K. Varma, "Optimized hydrophobic interactions and hydrogen bonding at the target-ligand interface leads the pathways of drug-designing," *PloS One*, vol. 5, no. 8, p. e12029, 2010.

[144] X. Chen, H. Li, L. Tian, Q. Li, J. Luo, and Y. Zhang, "Analysis of the physicochemical properties of acaricides based on lipinski's rule of five," *Journal of Computational Biology*, vol. 27, no. 9, pp. 1397–1406, 2020.

[145] J. G. M. Mvondo, A. Matondo, D. T. Mawete, S.-M. N. Bambi, B. M. Mbala, and P. O. Lohohola, "In silico adme/t properties of quinine derivatives using swissadme and pkcsm webservers," *International Journal of Tropical Disease and Health*, vol. 42, no. 11, pp. 1–12, 2021.

[146] A. Biharee *et al.*, "Flavonoids as promising anticancer agents: An in silico investigation of admet, binding affinity by molecular docking and molecular dynamics simulations," *Journal of Biomolecular Structure and Dynamics*, vol. 41, no. 16, pp. 7835–7846, 2023.

[147] M. N. Wickramaratne, J. Punchihewa, and D. Wickramaratne, "In-vitro alpha amylase inhibitory activity of the leaf extracts of adenanthera pavonina," *BMC Complementary and Alternative Medicine*, vol. 16, pp. 1–5, 2016.

[148] I. Ignat, I. Volf, and V. I. Popa, "A critical review of methods for characterisation of polyphenolic compounds in fruits and vegetables," *Food Chemistry*, vol. 126, no. 4, pp. 1821–1835, 2011.

[149] J. Bashyal, "Column chromatography: Principle, instrumentation," Dec 2022. [Online]. Available: https://scienceinfo.com/column-chromatography-principle-instrumentation-types-procedure-advantages

[150] L. M. Cheung, "Evaluation of the antioxidant activity and characterization of extracts from three edible chinese mushrooms," Ph.D. dissertation, Chinese University of Hong Kong, 2001.

[151] I. I. Koleva, T. A. Van Beek, J. P. Linssen, A. de Groot, and L. N. Evstatieva, "Screening of plant extracts for antioxidant activity: a comparative study on three testing methods," *Phytochemical Analysis: An International Journal of Plant Chemical and Biochemical Techniques*, vol. 13, no. 1, pp. 8–17, 2002.

[152] M. Hafeez, S. M. Hassan, S. S. Mughal, M. Munir, and M. K. Khan, "Antioxidant, antimicrobial and cytotoxic potential of abelmoschus esculentus," *Chemical and Biomolecular Engineering*, vol. 5, no. 4, p. 69, 2020.

[153] S. A. Petropoulos, S. Plexida, N. Tzortzakis, and I. C. Ferreira, "Phytochemicals content and health effects of abelmoschus esculentus (okra)," in *Phytochemicals in Vegetables: A Valuable Source of Bioactive Compounds*. Bentham Science Publishers, 2018, pp. 404–443.

[154] Y. Velioglu, G. Mazza, L. Gao, and B. Oomah, "Antioxidant activity and total phenolics in selected fruits, vegetables, and grain products," *Journal of Agricultural and Food Chemistry*, vol. 46, no. 10, pp. 4113–4117, 1998.

[155] F. O. Jimoh, A. A. Adedapo, and A. J. Afolayan, "Comparison of the nutritive value, antioxidant and antibacterial activities of sonchus asper and sonchus oleraceus," *Records of Natural Products*, vol. 5, no. 1, pp. 29–42, 2011.

[156] S. M. Mohsen and A. S. Ammar, "Total phenolic contents and antioxidant activity of corn tassel extracts," *Food Chemistry*, vol. 112, no. 3, pp. 595–598, 2009.

[157] K. Thongprajukaew, A. Choodum, B. Sa-E, and U. Hayee, "Smart phone: a popular device supports amylase activity assay in fisheries research," *Food Chemistry*, vol. 163, pp. 87–91, 2014.

[158] P. M. d. Sales, P. M. d. Souza, L. A. Simeoni, P. d. O. M. D. Batista, and D. Silveira, "α-amylase inhibitors: a review of raw material and isolated compounds from plant source," *Journal of Pharmacy and Pharmaceutical Sciences*, 2012.

[159] C. N. Kunyanga, J. K. Imungi, M. W. Okoth, H. K. Biesalski, and V. Vadivel, "Total phenolic content, antioxidant and antidiabetic properties of methanolic extract of raw and traditionally processed kenyan indigenous food ingredients," *LWT-Food Science and Technology*, vol. 45, no. 2, pp. 269–276, 2012.

[160] M. Suzery, A. Ningrum, B. Nudin, N. Mulyani, and B. Cahyono, "Determination of quercetin and rutin in red galangal rhizomes (alpinia purpurata) and white galangal (alpinia galanga) with high performance liquid chromatography method," in *IOP Conference Series: Earth and Environmental Science*, vol. 292, no. 1. IOP Publishing, 2019, p. 012064.

[161] F. Stanzione, I. Giangreco, and J. C. Cole, "Use of molecular docking computational tools in drug discovery," *Progress in Medicinal Chemistry*, pp. 273–343, 2021.

[162] H. Prabhavathi, K. R. Dasegowda, K. H. Renukananda, P. Karunakar, K. Lingaraju, and H. R. Naika, "Molecular docking and dynamic simulation to identify potential phytocompound inhibitors for egfr and her2 as anti-breast cancer agents," *Journal of Biomolecular Structure and Dynamics*, vol. 40, no. 10, pp. 4713–4724, 2020.

[163] M. I. Hosen, "In-silico approach to characterize the structure and function of a hypothetical protein of monkeypox virus exploring chordopox-a20r domain-containing protein activity," *Antiviral Therapy*, vol. 29, no. 3, 2024.

[164] S. C. Moldoveanu and V. David, "Properties of analytes and matrices determining hplc selection," in *Elsevier eBooks*, 2017, pp. 189–230.

[165] D. G. Gamage, A. Gunaratne, G. R. Periyannan, and T. G. Russell, "Applicability of instability index for in vitro protein stability prediction," *Protein and Peptide Letters*, vol. 26, no. 5, pp. 339–347, May 2019.

[166] S. Panda and G. Chandra, "Physicochemical characterization and functional analysis of some snake venom toxin proteins and related non-toxin proteins of other chordates," *Bioinformation*, vol. 8, no. 18, pp. 891–896, Sep 2012.

[167] H. Duan, A. Er-Bu, Z. Dongzhi, H. Xie, B. Ye, and J. He, "Alkaloids from dendrobium and their biosynthetic pathway, biological activity and total synthesis," *Phytomedicine*, vol. 102, p. 154132, Apr 2022.

[168] J. Kyte and R. F. Doolittle, "A simple method for displaying the hydropathic character of a protein," *Journal of Molecular Biology*, vol. 157, no. 1, pp. 105–132, May 1982.

[169] C. N. Pace, F. Vajdos, L. Fee, G. Grimsley, and T. Gray, "How to measure and predict the molar absorption coefficient of a protein," *Protein Science*, vol. 4, no. 11, pp. 2411–2423, Nov 1995.

[170] R. D. Requião, L. Fernandes, H. J. A. de Souza, S. Rossetto, T. Domitrovic, and F. L. Palhano, "Protein charge distribution in proteomes and its impact on translation," *PLoS Computational Biology*, vol. 13, no. 5, p. e1005549, May 2017.

[171] D. A. Korasick and J. M. Jez, "Protein domains: structure, function, and methods," in *Elsevier eBooks*, 2015, pp. 91–97.

[172] S. Hunter *et al.*, "Interpro: the integrative protein signature database," *Nucleic Acids Research*, vol. 37, no. Database, pp. D211–D215, Oct 2008.

[173] E. H. Bowler-Barnett, J. Fan, J. Luo, M. Magrane, M. J. Martin, and S. Orchard, "Uniprot and mass spectrometry-based proteomics—a 2-way working relationship," *Molecular & Cellular Proteomics*, vol. 22, no. 8, p. 100591, Jun 2023.

[174] A. Volkamer, D. Kuhn, T. Grombacher, F. Rippmann, and M. Rarey, "Combining global and local measures for structure-based druggability predictions," *Journal of Chemical Information and Modeling*, vol. 52, no. 2, pp. 360–372, 2012.

[175] I. V. Ferrari and P. Patrizio, "Development and validation molecular docking analysis of human serum albumin (hsa)," p. 2021.07.09.451789, 2021.

[176] A. C. Wallace, R. A. Laskowski, and J. M. Thornton, "Ligplot: a program to generate schematic diagrams of protein-ligand interactions," *Protein Engineering Design and Selection*, vol. 8, no. 2, pp. 127–134, Jan 1995.

[177] R. Roskoski, "The erbb/her family of protein-tyrosine kinases and cancer," *Pharmacological Research*, vol. 79, pp. 34–74, Nov 2013.

[178] L. Guan *et al.*, "Admet-score – a comprehensive scoring function for evaluation of chemical drug-likeness," *MedChemComm*, vol. 10, no. 1, pp. 148–157, Nov 2018.

[179] S. Ghosh, V. Arer, and D. Kar, "Antibiotic pharmacology and biopharmaceutics," in *Biomedical and Life Sciences (R0)*, 2024, pp. 153–177.

[180] K. A. Azzam, "Swissadme and pkcsm webservers predictors: an integrated online platform for accurate and comprehensive predictions for in silico adme/t properties of artemisinin and its derivatives," *Kompleksnoe Ispolzovanie Mineralnogo Syra = Complex Use of Mineral Resources*, vol. 325, no. 2, pp. 14–21, Nov 2022.

[181] D. A. M. Adnyaswari, A. W. Indrayani, and I. G. A. Artini, "In silico toxicity and pharmaceutical properties to get candidates for antitumor drug," *Journal of Pharmaceutical Research International*, vol. 36, no. 2, pp. 1–11, Feb 2024.

[182] O. K. Didigwu and C. O. Nnadi, "Theoretical drug-likeness, pharmacokinetic and toxicities of phytotoxic terpenoids from the toxic plants-phytotoxins," *Tropical Journal of Natural Product Research*, vol. 8, Nov 2024.

[183] P. D. Utami, V. Yudo, and R. Budiarti, "Blockade of multiple pathways of p. falciparum by quinoxaline from curry fish (s. hermanni) using an in silico approach," *Indian Journal of Pharmaceutical Education and Research*, vol. 59, no. 1, pp. 326–337, Jan 2025.